*Università degli Studi di Trieste*

**Graduate School in MOLECULAR BIOMEDICINE**

PhD Thesis

# Activation of the proteasome machinery by NRF2/mutant p53 axis and its therapeutic implications for triple negative breast cancer

*Kamil Lisek*

**Anno Accademico 2014-2015**

# Università Degli Studi di Trieste

## XXVII CICLO DEL DOTTORATO DI RICERCA IN BIOMEDICINA MOLECOLARE

# Activation of the proteasome machinery by NRF2/mutant p53 axis and its therapeutic implications for triple negative breast cancer

Settore scientifico-disciplinare: **BIO/13**


DOTTORANDO
**Kamil Lisek**

COORDINATORE
**PROF. Guidalberto Manfioletti**

SUPERVISORE DI TESI
**PROF. Giannino Del Sal**

CO-SUPERVISORE DI TESI
**DOTT. Dawid Walerych**


**ANNO ACCADEMICO 2014 / 2015**

*"… you see (…) it takes all the running you can do, to keep in the same place. If you want to get somewhere else, you must run at least twice as fast as that!"*

*“ ….bo widzisz (…) trzeba biec z całą szybkością, na jaką ty w ogóle możesz się zdobyć, ażeby pozostać w tym samym miejscu. A gdybyś się chciała gdzie indziej dostać, musisz biec przynajmniej dwa razy szybciej.”*

Lewis Carroll

(1832-1898)

To my wonderful family,for always being there for me.

Mojej wspaniałej rodzinie, za to że zawsze jesteście moim oparciem.

# Table of Contents

# ABSTRACT

Triple negative breast cancers (TNBC) are an aggressive group of tumors prone to recurrence, metastasis and become resistant to chemotherapy - therefore finding novel targets for possible treatment is crucial. Interesting hallmark of these neoplasms is high mutation rate in TP53 loci reaching more than 50% of cases.TP53 is the most frequently mutated gene in human cancers. Mutations of TP53 have been established to contribute to carcinogenesis by causing the loss of the tumor suppressor activities and exerting dominant negative effects over the wild type allele as well as arming the mutant p53 with novel oncogenic gain-of-function (GOF) properties. Until now, no universal mutant p53 gain-of-function program has been defined.

In this thesis I describe the identification of proteasome machinery as a common target of p53 missense mutants by multi-omic analyses (proteome, DNA-interactome and transcriptome). I show how the pathway is regulated at the transcriptional level by the cooperation of mutant p53 with transcription factors (TFs) among which NRF2 (NFE2L2) - the master regulator of oxidative stress response - was discovered as the common interactor of all investigated p53 mutant variants. Upregulation of proteasome activity by p53 GOF mutants allows the TNBC cells to foster the chemoresistance to proteasome inhibitors. Aiming the p53 mutant proteins with mutant p53 targeting drugs (APR-246) gives the opportunity to blunt the activity of NRF2-mediated mechanism of an induced transcription of proteasome encoding genes in response to the treatment with proteasome inhibitors - known as the “bounce back response”.

In summary, results of this thesis suggest that the combination of mutant p53 targeting drugs together with proteasome inhibitors might be a promising therapeutic solution tailored for treating TNBC and other tumors where p53 is mutated.

# INTRODUCTION

## Breast Cancer

Cancer is a one of the leading cause of death worldwide, accounting for 8.2 million deaths in 2012 (World Cancer Report 2014). This multistep process of progressive changes leads to deregulation of various biological pathways in a normal cell and its subsequent tumor transformation. Six essential steps for sustaining tumor growth and metastatic capabilities must be achieved to allow the cancer cell to survive, proliferate and disseminate. These steps, termed "the hallmarks of cancer" consist of sustained proliferative signaling, evading growth suppressors, resisting cell death, enabling replicative immortality, inducing angiogenesis and activating invasion and metastasis (Hanahan & Weinberg 2000). In addition to these six hallmarks, tumor formation may benefit also from the inflammatory microenvironment (Mantovani 2009) and from changes in cell metabolism to sustain deregulated cell proliferation (Hanahan & Weinberg 2011).

IARC (International Agency for Research on Cancer) pinpoints breast cancer as the most frequently diagnosed human cancer and as the disease that leads to the most women deaths worldwide. In recent years the decline in the death rates of breast cancer patients (especially women below the age of 50) is striking. This positive trend can be linked to an increased awareness, earlier and more precise detection and description as well as more advanced therapeutic approaches. The clinicopathological characteristics like: histopathological grade, size of the tumor, the involvement of lymph node and the expression of the estrogen receptor (ER), progesterone receptor (PR) and human epidermal growth factor receptor 2 (HER2) reported during the diagnosis allow to estimate an overall progression of the disease. However despite improved therapies and better diagnosis there are still challenges in the treatment of this complex and multilayered disease – mainly the resistance of various types of cancer to the therapies as well as difficulties in the detection and curing of the distant metastasis. At the molecular level, several distinct subtypes of breast cancer have been identified based on the gene expression profiling (Perou et al. 2000; Curtis et al. 2012) The most commonly used classification divides the breast cancer in six subtypes: luminal A, luminal B,

Her2, claudin low, basal-like breast cancer and normal (Perou et al. 2000; Prat et al. 2010). More recently however analysis of large numbers of tumor samples as part of the METABRIC study identified 10 pathologically distinct subtypes of breast cancer (Curtis et al. 2012) . Representing about fifteen percent of total number of breast cancer cases the triple negative breast cancer (TNBC) (Oakman et al. 2010) is a rough target for the molecular biomedicine studies due to its aggressive biological characteristics and poor prognosis arising from absence of a standard therapy available for treatment (Gusterson 2009). TNBC is a heterogeneous group of aggressive tumors of mammary epithelial tissue that is characterized by the absence of three growth factors receptors: estrogen (ER), progesterone (PR) and EGF (HER2/ERBB2) (Turner et al. 2013). Interestingly the mutation in TP53 gene locus which - according to recent genome-wide studies - occurs in 50-60% of all TNBC cases and up to 80% of basal-like TNBCs making it a distinctive thus potentially targetable genomic trait of this type of tumor (Curtis et al. 2012; Shah et al. 2012). Basal-like and triple negative breast cancer are often considered synonymous, TNBC however represent most but not all cases of basal-like breast cancer (Lehmann et al. 2011). In well-differentiated and hormone receptor positive subtypes TP53 mutations are usually uncommon unlike the HER2 and basal-like tumors where they tend to be more prevalent (Rivlin et al. 2011).

## The p53 tumor suppressor pathway

Deregulation of tumor suppressive genes is a common hallmark of cancer, hallmark in which p53 plays the central role. p53 is a potent transcription factor (TF) that in order to maintain the genetic stability on both transcriptional and non-transcriptional levels, becomes activated in response to a wide range of stress stimuli as various as: γ-rays, UV light, DNA damage, hypoxia, ribonucleotide depletion or deregulated oncogenes (Murray-Zmijewski et al. 2008) (Fig. 1). Upon its activation and stabilization by intra- or extra- cellular factors, p53 coordinates complex response through a combination of post-translational modifications and interacting protein partners leading to the DNA repair, senescence, cell-cycle arrest, or apoptosis (Vousden & Prives 2009). Under unstressed conditions activities of p53 are blunted by degradation mechanism mediated mainly by MDM2 E3-ubiquitine ligase as well as

MDM4 (MDMX in humans) - protein belonging to the same E3 ligase family. Post-translational modifications of both p53 and its E3 ligases MDM2/MDM4 induced by stress abolish interaction between p53 and MDM2/MDM4 leading to p53 accumulation and the enhancing its transcriptional activity (Toledo & Wahl 2006; Vousden & Prives 2009).

The family of p53 related factors contains two other proteins important for cellular homeostasis, p63 and p73 (Joerger et al. 2009). p63 and p73 that play a vital role in the development and both possess tumor suppressive activities in human tumors (Murray-Zmijewski et al. 2008). Due to a partial structural homology, p53 family members have some overlapping functions mediated by the transactivation of common targets (Stiewe 2007).

## Gain of function of mutant p53

Mutations in the TP53 loci occur with different frequency in various types of cancer, starting with 10% in hematopoietic malignancies, up to 96% in high grade ovarian serious carcinoma (Rivlin et al. 2011) overall making it the most commonly mutated tumor suppressor gene in human cancers (Kandoth et al. 2013). Majority of studies associate bad prognosis in various cancer types with the presence of mutated variant of p53. TP53 mutations are known mostly for their abilities to inactivate the oncosuppressive transcription factor properties of wild-type p53 protein - loss of function activities (LOF) (Walerych et al. 2015). Since p53 acts as a tetramer, an expression of p53 mutant variants allows them to exert a dominant negative (DN) effect over their wild-type counterpart, additionally arming cancer cells with novel oncogenic gain-of-function (GOF) activities (Freed-Pastor & Prives 2012; Walerych et al. 2012; Muller & Vousden 2013) (Fig. 2c). TP53 mutations in about 70% of cases are missense, most frequently they occur within the region encoding for the core DNA binding domain of the p53 protein (Petitjean et al. 2007) (Fig. 2a). Interestingly, although the range of missense mutations in TP53 counts more than 1,500 different amino-acid changes (Soussi 2011) some of the point mutations (termed: hotspot TP53 mutations) particularly targeting residues R273, R248, R175, and G245 of the p53 protein, occur with a frequency higher in both sporadic tumors (together over 21% of total missense

mutations) as well as in individuals with the Li–Fraumeni syndrome (Walerych et al. 2015) (Figure 2b). Li-Fraumeni syndrome (LFS) is a genetic disorder caused by inherited TP53 mutations that predispose carriers to an early-onset development of various cancers (Malkin 2011). In LFS wild-type TP53 allele is usually present, however in tumors it is likely to be inactivated (40-60% of the cases) (Varley 2003). This loss of heterozygosity (LOH) is a phenomenon occurring through various mechanisms of wild type p53 inactivation in humans and LFS mice models alike (Olive et al. 2004; Varley 2003). Interestingly, it was reported recently that in the embryonic stem cells from LFS mice it is the mutant allele that is lost, suggesting that a bi-directional TP53 LOH process plays a role of cell-fate checkpoint and that there exists a selective pressure against the heterozygous TP53 state (Shetzer et al. 2014) .

Hotspot changes in p53 are traditionally divided in two groups: "conformational mutants" - which disturb the correct folding of the core domain of p53, not allowing the p53 protein to bind the promoters of its target genes and the "DNA contact" mutations in residues that are responsible for directly binding DNA, with a near-native core domain structure (Bullock et al. 2000; Cho et al. 1994). As previously mentioned, the wild-type p53 is a short-lived protein whose levels are kept low in non-stressed conditions by the action of E3 ligase MDM2 leading to the wild type p53 protein ubiquitination and its subsequent degradation, however this negative feedback is abrogated in a tumor microenvironment and mutant p53 proteins are protected from degradation which results in their increased protein levels (Terzian et al. 2008). Importance of the accumulation of mutant p53 protein variants was underlined by the Li-Fraumeni mouse models where R172H KI mice (equivalent of human R175H p53 missense mutant) crossed with $MDM2^{-/-}$ mice resulted in a drastic shortening of mice survival and significant increase of mutant p53 protein levels (Lukashchuk & Vousden 2007). Since the mutant p53 proteins are not intrinsically resistant to degradation, it is possible that tumor-associated stress which normally stabilizes wild-type p53 provokes a futile accumulation of mutant protein as well (Muller & Vousden 2013). Despite the fact that mutant p53 variants can still be ubiquitinated by MDM2 as well as other E3 ligases and subsequently degraded by the proteasome, ubiquitination-dependent degradation can be counteracted in tumor cells by several mechanisms such as: stabilization of GOF p53 mutant proteins by binding to Hsp90 (Muller et al. 2008) or

the activities of upregulated p16INK4 (Zhang et al. 2006). Moreover, mutant p53 like its wild-type counterpart undergoes several post-translational modifications, that can affect its stability and function. For example the mutant p53 phosphorylation at Ser 392 effects in its enhanced MDM2-mediated degradation and reduced transforming activity (Gillotin et al. 2010; Yap et al. 2004), while phosphorylation by JNK or PLK2 enhances mutant p53 oncogenic potential (Valenti et al. 2011; Girardini et al. 2011). The loss of tumor suppressive functions of the wild-type p53 counterpart is not the only advantage that the cancer cell acquires from the missense mutation in core domain of p53. GOF p53 mutants were linked to be the cause for an aberrant regulation of several cancer-relevant pathways that include: DNA repair (Song et al. 2007), integrin recycling (Muller et al. 2009) regulation of mevalonate pathway and steroid synthesis (Freed-Pastor et al. 2012), inactivation of tumor suppression mediated by p73/p63 (Agostino et al. 2008; Adorno et al. 2009), activation of the cell cycle drivers (Javier E Girardini et al. 2011; Di Agostino et al. 2006), the vitamin D3 receptor signaling (Stambolsky et al. 2010), nucleotide biosynthesis (Kollareddy et al. 2015) or inhibition of oncosuppressive miRNA biogenesis (Garibaldi et al. 2016) (Fig. 3). Most of these tumorigenic activities of GOF p53 mutant variants are exerted by their direct impact on proteins through the interplay with a broad repertoire of interactors in the nucleus that significantly impact on the change of the gene expression (Girardini et al. 2014) and through some particular activities in the cytoplasm (Di Minin et al. 2014).

Target binding site of mutant p53, similar to the one of wild-type p53, was not determined in any of available mutant p53 ChIP-sequencing data. Thus the transactivation of mutant p53 in the nucleus most likely occurs through the interaction with the help of other transcription factors like: NF-Y family members, SREBP 1 and 2, and ETS2 (Freed-Pastor et al. 2012; Di Agostino et al. 2006; Martinez 2016). The cytoplasm specific activities of GOF p53 mutant variants are somehow less investigated: their activities however are relevant for tumor progression and include regulation of the DAB2IP protein which affects TNFα- dependent signaling (Di Minin et al. 2014) as well as the regulation of activity of PARP and its localization (Polotskaia et al. 2015).

Mutant p53 knock-in (KI) mice studies underlined the significance of GOF p53 mutant activities in tumor progression. Presence of mutated protein p53 variants promotes the growth of the tumor with higher metastasis rate, moreover the tissue spectrum of these tumors is different than the one observed in the absence of wild-type p53 (Olive et al. 2004; Lang et al. 2004). These *in vivo* studies proved the initial observations of cell line models suggesting that mutant p53 missense variants may actively foster the cell transformation (Dittmer et al. 1993; Halevy et al. 1990). However Chen and colleagues in a study of KI mice with the R246S p53 mutant (R249S GOF p53 mutant in human that had been demonstrated to induce growth, chemoresistance, and a specific mutant p53 transcriptional program in several studies of human cell line based experiments (Yan & Chen 2010; Zhu et al. 2015)), showed no clear indication of its GOF oncogenic activities in vivo (Lee et al. 2012). This particularity indicated that mouse models despite being very informative may possess their own specific limitations and require a careful validation of their significance in human systems.

## GOF p53 mutant variants - one oncoprotein with shared, common program or various oncoproteins with unique activities?

Only a minority of studies that would help to determine a common GOF program of different p53 mutant variants is based on mutant p53 KI mouse models. However some major discoveries in the field were made with their help as for example: human TP53 KI "HupKI" mouse model that demonstrated the inhibitory role of mutant p53 on MRE11 protein and the induction of genomic instability (Song et al. 2007); mutant p53 dependent - transcription-based activation of PDGFRβ signaling in pancreatic cancer model (Weissmueller et al. 2014); the transcriptional activation of oncogenic Pla2g16 phospholipase by p53 mutant variants (Xiong et al. 2014), and the confirmation of previous cell-based observations of a mutant p53-mediated inhibition of the p63/p73 oncosuppressive activities (Olive et al. 2004; Lang et al. 2004). The LFS mouse-model-based studies underlined differences between GOF properties of different p53 mutants and among the consequences of TP53 mutations in human and in mouse.

Studies comparing the R270Hand R172H p53 proteins in KI mice and human counterparts of these p53 mutant variants – R273H and R175H – in patients with LFS reported however different tumor spectra confirming the notion that the GOF of p53 mutants may in fact differ (Olive et al. 2004; Malkin 2011).

Vast data collected through the 25 years of studies using single initial *in vivo* and *in vitro* models that led to the discovery of numerous pathways controlled by p53 mutant variants, did not clarify whether these pathways have the same central role in diverse cellular contexts and are exerted by different GOF p53 mutant proteins in similar manner. Despite being profoundly investigated, the significance of oncogenic activities related to GOF p53 mutant variants are still concerned arguable by some researchers. Relevance of this issue is high - the lack of definition of the common gain-of-function molecular mechanism rendered it difficult to propose a universal therapeutic approach tailored to the presence of mutant p53. Many studies that aimed at determining the common or specific GOF program of p53 mutants were based on an overexpression of multiple mutant p53 variants in a p53-null or wild-type p53 background. Experiments performed in H1299 - p53-null background of non-small lung carcinoma cells demonstrated the role of mutant p53 variants in integrin recycling (Muller et al. 2009), NF-κB signaling (Scian et al. 2005), and in the Warburg effect (Zhang et al. 2013) as well as a role of TopBP1 in the upstream regulation of mutant p53 (Liu et al. 2011). Interestingly Neilsen and colleagues showed that genes activated by mutant p53 largely overlap between overexpressed different p53 mutant variants in H1299 and, moreover, they often share promoter sequences with p63 and wild-type p53 indicating that the promoter activation mediated by mutant p53 may be an aberrant representation of the interaction of wild-type p53 with transcription factors in normal cells (Neilsen et al. 2011).

Overexpression of mutant p53 variants in cells of wild-type p53 background (as for example MCF10A - the normal breast epithelium cells) led to the dissection of a mutant p53 dependent regulation of the epithelial-to-mesenchymal transition (EMT) phenotype (Zhang et al. 2011) as well as the cooperation of mutant p53 with the Ras oncogenic program in WI-38 human embryonic lung fibroblasts (Solomon et al. 2012). Over the course of transformation, cell lines carrying endogenous TP53 mutations become

addicted to the presence of mutant p53 variants and its GOF activities. Frequently their growth or the abilities of migration and invasion are compromised upon mutant p53 depletion (Bossi et al. 2006; Girardini et al. 2011; Di Minin et al. 2014; Zhu et al. 2015). Conversely, p53-null and wild-type p53 cell lines are able to survive and proliferate without the presence of mutant p53, suggesting that likely the GOF program observed under such conditions only partially resembles the cancer-related one.

The answer to the limitations of *in-vivo/in-vitro* systems may be the approach of initial analysis of different p53 mutants in their endogenous backgrounds. By comparing the downstream programs on both molecular and the phenotypic level it would be possible to address the question to what extent do the p53 mutants share one "core" oncogenic program, or if some of the mutants possess unique mode of actions.

The existence of a common oncogenic program exerted by various GOF p53 mutant proteins has been suggested by a recent study of Zhu and colleagues which describes a DNA interaction pattern common for three distinct p53 GOF mutants endogenously present in different breast cancer cell lines: (Bt-549, HCC70, MDA-MB-468) by comparing it with the one obtained from two cell lines bearing wild-type p53 (MCF7 and MDA-MB-175VII) (Zhu et al. 2015). Common DNA – mutant p53 interaction pattern pointed out the chromatin regulatory genes (MLL1 and MLL2) as the ones regulated by different mutants in their respective cellular backgrounds through their interplay with the transcription factor ETS2 - a well-established mutant p53 interactor (Martinez 2016). The relevance of mutant p53/ETS2 cooperation has been confirmed as a general feature in several mutant p53 expressing cell lines and thanks to the transcriptional program perturbed, as a critical modulator of the chromatin modification (Zhu et al. 2015).

Apparently this is only the beginning of a deeper understanding of both specific and general picture of mutant p53 GOF in cancer. In ordered to properly distinguish specific vs the common GOF p53 mutant program, the multiple cellular/cancer models have to be studied simultaneously in an unbiased, large-scale manner, by comparing the wider spectrum of mutant p53 variants, also including the non-hotspot mutations. Another important issue is how these discoveries could be transferred into clinical applications

## Targeting the oncogenic GOF p53 mutants for cancer therapy

The fact that the accumulation of mutant p53 proteins is observed in various tumors at high level and that TP53 is being one of the most frequently mutated genes in cancer creates a tempting opportunity to target it for more precise cancer therapy. Reactivation of oncosuppressive properties of wild-type p53 while blunting or eliminating the GOF activities of the mutant p53 could be an instrumental tool in the treatment of thousands cancer patients worldwide in more personalized clinical approach.

First drugs developed in order to target mutant p53 proteins were the inhibitors of Hsp90, a molecular chaperone that plays role in creation of a multiprotein complex stabilizing the conformational GOF p53 mutant variants. Geldanamycin was the first Hsp90 inhibitor demonstrated to reduce the levels of p53 mutants as well as its nuclear translocation (Blagosklonny et al. 1996; Dasgupta & Momand 1997). Recently, a geldanamycin derivative 17-DMAG and a new generation of Hsp90 inhibitors – ganetespib were both shown to significantly increase the survival of mutant p53 KI mice (Alexandrova et al. 2015). Of note, other drugs like sodium butyrate (NaB) (Yan et al. 2013), histone deacetylase inhibitor SAHA (Li et al. 2011) or arsenic compounds (Yan et al. 2014) were demonstrated to impinge on the stability of the mutant p53 proteins in various cancer models.

Another approach of targeting the oncogenic activities of GOF p53 mutant variants is to aim at the upstream oncogenic activators of p53 mutant proteins like ToBP1 (Liu et al. 2011) or Pin1 (Girardini et al. 2011). By blocking the activities of mutant p53 upstream activators for example - Pin1 with ATRA (Wei et al. 2015) or TopBP1 with Calcein (Chowdhury et al. 2014) the GOF properties of p53 mutant variants are suppressed. Third and most clinically advanced strategy to specifically target, blunt and deactivate the oncogenic properties of GOF p53 mutant variants is the treatment with small molecules that reactivate the oncosuppressive potential of the wild-type p53 counterpart by restoring its proper folding and conformation and upregulating its transcriptional targets. A number of small peptides were reported to directly and efficiently target mutant p53 proteins (Guida et al. 2008; Selivanova et al. 1997). Although the promising

results in inhibiting the tumorigenic GOF activities of p53 mutants were reported, clinical potential of these peptide aptamers is not profoundly investigated. CP-31398 was the first reported mutant p53 targeting micromolecule (Foster 1999) and after 15 years from initial description is still considered to be a promising drug candidate (He et al. 2015). Recently Tal and coworkers reported the synthetization of a number of novel peptides that are able to restore the proper p53 folding and activity. Treatment of cancer cells with chosen peptides lead to a dramatic regression of aggressive tumors in mouse breast and ovarian xenograft models (Tal et al. 2016).

Among compounds restoring the wild type p53 activities like STIMA-1, MIRA, RITA-1 and others (Parrales & Iwakuma 2015) the best described and most studied mutant p53 reactivating drug however is PRIMA-1 (Bykov et al. 2002) and its more potent and less toxic derivative PRIMA - 1MET/APR-246 (Bykov & Wiman 2014). This molecule is able to bind directly and modify the thiol residues in mutant p53 transforming it into a wild-type-like protein conformation (Lambert et al. 2009), thus allowing it to activate wild-type p53 transcriptional targets, such as NOXA, GADD45B, or CDKN1A (p21) inducing *in vitro* and *in vivo* cell cycle arrest or apoptosis in human cancer cells (Zache et al. 2008; Lambert et al. 2010).

An important and surprisingly underscored strategy of mutant p53 targeting is the treatment based on the drugs that downregulate oncogenic pathways activated downstream of GOF p53 mutants. Mainly, by tailoring the therapy to target the pathways dependent on mutant p53, it is possible to induce apoptosis in cells bearing specifically mutant and not wild- type p53 variant. Examples of drugs that take advantage of cancer cell dependency to mutant p53 induced pathways are statins that inhibit the mevalonate pathway (Freed-Pastor et al. 2012), Imatinib targeting the PDGFRβ (Weissmueller et al. 2014), or COMAPSS complex inhibitors (Zhu et al. 2015). The problem with application of the therapies based on mentioned drugs is that despite the results of their work are promising the limited knowledge of their performance in various mutant p53 context as well as the context of different genetic backgrounds contexts is making them difficult to apply.

Another important drawback of mutant p53 tailored therapies is their long time before they could be used in clinics due to the fact that most of the therapies are still in an early stage of development (Parrales & Iwakuma 2015). Treatment of the TNBC

cells with mutant p53 or p53 deficiency status by Chk1 inhibitors gave promising results in both *in vitro* and in mice cells (Origanti et al. 2013; Ma et al. 2012), however they failed to show a significant improvement in human patients (Ma et al. 2013). Meanwhile some of the drugs that could potentially benefit patients bearing mutant p53 variant like HDAC or Hsp90 inhibitors and statins, are currently involved in already ongoing clinical trials in cancer where mutant p53 status is not known or considered (Gonyeau 2014; Sidera & Patsavoudi 2014; West & Johnstone 2014). The only drug that directly targets GOF p53 mutant variants that reached the clinical stage is PRIMA-1MET/APR-246. APR-246 successfully went through phase I/II clinical trial in hematological malignancies and prostate cancer involved patients bearing mutant p53.

By combining drugs targeting mutant p53 directly and the ones that are able to downregulate pathways regulated by p53 mutant variants in cancer it is conceivable that the combination of the drugs might have an additional, beneficial effect in killing the cancer cells by decrease their responses involved in the compensation to the effects of the drugs and dosage toxicity. This synergistic or additive effects are observed in number of studies reporting combination of PRIMA-1 and APR-246 with chemotherapeutics like cisplatin (CDDP) and doxorubicin (andramicin) in effectively killing the mutant p53 bearing cancer cells (Bykov et al. 2005; Mohell et al. 2015) suggesting that also other compounds are worth being tested together with mutant p53 targeting drugs, such as PRIMA-1MET/APR-246 (Fig. 4)

## Proteasome

The loss of the cell cycle checkpoint control is one of the hallmarks of tumor cells. Tumors lose their DNA replication fidelity and acquire an increased rate of genomic mutations as a result of enhanced lifespan and eventual immortality. This leads to an accumulation of large quantities of misfolded or aberrantly overexpressed proteins which potentially may be highly toxic to the cells. In order to respond to these microenvironmental challenges, tumors cells are able to upregulate their expression of proteasomes in order to get rid of misfolded, damaged or tumor-suppressor proteins (Grigoreva et al. 2015) (Fig. 5). Main role in maintaining the cellular homeostasis plays the ubiquitin-mediated targeting of misfolded proteins for 26S proteasomal degradation (UPS - ubiquitin-proteasome degradation system) (Ciechanover 2005). However degradation of tumor suppressors is not entirely controlled by polyubiquitination – there is a growing number of known cancer-relevant proteasome substrates that are degraded by the 20S proteasome without the necessity of being ubiquitinated (Ben-Nissan & Sharon 2014). *S*ome studies indicate that even 20% of total cell protein content may be degraded without polyubiquitination (Baugh et al., 2009). The 26S proteasome is a complex protein degradation machinery with fourteen subunits constituting its catalytic 20S core (encoded by genes *PSMA1-7* and *PSMB1-7*), twenty subunits forming a regulatory 19S cap (encoded by *PSMC/Rpt1-6* and *PSMD/Rpn1-14*) and three alternative core subunits defining an antigen peptide-processing immunoproteasome (Gu & Enenkel 2014) (Fig. 5). Unlike the yeast, where all the proteasome subunits encoding genes are controlled by protein Rpn-4 (Shirozu et al. 2015), the mammal proteasome transcriptional regulation is controversial. The regulation of the transcription of 19S and 20S proteasome was implied to be regulated by several transcription factors to different extent: like NF-YA (Xu et al. 2012), STAT3 (Vangala et al. 2014), NF-kB (Arlt et al. 2009) or CNC bZIP family of TFs NRF1/TCF11 (Koch et al. 2011) and NRF2 (Höhn & Grune 2014) (Fig. 6). It is now widely established that the UPS plays a critical role in regulating a wide variety of cellular pathways, including cell growth and proliferation, apoptosis, protein quality control, DNA repair, transcription, and immune response (Eldridge & O'Brien 2010). However defects in

UPS have been implicated in a number of human pathologies, most notably in cancer and neurodegenerative disease (Crawford et al. 2011). In cancer an increased 26S proteasome and immunoproteasome activity results in the degradation of tumor suppressor proteins, the knowledge of which has been limited mostly to cell cycle and apoptosis-related factors (Eldridge & O'Brien 2010). Proteasome inhibitors Bortezomib ($1^{st}$ generation) and Carfilzomib ($2^{nd}$ generation) are clinically approved for the multiple myeloma treatment, while their application in solid tumor therapies did not progress beyond clinical trials (Johnson, 2015). Although the proteasome may represent point of weakness of solid tumors (Nijhawan et al. 2012; Petrocca et al. 2013) and a number of studies suggest the therapeutic potential of proteasome inhibitors in these malignancies, a prevalence of resistance mechanisms was reported (Johnson 2015).

# NRF2

Maintaining redox homeostasis in living cells requires a constant availability of intracellular antioxidants. In aerobic conditions, cells are permanently exposed to the generation of reactive oxygen species (ROS) that can impact proteins, lipids, and DNA, playing a pathological role in the development of various human diseases and cancer. Therefore in response to the oxidative or nucleophilic stress and to maintain ROS at low physiological levels cells evolved an endogenous defense mechanisms. The core of this antioxidant response is NRF2 (NFE2-related factor or Nuclear factor (erythroid-derived 2-like 2) (Gorrini et al. 2013). Ability to survive and adapt under conditions of inflammatory, oxidative and electrophilic stress relays on the expression of a complex network comprising nearly 500 genes that can be regulated by NRF2 encoding for proteins with different cytoprotective and antioxidant functions (Sporn et al. 2012).

In the first 10 years since its discovery in 1994, NRF2 had been an obscure protein with numerous studies conducted by few research groups around the world that were focused on investigating its involvement in suppression of the oxidative and electrophilic stress and possible potential in inhibiting the tumorigenesis (Moi et al. 1994; McMahon et al. 2001). With the understanding of the complex effects caused by the extrinsic and intrinsic insults such as: xenobiotics and oxidative stress, to the cellular homeostasis, the role of main cellular defense mechanism orchestrated by NRF2 moved the oxidative stress response pathway from the backstage of molecular and cell biology research topics to its spotlight (Gorrini et al. 2013) counting 966 in 2014 and over 1200 publications reported in PubMed last year (2015). Over the years hundreds of studies worldwide started to link the role of NRF2 mediated cellular defense response with protection from many diseases in which oxidative and inflammatory stress are crucial for pathogenesis like: the neurodegenerative diseases, aging, inflammation, acute pulmonary injury, photo-oxidative stress, cardiovascular disease, diabetes, pulmonary fibrosis, as well as cancer (Jaramillo & Zhang 2013; Sporn et al. 2012; Hayes & Dinkova-Kostova 2014). Ample evidence established NRF2 as a pivotal player in regulating processes as diverse as proliferation, inflammation, apoptosis, cell

differentiation, tissue regeneration and metabolism (Wakabayashi et al. 2010) impinging on such important and well investigated pathways as NF-kB (Lee et al. 2009), p53 (You et al. 2011; Bui & Shin 2011), mTOR (Shibata et al. 2010), NOTCH1 (Wakabayashi et al. 2014), AP-1 (Kim et al. 2010) and proteasome (Kwak et al. 2003). These observations consolidated the role of NRF2 as key regulator of cellular homeostasis and main regulator of cell survival (Fig. 7). Recently however the dark side of NRF2 emerged, various cancers types were shown to hijack NRF2 pathway by upregulating its mRNA and protein levels or to enhance its transcriptional activity thus creating a favorable environment as well as increasing the cancer cell resistance to standard chemotherapeutic agents thus lowering overall survival of patients (Wang et al. 2008). The role that this potent transcription factor plays in cellular homeostasis became a controversy. This dispute is important from the clinical point of view due to the fact that many chemotherapeutic approaches used to treat cancer or other diseases (ex. Sulphoraphane - SFN) as well as food preservatives (ex. tBHQ – tetr-Butyl hydroquinone) activate the NRF2 pathway in direct or indirect way. Opposite approach suggests that in various cancer types the inhibition of NRF2 (ex. Brusatol) pathway would be a tempting path for the treatment development to follow (Sporn et al. 2012; Jaramillo & Zhang 2013).

## NRF2 – the master regulator of oxidative stress response

Encoded by *Nfe2l2* gene NRF2 belongs to the Cap'n'Collar (CNC) basic leucine zipper (bZIP) transcription factors family (Moi et al. 1994) that comprises of NFE2-related factors: NF-E2 p45, NRF1/TCF11 (*Nfe2l1*), NRF2 (*Nfe2l2*), and NRF3 (*Nfe2l3*) (Chevillard & Blank 2011). NRF2 was cloned in the laboratory of Yuet Wai Kan and described as a protein that could bind a tandem repeat of the consensus site for AP-1 (Transcription Factors Activating Protein 1) and NF-E2 (Nuclear Factor-Erythroid 2) (Moi et al. 1994). The function of NRF2 was not clear in the initial stage of research due to no evident phenotype of mice knock-out for NRF2 (Chan et al. 1996). NF-E2 binding site however (5'-$^{A}/_{G}$TGA$^{C}/_{G}$TCAGCA-3') shared by NRF2 with other family members closely resembles the Antioxidant/Electrophile Response Element (ARE/EpRE – 5'-TGACNNNGC-3') (Rushmore et al. 1991; Friling et al. 1992). Based on sequence homology between ARE and MAF-recognition element (MRE), further

studies proved that small MAF and bZIP Cap'n'Collar transcription factors interact with ARE and both families heterodimerize on the gene promoters transactivating the genes responsible for oxidative stress response (Motohashi et al. 2004). In order to test the hypothesis that NRF2 controls enzymes involved in metabolism of the drugs *in vivo*, in a landmark study Itoh and colleagues revealed that induction of various GST subunits, as well as NQO1, by BHA (butylated hydroxyanisole) was greatly diminished in $Nrf2^{-/-}$ mice demonstrating the role that NRF2 plays in the oxidative stress response (Itoh et al. 1997). As mentioned before NRF2 KO mice do not present an obvious phenotype however they possess markedly higher susceptibility to carcinogen-induced tumor development in various organs, including colon, skin, breast, bladder and liver (Jaramillo & Zhang 2013). Further studies established NRF2 as a master regulator of the expression of various Phase I/II drug-metabolizing enzymes, as well as the battery of multi- drug resistance associated protein (MRP) transporters: MRP2, MRP3, MRP4, and MRP5 (Sporn et al. 2012). However today an ample evidence supported by various high-throughput analyses established NRF2 to control pathways spreading wide beyond only the oxidative stress response and multi drug-resistance-associated proteins programs in both in health and the disease (Chorley et al. 2012; MacLeod et al. 2009; Malhotra et al. 2010; Hayes & Dinkova-Kostova 2014). For the list of genes reported to be regulated in NRF2 dependent manner see Tab. 1 modified after (Hayes & Dinkova-Kostova 2014).

## Structure of NRF2

NRF2 is composed of seven conserved NRF2-ECH homology (Nef) domains (Fig. 7). Nef1 contains the CnC-bZIP motif that facilitates the binding of NRF2 to the ARE sequences and heterodimerizes with small Maf proteins on the gene promoters (Itoh et al. 1997). This domain interacts with UbcM2, an E2 ubiquitin conjugating enzyme, which regulates the Nrf2 protein stability (Plafker et al. 2010). Nef1 controls the NRF2 mediated transcriptional activity by binding and subsequent acetylation of its multiple lysine residues by p300/CBP in response to the arsenite induced oxidative stress (Z. Sun et al. 2009). C-terminally oriented region Neh3 domain helps with NRF2

transactivation through the interaction with chromatin remodeling protein CHD6 (Nioi et al. 2005) and is the domain regulating NRF2 activity through acetylation/deacetylation events that shuttle NRF2 between the nucleus and the cytoplasm regulating HO-1 activity among oxidative stress response genes (Kawai et al. 2011). Transactivation of ARE response genes is regulated also by domains Neh4 and Neh5 that are bound by CBP (Katoh et al. 2001) or nuclear cofactor RAC3 (Kim et al. 2013). The redox-insensitive Neh6 domain contains DSGIS and DSAPGS motifs and regulates Nrf2 stability. Phosphorylation of the DSGIS motif by GSK-3β enhances the ability of β-TrCP to ubiquitinate NRF2 and promotes its rapid turnover (McMahon et al. 2004; Chowdhry et al. 2013)**.** Neh7 which is localized between Neh5 and Neh6 domain of NRF2 interacts with the retinoic acid receptor α (RARα) and is able to repress NRF2 target gene expression (H. Wang et al. 2013)**.**

The best described and most profoundly investigated NRF2 domain is Neh2. Neh2, located at the N- terminal end of the NRF2, is its major regulatory domain, that contains two motifs important for NRF2 stability ($^{29}$DLG$^{31}$ and $^{79}$ETGE$^{82}$ motifs) divided by short linker sequence comprising seven lysine residues responsible for the conjugation of ubiquitin (McMahon et al. 2006). With $^{29}$DLG$^{31}$ and $^{79}$ETGE$^{82}$ NRF2 binds the KEAP1 – a dimeric redox sensitive substrate adaptor for the CUL3 RING ligase complex (McMahon et al. 2006) that sequesters NRF2 in the cytoplasm and represses its transcriptional activity and nuclear translocation by promoting its ubiquitination and directing for constant degradation (Cullinan et al. 2004; Zhang et al. 2004). (Fig. 7)

## Regulation of NRF2

Under basal condition of low oxidative stress NRF2 is sequestered in cytoplasm by its inhibitor - KEAP1 that binds NRF2 dimer with two KELCH domains. This binding, subsequent polyubiquitination of NRF2 and recognition by CUL3 RING ligase directs it for degradation by the 26S proteasome. Two KELCH domains of KEAP1 bind two specific motifs within the Neh2 domain ($^{29}$DLG$^{31}$ and $^{79}$ETGE$^{82}$) of NRF2. Both motifs have different affinity to the KEAP1 - binding ETGE being 20 times stronger

than DLG (Tong et al. 2007). This difference in affinity of the binding is explained by hinge and latch regulation model of NRF2. To be efficiently degraded NRF2 needs to bind the KEAP1 with both of the domains, the loss of binding with DGE motif (hinge) is enough, regardless of the binding to ETGE (latch), to lose the efficient ubiquitination and degradation of NRF2, thus allowing its detachment from the complex, subsequent translocation to the nucleus and transcription of its target genes (Canning et al. 2015) (Fig. 7).

Disruption of the binding between NRF2 and KEAP1 occurs upon oxidative stress stimuli, the KEAP1 loses its ability to bind NRF2 leading to its disassociation from the KEAP1-NRF2-CUL3 degradation complex and translocation to the nucleus. KEAP1 through its 25 reactive cysteine residues plays the role of an oxidative stress sensor that according to the intensity as well as the origin of recognized electrophilic insult tunes the activation of NRF2 which in literature forged a term of "cysteine code" of KEAP1 (Kobayashi et al. 2009; Ma 2013). Apart from mechanism of KEAP1 cysteine residues oxidation other regulations of NRF2-KEAP1 pathway were reported: proteins with higher affinity to the DLG motif recognized by KEAP1 on NRF2 are able to compete with KEAP1 to the binding to NRF2 (Chen et al. 2009) and the covalent modification of NRF2 by phosphorylation/dephosphorylation (Huang et al. 2002; Zheng Sun et al. 2009; Pi et al. 2007; Cullinan & Diehl 2004) and acetylation/deacetylation (Z. Sun et al. 2009; Kawai et al. 2011), that were mentioned briefly before and are responsible for the nuclear translocation/export, transcription activation, and degradation of NRF2 in response to induction signals.

## NRF2 in cancer

Activation of NRF2-KEAP1 pathway protects from various diseases and harmful intra- and extra- cellular agents, however chronic and constitutive upregulation of NRF2 activity was established to foster the progression of several types of cancer like breast, neck, lung, ovarian, and endometrial carcinomas (Lau et al. 2008; DeNicola et al. 2012; DeNicola et al. 2015; Mitsuishi et al. 2012; Q. Wang et al. 2013; Kim et al. 2010) In some cancer types the high expression of Nrf2 and its targets correlates with

poor prognosis of patients (Sasaki et al. 2013; DeNicola et al. 2015; Wang et al. 2008). Due to the oncogene activation in transformed cell environment, ROS and thus the oxidative stress levels are already high in non-induced conditions (Ogrunc et al. 2014). This situation leads to a chronic oxidative insult causing a constant NRF2 activation and nuclear presence of a substantial fraction of NRF2 protein even without additional exogenous oxidative stress (Chen et al. 2009). (Fig. 8) In cancer NRF2 can be activated by various mechanisms, to the most relevant belong: mutations in one of the genes comprising the NRF2-KEAP1-CUL3 inhibitory complex - both mutations of KEAP1 and CUL3 were reported to abrogate the degradation of NRF2 (Padmanabhan et al. 2006; Sjöblom et al. 2006; Ooi et al. 2013); mutations in NRF2 itself - although much less frequent than in KEAP1- are enhancing its activity mainly by blocking the proper and efficient binding to KEAP1 (Shibata et al. 2008; Singh et al. 2010); an epigenetic silencing of KEAP1 by the hypermethylation of its promoter (Muscarella et al. 2011), miRNA targeting KEAP1 (Eades et al. 2011) or NRF2 itself (Yamamoto et al. 2014); upregulation of proteins that can interfere with the interaction between NRF2 and KEAP1 such as p21 (Chen et al. 2009) that has stronger affinity to bind the DLG motif of NRF2 than KEAP1 (activation of NRF2) or p62/SQSTM (Komatsu et al. 2010) whose STGE motif in comparison to ETGE of NRF2 possess higher than affinity to bind KEAP1 (degradation of KEAP1); inhibition of Keap1 by metabolic intermediates such as fumarate (Ooi et al. 2011).

As reported by DeNicola and colleagues oncogenes can also upregulate the transcription of NRF2. In their study oncogenic alleles of KRAS ($KRAS^{G12D}$) BRAF ($BRAF^{V619E}$) and C-MYC ($C\text{-}MYC^{ERT12}$) increased the level of NRF2 mRNA as well as its canonical anti-oxidative genes (HO-1, NQO1) and upregulated levels of GSH/GSSG ratio resulting in an increase of cytoprotective activity in the cell and, most notably, a decrease in ROS levels thus creating more reduced intracellular redox environment for the survival of tumor cells. Interestingly the binding site for Jun and Myc was found in the TSS of the Nrf2 - it has been proposed that their action mediate the NRF2 oncogene dependent regulation (DeNicola et al. 2012)

NRF2 regulates the transcription of the most abundant antioxidant within all cells - glutathione (GSH). GSH is synthesized in a two-step process; the rate limiting

step driver by glutamate cysteine ligase (GCL), a heterodimer of catalytic (GCLC) and modifier (GCLM) subunits (Meister 1983). Recently the laboratory of Tak W. Mak reported that the synthesis of glutathione driven by GCLM is required for cancer initiation *in-vivo* and *in-vitro*. Genetic loss of *Gclm* prevents a tumor's ability to drive malignant transformation - they indicate that this process is likely to be NRF2 dependent. Combined downregulation of glutathione by buthionine sulfoximine (BSO) together with inhibition of other oxidative stress defense mechanism driven by thioredoxine (TXN) by auranofin (AUR) or sulfasalazine (SSA) efficiently leads to a synergistic cancer cell death *in vitro* and *in vivo*, demonstrating the importance of these two antioxidant pathways for tumor progression and as potential targets for clinical approach (Harris et al. 2015).

Mounting evidence associates NRF2 activity and cancer cells resistance to the therapies. NRF2 confers both intrinsic and acquired chemo- and radio- resistance abilities of cancer cells. High NRF2 activity and the resulting target gene expression confers cancer cell the protection against the oxidizing microenvironment in cancer cells makes them less sensitive to cytotoxic chemotherapeutic agents such as etoposide, doxorubicin, carboplatin, cisplatin and 5- fluorouracil through enhanced detoxification of anticancer agents and improved antioxidant capacity (Jaramillo & Zhang 2013; Hayes et al. 2010).

Recently chemoresistance to cisplatin and doxorubicin of MCF7 breast cancer cells and cancer stem cells derived from MCF7 were demonstrated to be fostered by the NRF2 and its upregulation of genes encoding for GSTA2, GSTP1, CYP3A4, HO-1, MRP1, and MRP5 (Kang et al. 2014; Syu et al. 2016). Cancer cells in which expression of NRF2 and its targets was high were more resistant also to the radiation induced toxicity and the ablation of NRF2 expression by siRNA in non-small cell lung cancer cell lines sensitized these cells to the ionizing radiation toxicity (Singh et al. 2010).

Apart from crucial role of NRF2 in regulating oxidative stress response by inducing genes like HMOX1 and NQO1 or genes involved in gluthatione/thioredoxine systems whose oncogenic potential has been a main subject of studies describing the dark side of NRF2 (Wang et al. 2008; DeNicola et al. 2012) some pathways regulated in NRF2 dependent manner also apart from the additional oxidative insult in cancer cells

were recently unraveled (Huang et al. 2015). This still under-addressed issue is a scope of an interesting study by Lacher and colleagues that focused their work on determining the most ancient NRF2 dependent pathway conserved from *D. melanogaster* to human beyond the oxidative stress response. The most conserved NRF2 mediated program is indicated to regulate genes associated with: lipid or glucose metabolism, proteasome degradation pathway, autophagy and genes encoding proteins involved in oxidation/reduction reactions – listed and indicated in Table1 (Lacher et al. 2015).

Recently Mitsushi and colleagues identified novel NRF2 target genes involved in the pentose phosphate pathway that are responsible for NADPH regeneration such as: G6PD, PGD, TKT and TALDO as well as other metabolic genes, including ME1, PPAT, MTHFD2, and IDH1. NRF2 bound directly ARE sequences in the promoters of G6PD, PGD, TKT, TALDO1, ME1 and IDH1 enhancing their expression and activity. These proteins participate in synthesis of purines which are necessary building blocks for DNA and RNA and are involved in acceleration of proliferation of cancer cells as well as they support the glucose flux (Mitsuishi et al. 2012).

Serine and glycine are biosynthetically linked, and together they provide essential precursors for synthesis of proteins, nucleic acids, and lipids that are crucial for cancer cell growth (Amelio et al. 2014; DeNicola & Cantley 2015). Recently DeNicola and co-workers by analyzing the metabolic tracing combined with transcriptional profiling reported that the regulation of the serine/glycine biosynthetic pathway in large panel of NSCLC cell lines is orchestrated by NRF2 through its control of the key serine/glycine biosynthesis enzymes as PHGDH PSAT1 and SHMT2 via ATF4 to support glutathione and nucleotide production (DeNicola et al. 2015). Interestingly the laboratory of Cantley developed also a peptide targeting the crucial enzyme (PHGDH) of the first steps of serine biosynthesis pathway that is able to efficiently block the activity of enzyme and specifically target NSCLC and TNBC cancer cells that survival depend on enhanced serine/glycine biosynthesis (Mullarky et al. 2016).

Oxidized and damaged proteins caused by high levels of ROS or oxidative stress inducing agents that accumulate in the cell are the reason for enhanced increased proteasomal activity and increased proteasome encoding genes transcription (Kwak et

al. 2003). Increased proteasome activity as mentioned before is an important feature of human cancers that allows to drive signaling pathways crucial for proliferation and survival (Crawford et al. 2011). NRF2 controls a battery of genes encoding for proteasomal subunits of both the 20S core and the 19S regulatory particle are targets direct targets of NRF2 (Jung & Grune 2013). Both 20S and 19S proteasome encoding genes possess ARE-like sequences in their promoters (Pickering et al. 2012). Despite that no TF is reported to possess exclusive master control over transcription of whole proteasome machinery encoding genes in mammals, its regulation by NRF2 is reported to be an ancient existing axis shared by human NRF2 and its homologues in *D. melanogaster* - *CncC* (Lacher et al. 2015) and *C. elegans* - *SKN-1* (Pickering et al. 2012). It is important to underline that the impact of the NRF2 on proteasome genes transcription and proteasome activity might strongly vary depending on the cellular context (Sporn et al. 2012) and some other transcription factors activities (like ex. NRF1/TCF11) might be involved in the regulation (Koch et al. 2011). Proteasome inhibitors used in therapy for treating multiple myeloma are shown to induce NRF2 activity thus engaging a compensatory mechanism of *de novo* synthesis of proteasomal subunit proteins called the *"bounce-back"* response. Enhanced NRF2 activity is considered to be one of the main issues responsible for failure of PI-based therapies in solid tumors (Rushworth et al. 2011) (Fig. 7).

To underline the complexity of NRF2-KEAP1 pathway it is interesting to mention a recent and conceptually provocative work of Zucker and colleagues showing that NRF2 – the master regulator of anti-oxidant response – induces ROS levels. When intracellular ROS levels cross a critical cellular threshold, NRF2 is not able to efficiently bind promoters of the canonical antioxidant genes and increase their expression, but, by inducing the expression of Klf9 transcription factor instead, causes further Klf9-dependent increase in ROS levels leading to induction of cell death (Zucker et al. 2014).

In sum, although recent studies started to unravel the roles of NRF2 in oncosuppression and tumorigenesis, the mechanism of action of this potent transcription factor in various cellular contexts requires further investigation.

# AIM OF THE THESIS

This thesis focuses on Triple-Negative Breast Cancers: model of an aggressive group of tumors of high mutation rate in TP53 loci. TNBC tumors are prone to recurrence, metastasis, become resistant to chemotherapy and currently they lack targeted therapies - therefore finding novel targets for possible treatment is necessary. The fact that the accumulation of mutant p53 proteins is observed in various tumors at high level and that TP53 is the most frequently mutated genes in cancer, creates a tempting opportunity to target it for more precise cancer therapy. Point mutations of TP53 have been established to contribute to carcinogenesis by: losing the tumor suppressor activities of the wild-type p53, exerting dominant negative effects over the wild type allele and providing the mutant p53 with novel oncogenic gain-of-function (GOF) properties. Common GOF program shared by many mutant p53 variants has not been defined. However, current approaches are only starting to resolve whether missense p53 mutants can be regarded as one oncoprotein with a conserved tumorigenic activity, or if they represent a population of different oncoproteins, each exerting its unique program. This renders it difficult to propose a universal therapeutic approach tailored to the presence of mutant p53 in standard clinical practice.

Aims of this work are: 1) determining the common GOF program of various p53 mutant proteins; 2) understanding the molecular mechanism behind the regulation of this program; 3) proposal of a therapy tailored for GOF p53 mutant variants presence and their shared oncogenic activities.

# RESULTS

## Proteasome pathway is a common transcriptional target of various p53 missense mutants in TNBC cells

In order to gain novel insights into the oncogenic gain-of-function of mutant p53 in cancer cells, we utilized a combination of large-scale approaches in the MDA-MB-231 cells (Fig. 9a, c) – a well-established TNBC cellular model, whose transformed phenotype relies on the high level of a R280K mutant variant of p53 (Girardini et al. 2011). RNA-sequencing coupled to whole cell lysate proteomic analysis and chromatin immunoprecipitation sequencing (ChIP-sequencing) allowed us to understand to what extent mutant p53 dependent changes in the levels of proteins match the transcriptional control exerted by mutant p53. As shown in Fig. 9a, we observed upon silencing of mutant *TP53* that 56% of the significantly up- and down-regulated proteins identified by a differential whole cell proteome analysis (p-value≤0.05) match their corresponding transcripts, identified by RNA-sequencing (Benjamini-Hochberg adjusted p-value≤0.05). In parallel (Fig. 9a), upon silencing of mutant *TP53*, we observed significant changes in the levels of transcripts (B-H adjusted p-value≤0.05) for the 59% of corresponding transcription start sites that were identified by mutant p53 in ChIP-sequencing analysis (FDR≤0.05, +/- 500 bp from adjacent TSSes). These results suggested that in MDA-MB-231 cells the majority of the observed mutant p53-dependent protein changes are related to its transcriptional activity and that a binding of mutant p53 to the majority of gene promoters in the proximity of TSSes results in a significant modulation of transcription at the corresponding loci. Overlapping the lists of transcripts matched to the corresponding proteins and transcripts matched to the mutant p53-bound TSS regions, we obtained a 72-gene signature (Venn diagram in Fig. 9a) linked to the presence of mutant p53 in the MDA-MB-231 cells ("integrated signature"). Pathway/GO-term enrichment analysis (independently – by Ingenuity Pathway Analysis and Cytoscape-ClueGO software) of the integrated signature suggested the proteasome-ubiquitination pathway to be the most affected process (Fig. 9a).

Having demonstrated that the transcriptional activity is pivotal to the R280K mutant p53 GOF in MDA-MB-231 cell line, we decided to focus our attention on mutant p53-regulated transcriptomes to investigate whether the GOF program is shared among other p53 missense mutants and conserved in different cellular contexts. The MDA-MB-231 transcriptome was compared with mutant p53 mRNA profiles obtained from 4 other TNBC cell lines (all at B-H adjusted p-value≤0.05 cutoff) carrying diverse missense mutations of *TP53,* upon mutant *TP53* silencing (Fig. 9b, c). The p53 variants in these cell lines differ in their biophysical properties – two contact and three conformational p53 mutant variants (Bullock & Fersht 2001). The analysis allowed us to distinguish between mutant-specific and common mRNA signatures associated with the presence of the missense p53 mutants. Applying the -/+ 0.4 logarithmic fold change (LFC) cutoff to the shared mutant p53 transcriptional program, we obtained a 205-gene common signature (Fig. 9b, c). Strikingly, the common signature, just like the integrated signature obtained from MDA-MB-231 cells, was most significantly enriched with genes belonging to the proteasome-ubiquitination pathway (Fig. 9b). Notably, among the extensive number of wt p53 targets identified in recent transcriptomic/ChIP-seq studies carried out in various cell models there are no proteasome-ubiquitination pathway genes shared with the integrated or common mutant p53 signatures shown in Fig. 9 (Allen et al. 2014; Tonelli et al. 2015)

Both integrated and common mutant p53 signatures contain multiple 26S proteasome and immunoproteasome subunit genes which partially overlap in the two signatures and are overrepresented in the top enriched pathways , all but three 26S proteasome subunit mRNAs were on average downregulated upon silencing the mutant *TP53*. To clarify and validate this data, we have quantified the mRNA levels for all the 37 proteasome subunit genes expressed in humans by qPCR in the 5 TNBC cell lines of interest. In all the cell lines, transcription of the genes encoding all the components of a 20S proteasome core, a 19S regulatory cap and 3 subunits of the immunoproteasome was downregulated upon the mutant *TP53* knockdown (Fig. 9d), accompanied by a downregulation of the corresponding proteins (Fig. 16a). Several other candidate mutant p53 target genes related to the proteasome-ubiquitination pathway, such as the PSME1/2 (Pa28αβ) proteasome regulatory subunits, did not pass this validation step.

Silencing-rescue experiments in MDA-MB-231 cells demonstrated that the 5 different full-length mutant p53 variants derived from the panel of TNBC cell lines of interest are interchangeable with respect to their ability to upregulate the expression of 10 tested proteasome genes that represent all the proteasome components (Fig. 16b). This evidence further confirms that proteasome machinery encoding genes are targets shared by different p53 missense mutants within a common transcriptional program.

## The proteasome expression signature is strongly associated with poor prognosis and mutant status of TP53 in cancer patients

We next explored the association between the expression levels of the identified mutant p53-related gene sets, the prognosis in cancer patients' datasets or the presence of mutant *TP53* in clinical samples.

The mutant p53 common signature, derived from the panel of TNBC cell lines, showed more significant association with a poor prognosis in breast cancer than any mutant p53 signature derived from the 5 TNBC cell lines individually (Fig. 10a; for each signature we selected the top 30 upregulated and the top 30 downregulated genes) This result suggests that in breast cancer the most significantly oncogenic GOF transcriptional program is shared between different mutants and cell backgrounds rather than associated with the individual mutant p53 variants in their cellular contexts. Having shown that the GOF p53 mutants activate all the subunits of the 26S proteasome and immunoproteasome in the 5 TNBC cell lines (Fig. 9d) we tested the association between the “whole proteasome” 37-gene signature and the prognosis of breast cancer patients. Strikingly, high expression level of the whole proteasome 37-gene signature was able to more effectively discriminate a poor outcome of the patients than the mutant p53 common signature or any other signature derived from the individual TNBC cell lines (Fig. 10a).

Since all the 37 proteasome genes are upregulated by mutant p53 (Fig. 9d), we decided to test the association between the mutational status of *TP53* and this signature in breast cancer. As a control, we also analyzed an equal number of upregulated genes in common and cell line-specific signatures. The association of the signature expression level with wt/mutant status of *TP53* (*TP53*-null status was excluded) is represented in

Fig. 10b by box plots with Mann–Whitney U test p-values and indicated differences between means. We used the Pearson's Chi-squared ($\chi^2$) test with Yate's continuity correction (shown as test values for degrees of freedom=1 and supporting p-values) to verify whether the mutant status of *TP53* and the expression of the signatures are independent (Fig. 10b). Also in this case, the high expression of the 37-gene whole proteasome signature was most strongly associated with the *TP53* mutations and had the highest Chi-squared test value as well as the lowest p-value, allowing us to reject the null hypothesis that the mutant *TP53* status and the high proteasome expression are independent (Fig. 10b). This observation supported the significance of the proteasome-related GOF program shared by the studied p53 mutants regardless of the cell backgrounds.

## Mutant p53 proteins increase the activity of the proteasome machinery in in vitro and in vivo cancer models

In line with the expression data, depletion of mutant p53 in the TNBC cell lines, but not of wild-type p53 in MCF7 breast cancer cells, nor in non-transformed breast epithelium MCF10A cells, resulted in a significant decrease of the proteasome rate-limiting Chymotrypsin-like (Fig. 11a) and Trypsin-like activities (Fig. 16c). As a positive control of the proteasome downregulation we used a silencing of the essential proteasome 20S core subunit gene *PSMA2* – strongly downregulated transcriptionally and on a protein level upon mutant *TP53* silencing (Fig. 9d, Fig. 16a) - and two clinically approved proteasome inhibitors – Bortezomib and Carfilzomib.

In frozen primary tumor samples obtained from 15 basal-like breast cancer patients (including 10 TNBCs), the presence of the elevated proteasome activity correlated with the presence of p53 missense mutants determined by *TP53* mRNA sequencing and immunohistochemical staining (Fig. 11b, Fig.16d).

Expression of each of the *TP53* mutant variants, characterizing the 5 TNBC cell lines in MCF10A cells with depleted endogenous wt p53, caused a significant increase of the proteasome activity and protein levels of selected proteasome subunits (Fig. 11c, Fig. 16e). This effect was accompanied by an increased transcription of proteasome subunit genes (Fig. 16f). The result indicates that the activation of the proteasome is an

inherent process linked to the expression of the various *TP53* mutants in a non-transformed background. Although the basal proteasome activity is lower in MCF10A than in TNBC cells, the introduction of the p53 mutants caused it to increase to levels that are comparable to the TNBC cell lines (Fig. 11c *vs* Fig. 16g).

Importantly, we observed a significant decrease in the proteasome activity and in the proteasome subunits transcription upon mutant *TP53* silencing in other cancer-derived cell lines - of hepatic, ovarian, pancreatic, prostatic and colonic origin – carrying various GOF p53 mutants (Fig. 11d, Fig. 16h). Therefore, the dependence of high proteasome expression and activity on mutant p53 is an inherent trait of cancer cells with p53 mutants.

In line with the above observations, proteasome activity was significantly increased in thymic lymphomas and lymphoma-infiltrated enlarged livers derived from mutant *TP53* knock-in mice (expressing p53 variant R172H), as compared with *TP53* knock-out and normal thymi or livers in control mice (Fig. 11e). These organs were chosen for comparative analysis in mouse models since their transformation-related changes are pathologically comparable in both mutant *TP53* R172H KI and *TP53* KO mice (Lang et al. 2004). However, despite these similarities, the strongly elevated proteasome activity was characteristic only of the mutant *TP53* KI genotype. Also in mouse embryo fibroblasts (MEFs) derived from the same mice as above the elevated proteasome activity correlated with the mutant *TP53* KI status and the effect was enhanced by an overexpression of the oncogenic *RAS* V12 variant (Fig. 13f).

Altogether, this *in vitro* and *in vivo* evidence strongly supports the dependence of proteasome activity on the presence of the p53 mutants in different cancer types, and suggests that the proteasome activation by different p53 missense mutants may be further increased in an oncogenic context.

## NRF2 transcription factor cooperates with GOF p53 mutants in binding the 26S proteasome subunit gene promoters

In order to investigate molecular mechanisms underlying the proteasome transcriptional regulation by the p53 mutants in cancer, we analyzed the ChIP-

sequencing data obtained from the MDA-MB-231 cell line (Fig. 9a). We defined candidate mutant p53-binding regions within promoters of 10 genes encoding proteasome subunits, selected to represent all proteasome functional parts which we have previously validated at the transcriptional level (Fig. 9d) and p53 ChIP-seq peaks of both weak and strong intensity. Irrespective of the ChIP-seq peak size, we confirmed a strong binding of mutant p53 to all these regions in the panel of 5 TNBC cell lines of interest, while regions mapping outside the ChIP-seq peaks in each gene locus showed no evidence of mutant p53 binding (Fig. 12a).

We next performed a bioinformatics analysis to identify consensus sequences significantly enriched in the mutant p53 bound regions in all 37 proteasome genes. We found that the most frequently represented sequence motifs match the binding sites of known transcription factors, with no indication of the wt p53 consensus binding site. These included motifs for NRF1 (NFE2L1, TCF11), NRF2 (NFE2L2), STAT3, NF-YA, NF-κB (Fig. 12b) that have been previously reported to control basal transcription of 26S proteasome and immunoproteasome genes (Steffen et al. 2010; Xu et al. 2012; Vangala et al. 2014; Moschonas et al. 2008; Höhn & Grune 2014), the latter two having been reported to directly cooperate with mutant p53 (Di Agostino et al. 2006; Weisz et al. 2007) (Fig. 12b). We silenced the expression of these factors in MDA-MB-231 cells to investigate their impact on the activity and transcription of the 26S proteasome (Fig. 12c). We selected *PSMA2* and *PSMC1* as the 26S proteasome machinery representative genes for further studies, as these genes were the most downregulated on average in the transcriptomic analysis and qPCR validation in the TNBC cell line panel (Fig. 9d) and were positively validated in all expression and ChIP experiments (Fig. 12a). Silencing of either *NRF1* or *NRF2* resulted in downregulation of both *PSMA2* and *PSMC1* transcription and proteasome activity to the levels comparable to the mutant *TP53* silencing. Conversely, silencing of *STAT3*, *NFYA* or *NFKB1* had a substantially weaker effect (Fig. 12c, for protein levels control see - Fig. 17b). Double knockdown experiments suggested that the effect of NRF1 is additive and as such independent of mutant p53 while the activities of NRF2 and mutant p53 are not additive and possibly interdependent (Fig. 12d; for an alternative *NRF2* siRNA see Fig. 17c).

Indeed, ChIP analysis confirmed that the recruitment of mutant p53 to *PSMA2* and *PSMC1* gene promoters relies on the presence of NRF2 but not NRF1, while NRF2 binding weakly depends on mutant p53 (Fig. 12e). In MDA-MB-231 cells, mutant p53 and NRF2 increase the recruitment of the acetyltransferase p300 at *PSMA2* and *PSMC1* promoters more strongly than NRF1 and induce the p300-dependent acetylation of Histone 3 K9 at these loci (Fig. 12f-g) – a marker of transcriptionally active chromatin (Drost et al. 2010). Conversely, wt p53 does not bind to the proteasome gene promoters in MCF7 cells (Fig. 17d).

These data indicate that mutant p53 is specifically recruited to the proteasome gene promoters by NRF2. Together with the fact that the silencing of *NRF2* in MDA-MB-231 cells significantly downregulated transcription of most subunits of the whole proteasome machinery (Fig. 17e) our results suggested that the transcriptional control of mutant p53 over proteasome subunit genes is dependent on NRF2.

## NRF2 interacts with p53 mutants but not with wild-type p53 and is required for the mutant p53-mediated transactivation of the proteasome genes

To deepen our understanding of the interplay between p53 mutants and NRF2 in regulating proteasome gene transcription, we evaluated their ability to interact. Co-immunoprecipitation experiments revealed that the endogenous NRF2 protein interacts with the p53 missense mutants in all tested TNBC cells but not with endogenous wild-type p53 in MCF7 and MCF10A cells (Fig. 13a). This interaction pattern was confirmed by a reversed co-IP with anti-NRF2 IgGs (Fig. 18a). In contrast, STAT3 and NF-YA interacted with the p53 mutants only in two TNBC cell lines, while neither NRF1 nor NF-κB (p65) interacted with any of the mutants characterizing the different TNBC cell lines (Fig. 13a). Thus, among the different transcription factors regulating the proteasome genes, only NRF2 was able to specifically and consistently bind all the GOF p53 mutants in their endogenous cellular backgrounds. Interestingly, upon treatment of MDA-MB-231 cells with PRIMA-1, a drug that binds and converts mutant p53 into a wild-type-like, active protein by covalently modifying its thiol residues (Lambert et al. 2009), we did not detect the p53-NRF2 interaction (Fig. 13b).

In normal, unstressed cells NRF2 is predominantly localized in the cytoplasm. Following an exposure to oxidative stimuli – such as a sodium arsenite treatment – NRF2 translocates to the nucleus and activates transcription of oxidative stress response genes (e.g. *HO-1/HMOX1*) and the proteasome (Fig. 18g-h) (Koch et al. 2011). As mentioned earlier in the introduction in cancer cells, likely due to the increased accumulation of reactive oxygen species (ROS) caused by oncogene activation, a substantial fraction of NRF2 is localized in the nucleus even without the exogenous oxidative stress (Fig. 18h-i) (Chen et al. 2009). We confirmed that in the MDA-MB-231 cell line NRF2 co-localizes in the nucleus with mutant p53, with or without the sodium arsenite-induced oxidative stress (Fig. 18e, h), and that the interaction of both proteins occurs in the nuclear fraction of these cells (Fig. 18f). Furthermore *NRF2* or *TP53* silencing reduces the mRNA levels of the proteasome genes in both control and oxidative stress conditions, while *TP53* silencing has an opposite effect on the expression of the oxidative stress response gene *HO-1*, as described earlier (Fig. 18g) (Kalo et al. 2012).

In the non-transformed MCF10A cell line, we did not detect the interaction between wt p53 and NRF2 in control conditions nor in the presence of high levels of wt p53 stabilized after Nutlin treatment. However, the presence of comparable levels of the stably overexpressed mutant p53 variants (R280K or R175H) in MCF10A resulted in a detectable mutant p53-NRF2 interaction (Fig. 13c; for co-localization see Fig. 18i). Consistently, expression of *PSMA2* and *PSMC1* genes was significantly downregulated by the *NRF2* or *TP53* silencing only in the presence of ectopically expressed mutant p53 variants which were upregulating the basal level of the proteasome gene transcripts (Fig. 13d). This result clearly indicates that the upregulation of the proteasome genes transcription by the p53 missense mutants requires the presence of NRF2.

We found the same regulation pattern in a p53-null background of H1299 lung carcinoma cells upon *TP53* overexpression. In this context the p53 mutants interacted with NRF2 more strongly than wt p53 in co-immunoprecipitation experiments (Fig. 18b), while the proteasome gene expression was significantly blunted by either *TP53* or *NRF2* silencing only in the presence of mutant p53 (Fig. 18d).

As a next step, we mapped the interaction domain of mutant p53 with NRF2 by *in vitro* binding assays using truncated versions of GST-tagged p53. GST-pull down experiments with NRF2 overexpressed in H1299 cells clearly showed that the interaction of both R175H and R280K p53 mutants with NRF2 is mediated by the DNA-binding domain (DBD) of these variants (Fig. 18c).

These data indicate that the ability of the p53 missense mutants to interact with NRF2 is mediated by the DNA-binding domain of p53, is conserved in all the tested mutant variants and cellular environments, and NRF2 presence is required for the mutant p53-dependent stimulation of the proteasome transcription.

## Targeting GOF p53 mutants with APR-246/PRIMA-1MET abrogates chemoresistance of TNBC cells to the proteasome inhibitor Carfilzomib

The observation that the concomitant silencing of mutant p53 and PSMA2 synergistically reduce viability of MDA-MB-231 (Fig. 19i) prompted us to investigate whether this effect could be significant in an *in vivo* tumor growth and metastasis model. Preliminarily we used in combination with Carfilzomib, two clinically-tested molecules known to inhibit mutant p53's oncogenic activity - a histone deacetylase inhibitor SAHA (Vorinostat) which downregulates mutant p53 level (Li et al. 2011) and PRIMA-1 which converts GOF p53 mutants into a wt-like proteins (Lambert et al. 2009; Bykov et al. 2016) and abolishes the mutant p53-NRF2 interaction as shown earlier in this study (Fig. 14b).

The combination of Carfilzomib and mutant p53-targeting drugs (PRIMA-1 or SAHA) acted synergistically to reduce cell viability and proteasome activity in the panel of 5 TNBC cell lines of interest, but not in MCF7 and MCF10A wild-type p53 cell lines (Fig. 19a-b). Both SAHA and PRIMA-1 cooperated with Carfilzomib in increasing the level of tumor suppressor KSRP and wt p53 targets (NOXA, PUMA and p21) (Fig. 19c). We therefore tested the activity of SAHA and PRIMA-1, individually or in combination with Carfilzomib, in an *in vivo* xenograft model of MDA-MB-231 cells injected into a mammary fat pad of immunocompromised SCID mice (Rustighi et al. 2009). After 4 weeks of treatment, the combination including PRIMA-1 was more

effective than the combination with SAHA in reducing the primary tumor growth (Fig. 19d).

Having selected PRIMA-1 as the more effective drug *in vivo,* we introduced its phase I/II clinically-tested derivative APR-246 (PRIMA-1MET) into further studies (Lehmann et al. 2012). APR-246, just like PRIMA-1, showed an inhibitory effect on the proteasome activity and induced the wt p53 targets in MDA-MB-231 cells (Fig. 19b-c). APR-246 was able to eradicate Carfilzomib-resistant clones in colony formation assays in MDA-MB-231 cells (Fig. 14a). In contrast, neither of the drugs (Carfilzomib or APR-246) was able to significantly increase the effect of other chemotherapeutic drugs such as Doxorubicin (Adriamycin), Cisplatin or Paclitaxel (Taxol) - used in sub-lethal concentrations, to allow emergence of resistant colonies (Fig. 19e).

Of note, ectopic expression of 5 GOF p53 mutants into an isogenic background of MCF10A cells with silenced endogenous wt *TP53,* significantly increased the resistance of cells to Carfilzomib but also increased sensitivity to the Carfilzomib/APR-246 combination (Fig. 19f).

In response to treatment with proteasome inhibitors, cells engage recovery mechanisms which up-regulate proteasome genes transcription through the action of NRF1 and NRF2. This effect is called a "bounce-back response" and leads to resistance to treatment (Arlt et al. 2012; Radhakrishnan et al. 2010). Based on our findings it is conceivable that, on a molecular level, the silencing of the GOF *TP53* mutants or *NRF2*, as well as the treatment with APR-246, could abrogate the bounce-back effect. To evaluate this we treated the 5 TNBC cell lines with Carfilzomib and observed a bounce-back increase of *PSMA2* and *PSMC1* gene expression that was abolished upon *NRF2*, mutant *TP53* silencing or by the APR-246 treatment (Fig. 14b and Fig. 19g). In cell lines harboring wt p53, such as MCF7 and MCF10A, the bounce-back response was less pronounced and, importantly, silencing of *TP53* or *NRF2* did not cause a strong effect (Fig. 19g). Of note, ectopic expression of the GOF p53 mutant R280K in MCF10A cells (with stably silenced endogenous wt *TP53*) caused the appearance of the bounce-back response during Carfilzomib treatment that was blunted by silencing of mutant *TP53* or *NRF2* or by treatment with APR-246 (Fig. 19g).

*In vivo*, the combination of Carfilzomib and APR-246 was more effective than any single drug treatment in reducing the primary tumor growth of the mammary fat pad xenografts of MDA-MB-231 with stably introduced luciferase gene (on average less than 50% tumor size of the DMSO treated control mice – (Fig. 14c-d, Fig. 19h), while the same drug combination had no effect on ER+ primary tumors of wt p53 MCF7 xenografts (Fig. 14e). Importantly, the Carfilzomib and APR-246 combination efficiently eradicated lymph-node and lung metastasis derived from the MDA-MB-231 xenograft (over 90% reduction on average in lymph node luciferase activity; the metastasis analysis was performed when the treated primary tumors reached sizes comparable to the control tumors (Fig. 19f-g;).

Analysis of the MDA-MB-231 primary tumor biopsies indicated that the Carfilzomib-induced "bounce-back" transcription of the proteasome genes, as well as the in-tumor proteasome activity, were both significantly blunted in mice treated with APR-246 (Fig. 14h-i), matching the *in vitro* results. No adverse effects associated with the APR-246 and Carfilzomib combined treatments were observed during the *in vivo* experiments.

In summary, only the combined drug-mediated inhibition of mutant p53 and the proteasome was able to effectively recover the tumor suppressive downstream targets of the mutant p53-proteasome axis, as well as to block proliferation and metastatic dissemination of the TNBC cells *in vivo* (Fig. 15).

# DISCUSSION

In this thesis I provide the evidence of a connection between the gain-of-function (GOF) p53 mutants and NRF2 mediated upregulation of proteasome that blunt the tumor-suppressive potential of cancer cell.

The proteasome machinery is a conserved representation of the mutant p53 transcriptional GOF. We thoroughly investigated this property in TNBC, also providing the evidence for a variety of other tumor types harboring *TP53* missense mutations: hepatic, ovarian, pancreatic, prostatic, colonic and a p53 KO/KI mouse lymphoma model. Interestingly, several previous studies reported regulation of the proteasome subunits by mutant p53, without investigating its relevance. In a mouse model of pancreatic cancer, two immunoproteasome subunits have been described among the main mutant p53 transcriptional targets (Weissmueller et al. 2014). Several 26S proteasome subunits were found in the mutant p53-regulated proteome in MDA-MB-468 TNBC cell line (Polotskaia et al. 2015). In mutant p53 ChIP-sequencing studies, the promoters of multiple proteasome subunit genes were reported to be bound by mutant p53 variants (Martynova et al. 2012; Do et al. 2012). These studies, however, did not compare high-throughput data from multiple models, and hence did not define which targets are shared between various p53 mutants and cell backgrounds. Our multi-omic and multi-model analyses led to identification of the proteasome subunits as the most overrepresented group of proteins whose upregulation is associated with the presence of several p53 missense mutant variants. Hence, at least the GOF p53 mutants which we have analyzed can be regarded as a uniform, potent oncogene with shared downstream transcriptional targets - a notion supported by a recent study on shared properties of DNA-interactomes of 3 mutant p53 variants (Zhu et al. 2015). We show here that the broad influence of mutant p53 on the protein content of a cancer cell extends beyond the control of chromatin and transcription, to the level of proteasome-mediated protein content regulation. Of note, although not observed in the TNBC cell line transcriptomes described here, a mutant p53 control over the transcription of the proteasome activator REGγ (*PSME3*) reported earlier (Ali et al. 2013), may contribute to the overall oncogenic effects of the mutant p53-proteasome axis under different conditions. According to our observations in the wt p53 cell lines MCF10A and MCF7, it is

reasonable to assume that the p53 dependent activation of 26S proteasome is a specific property of cells carrying *TP53* missense mutations. Supporting this notion, multiple large scale studies (Allen et al. 2014; Tonelli et al. 2015; Younger et al. 2015) did not detect proteasome genes among the identified wt p53 targets.

Secondly, among the GOF effects the p53 mutants exert through a formation of protein-protein complexes, the mutant p53 influence on the transcription factor NRF2 may play a key role. NRF2, whose both pro- and antitumorigenic activities are currently getting an increasing experimental support (Sporn et al. 2012), is a master regulator of the oxidative stress response, known to cooperate with multiple oncogenes (DeNicola et al. 2012). Mutant p53 has been previously shown to attenuate the expression of the oxidative stress-induced genes controlled by NRF2, such as *HO-1*, although no direct mutant p53-NRF2 interaction has been investigated (Kalo et al. 2012). Conversely, we show here that the proteasome genes are transactivated by NRF2 and mutant p53. The effect involves an interaction between the two proteins and is retained under the oxidative stress when *HO-1* is indeed repressed by mutant p53 (Fig. 18g). This evidence suggests that in cancer cells NRF2 has two modes of regulation of its target promoters, possibly orchestrated by mutant p53: one towards the proteasome genes house-kept in cancer cells by NRF2, and another towards the NRF2-induced canonical oxidative stress response genes. These two modes of NRF2 activity deserve further investigation, as they may help to better understand the dual role of NRF2 as the context-dependent oncoprotein or oncosuppressor (Jaramillo & Zhang 2013).

Moreover, mutant p53, when present, is responsible for the resistance of TNBC cells to proteasome inhibitors. As the resistance to proteasome inhibitors is a major issue in cancer treatment clinical practice, combinational therapies are being widely tested (Huang et al. 2014). In our *in vitro* and *in vivo* experimental setups PRIMA-1 and APR-246, turned out to be efficient and well tolerated in combination with Carfilzomib. APR-246 effectively decreased the Carfilzomib-induced bounce-back response of proteasome expression recovery, reduced primary tumor growth and eradicated metastasis in mutant p53 TNBC xenografts, while having no effect on primary tumor growth in wt p53 xenografts. The mutant p53-related proteasome activation may therefore at least partially explain the resistance to proteasome inhibitors observed in

clinical trials involving TNBC (Schmid et al. 2008; Irvin et al. 2010), despite the fact that the proteasome has been reported as a vulnerability in this tumor type (Petrocca et al. 2013).

The treatment strategy suggested by our data may also overcome the limitations of therapies which target only mutant p53 in solid tumors (Bykov et al. 2016; Girardini et al. 2014). The promising efficiency of simultaneous targeting of the p53 missense mutants and their major downstream pathways, such as the proteasome machinery, has not been previously shown *in vivo*.

In summary, our study defines a common mutant p53 gain-of-function transcriptional program and links it to proteasome machinery activation. Our findings explain how the transcriptional activity of mutant p53 and its consequent effects on the protein degradation machinery co-shape the protein landscape of cancer cells. The simultaneous targeting of both mechanisms by APR-246 and Carfilzomib (Fig. 15) provides a solution to overcome chemoresistance to proteasome inhibition in solid tumors harboring mutant p53.

# FUTURE PERSPECTIVES

Interplay between GOF p53 mutant variants and NRF2 reported in this thesis establishes a ground for interesting questions to be investigated in the future.

The double mode of NRF2 action in cancer cell – one exerted upon the oxidative stress stimuli and one kept by NRF2 in the basal condition without an oxidative insult allows hypothesizing that mutant p53 can be playing the role of a molecular switch between these two activities. Unraveling the mechanism behind NRF2 action towards the proteasome subunits encoding (basal oncogenic program) and anti-oxidative genes (induced oncogenic program) in cancer cells and cancer cells bearing GOF p53 mutant variants specifically, would allow to use it as a possible molecular target for a targeted therapy.

Since most of the high-throughput studies that aim at unraveling the possible novel targets of NRF2 are conducted upon NRF2 induction, the oncogenic program kept by NRF2 at basal level is significantly less known. For example, unlike in case of canonical oxidative stress response genes the regulation of the proteasome by NRF2 is not ubiquitously reported in all large scale datasets (Hirotsu et al. 2012; Chorley et al. 2012; Malhotra et al. 2010). This might be explained due to the fact that some of NRF2 activities are strongly dependent on the cellular and tissue context and thus the choice of the experimental model in mentioned studies might have a significant impact on the observed NRF2 regulated program (Sporn et al. 2012). A thorough, broad large-scale analysis focused on defining the NRF2 dependent program kept on basal and induced level in various cancer cell models would be necessary for proper understanding of oncogenic role of this potent transcription factor.

More pronounced nuclear localization of NRF2 (Fig. 18i) upon introduction of GOF p53 mutant into the normal cell background of MCF10A previously silenced for wild-type p53 variant, might suggest that biochemical properties of the GOF p53 mutant proteins, directly or indirectly regulate process of the translocation of NRF2 to the nucleus. This fact could explain the transcriptional activities of NRF2 towards proteasome gene promoters even without additional oxidative insult.

Since NRF2 transcriptional activities and nuclear localization are dependent on PTM events like phosphorylation/acetylation (Kawai et al. 2011; Pi et al. 2007), it would be interesting to investigate if GOF p53 mutant variants are involved in this type of NRF2 regulation. Further studies should determine if GOF p53 mutant proteins have an impact on phosphorylation/acetylation of NRF2 and if these PTM events have a functional effect on the transcription of particular set of NRF2 targets in cancer cells, thus explaining the dual mode of NRF2 action.

NRF2 exerts its transcriptional activities on the canonical oxidative stress response genes through heterodimerization with other transcription factors at the gene promoters (ex. small Maf proteins) (Hirotsu et al. 2012). Recent studies indicate novel transcriptional cofactors to interplay with NRF2 on gene promoters, like the ATF4 transcription factor that fosters aberrant transcriptional activities of NRF2 in cancer cells (Zucker et al. 2014; Ye et al. 2014). Thus it should be investigated further if mutant p53 requires other cofactors to induce the transcription of specific NRF2 target genes.

In mutant p53 bearing cancer cells the "bounce-back" chemoresistance response to proteasome inhibitors is mediated by NRF2 (Figure 14 a, b). Thus it is conceivable that NRF2 itself could be an interesting target of a therapeutic approach. Future studies should determine if the combination of NRF2 targeting drugs (Brusatol (Ren et al. 2011) or ATRA (Tan et al. 2008)) with proteasome inhibitors (Carfilzomib) could be an alternative therapeutic target for the resistant tumor cells.

In summary: understanding of the mechanisms of NRF2 dual action together with determining novel, specific programs that NRF2 engages in various tumors in both basal and induced conditions might give a reasoning of developing the therapies targeting specifically these tumors that rely on mutant p53 hijacking the broad activities of NRF2.

# EXPERIMENTAL PROCEDURES

**Cell lines**

Human cell lines MDA-MB-231 (p53 R280K), MDA-MB-468 (p53 R273H), HCC-1395 (p53 R175H), PANC-1 (p53 R273H), HT-29 (p53 R273H), 293GP (p53 wt) and Mouse Embryonic Fibroblasts (MEF – for p53 status see below) were cultured in DMEM medium (Sigma) supplemented with 10% FCS (ECS0180L, Euroclone), and antibiotics (DE17-602E, Lonza). BT-549 (p53 R249S), DU145 (heterozygous p53 - P223L/V274F), H1299 (p53-null) and TOV112 (p53 R175H) cells were cultured in RPMI medium (Sigma) supplemented with 10% FBS and antibiotics. SUM-149 (p53 M237I) cells were cultured in DMEM:F12 Ham's medium 1:1, supplemented with 10% FCS and antibiotics. MCF7 (p53 wt) were cultured in EMEM (Sigma), supplemented with 1% non-essential aminoacid solution (Sigma), 10% FBS and antibiotics. Malhavu cells (p53 R249S) were grown as MCF7, with addition of 2mM L-Glutamine. MCF10A (p53 wt, sh p53 and stable mutant p53 overexpressing cell lines) cells were maintained in DMEM:F12 Ham's medium 1:1, supplemented with 5% horse serum, insulin (10 μg/ml), hydrocortisone (0.5 μg/ml) and epidermal growth factor (EGF 20 ng/ml), if needed - with addition of selection antibiotics. All human cell lines were subjected to STR genotyping with PowerPlex 18D System and confirmed in their identity comparing the results to reference cell databases (DMSZ, ATCC, and JCRB databases). Mutant p53 cell lines have been confirmed to possess indicated mutant p53 variants by sequencing of the full-length p53 mRNA. MEFs were generated by crossing mice of the appropriate genotype, and collecting cells from 13.5 d.p.c. embryos. MEF KO p53 and MEF KI p53R172H were optionally immortalized through retroviral transduction of H-Ras V12 as described

All the cell lines have been tested by PCR/IF for the Mycoplasma presenceAll human cell lines were subjected to STR genotyping with PowerPlex 18D System and confirmed in their identity comparing the results to reference cell databases (DMSZ, ATCC, and JCRB databases). Mutant p53 cell lines were confirmed to possess the indicated mutant p53 variants by sequencing of the full-length p53 mRNA extracted from these cells.

**Western blot analysis**

Total cell extracts were prepared in RIPA buffer without SDS (150mM NaCl, 50mM Tris-HCl pH8, 1mM EDTA, 1% NP-40, 0.5% Na-deoxycholate) supplemented with 1 mM PMSF, 5 mM NaF, 1 mM Na3VO4, 10µg/ml CLAP protease inhibitor cocktail (SIGMA). Protein concentration was determined with Bio-Rad Protein Assay Reagent (Bio-Rad). Lysates were resolved by SDS/PAGE and transferred to nitrocellulose (Millipore). Western blot analysis was performed according to standard procedures using primary antibodies listed in. Western blots experiments were normally performed in at least 3 biological replicates, the representative is shown.

**Proteasome activity assay**

The assay was performed on the basis of the 20S Proteasome Activity Assay Kit (Chemicon-Millipore), using proteasome substrates: Substrate III (Suc-LLVY-AMC, chymotrypsin like activity), Substrate IV (Z-ARR-AMC, trypsin-like activity). 50 µg of protein lysates were incubated with the substrates at 37°C for 2h and measured at wavelengths of 380 nm excitation and 460 nm emission (3 biological replicates, for each means from 3 technical replicates were used).

**Protein stability determination**

Cells 24h with DMSO or Carfilzomib or 48h post indicated siRNA transfection were treated with 0.1mg/ml Cycloheximide (CHX; Sigma) and lysed in SDS-PAGE loading buffer directly on plates on the indicated time points. Lysates were subjected to western blots and the results were scanned and analyzed densitometricaly by the ImageJ software. The results were plotted in Excel and protein half-lives determined according to the fitted exponential decay curves' equations.

**Protein interaction studies**

Coimmunoprecipitation experiments with endogenous proteins were performed by lysing cells in the Co-IP buffer (NaCl 150mM, Tris-HCl pH8 50mM, EDTA 1mM, NP40 0.5%, glycerol 10%) with protease inhibitors. Samples were cleared by centrifugation for 30 min at 13000g at 4°C and incubated overnight at 4°C with the specific antibody. After 1h incubation with protein G-Sepharose (GE Healthcare),

immunoprecipitates were washed three times in Co-IP buffer, resuspended in a sample buffer, and analyzed by western blotting. For Co-IP of endogenous p53 or NRF2 – DO-1 (sc-126, Santa Cruz) and EP1808Y (ab62352, Abcam) primary antibodies were used respectively, and mouse or rabbit normal IgGs (Santa Cruz) as negative controls.

GST pull-down assay was performed essentially as described earlier. H1299 cells overexpressing the full length NRF2 were lysed in 300mM NaCl containing buffer (300mM NaCl, 50mM Tris, pH 7.5, 0.5% NP-40, and 10% glycerol) supplemented with protease and phosphatase inhibitors (CLAP - inhibitor cocktail, 1mM PMSF and 5mM NaF, 1mM $Na_3VO_4$). Lysates were then diluted 1:2 in the same buffer without NaCl and incubated for 2 h at 4 °C with 2 μg of Sepharose-GSH-bound GST proteins. After washing, the resin was resuspended in the SDS-PAGE loading buffer and subjected to western blot. NRF2 was detected using anti-NRF2 antibody and overexpressed GST-fusion proteins were dectected by Ponceau-Red staining of the western-blot membrane. NRF2 expression vector was a kind gift of prof. D.D. Zhang (Chen et al. 2009).

**Immunofluorescence**

IF has been performed as described (Sorrentino et al. 2014) using primary antibodies against p53 and NRF2: DO-1 (sc-126, Santa Cruz) and EP1808Y (ab62352, Abcam). The shown photos are representative of at least 3 biological replicates.

**Nucleus-cytoplasm fractionation**

To evaluate NRF2 and p53 cellular localization, nuclear and cytosolic fractions were prepared using the ProteoExtract Subcellular Proteome Extraction Kit (Millipore), following the manufacturer's instructions. Proteins were detected on western blots using indicated antibodies.

**Viability assay**

6-10x$10^4$ cells were plated in 96-well plates (white, transparent bottom), after 24h they were treated as indicated in figures and assayed for viability post 24h using ATPlite OneStep reagent (Perkin Elmer), according to the manufacturer's instructions. Luminescence intensity was measured using EnSpire plate fluorometer (Perkin Elmer). Most important results were reconfirmed (not shown) using a colorimetric WST

viability assay (Roche) as instructed by the manufacturer. 3 biological replicates were performed, for each means from 3 technical replicates (3 wells) were used.

**Colony formation assay**

4,000 cells were plated on 6cm plates in serum-containing medium. After 48h medium was supplemented with drugs as indicated in the figures. Medium and drugs were replaced every 3 days. After 12-14 days with drugs, cells were fixed (Formaldehyde 37%, diluted 1:10 in PBS) and stained for 15 min. with Giemsa diluted solution 1:10 in water (Fluka). Plates washed with water and dried were analyzed microscopically.

**Human breast cancer specimens**

Human breast cancer tissues for research's purposes were provided by institutional biobank at IRCCS Fondazione Salvatore Maugeri (FSM), Pavia, Italy. This study was approved by FSM Central Ethic Committee and subjected to patient's informed consent. Tumor samples were selected based on histopathological analysis performed by the Unit of Pathology at FSM. Frozen tumor tissue was fragmented by mortar and pestle in liquid nitrogen, fragments split 1:1 into Quiazol (see Total RNA extraction) and Lysis Buffer (see Proteasome activity assay) and homogenized mechanically. Samples were further processed according to RNA extraction and Proteasome activity assay protocols. For p53 cds mRNA sequencing the cDNA produced from total mRNA was used as a template for PCR of full length p53 cds and the product has been sequenced.

**Immunohistochemistry**

For p53 staining in breast cancer tissues, FFPE slices from each cancer sample along with its normal counterpart (as control) were processed. Epitope Retrieval was performed in pre-warmed TE buffer, pH 9 (Dako) for 40 minutes at 98°C. Incubation with monoclonal primary antibody, anti-p53 DO-7 (1:200, DAKO) was carried out at room temperature for 30 minutes. For antigen detection, samples were incubated with HRP-conjucted antibody from LSAB-Plus/HRP kit (Dako). Nuclei were counterstained with haematoxylin. p53 staining was evaluated by DM1000 Microscope (Leica) equipped with LAS Software (Leica) for images capture. Nuclear p53 localization was measured as percentage of cells. For each sample fifty randomly selected regions were

analyzed and compared with the staining in its normal tissue. Representative images are displayed at 200x magnification.

**Plasmids**

pSR-shRNAp53 PuroR used to stably silence *TP53* expression was a kind gift of R. Agami. N-terminally HA-tagged p53 constructs: pMSCV-HA-p53R175H, -p53M237I, -p53R249S, -p53R273H, -p53R280K were generated by first introducing 4 silent point mutations in the region targeted by p53 siRNA I/shRNA (the same target sequence) by site directed mutagenesis in pcDNA-HA-p53 (, subsequent introduction of missense point mutations and subcloning of sequenced p53 cds constructs to pMSCV-HA BlastR retroviral vector to obtain pMSCV with N-terminally HA-tagged p53 cds.

**Transfection**

For retrovirus production (stable silencing of *TP53* and ectopic overexpression of mutant p53s) low confluent HEK 293GP packaging cells were transfected with appropriate vectors by calcium phosphate precipitation. After 48–72 hr the virus-containing medium was filtered and added to target cells (MDA-MB-231 or MCF10A). Cells were selected with puromycin (0.5 μg/ml) and/or blasticidin (2 μg/ml). H1299 cells were transfected using Lipofectamine 2000 reagent (Invitrogen) as in the manufacturer's instructions. For siRNA transfections, all cells lines were transfected at 40-60% confluence two times with 24h interval (to increase efficiency of silencing), with 50 nM siRNA oligonucleotides using Lipofectamine RNAiMax (Invitrogen), following manufacturer's instructions. After 48 hr of the second silencing, cells were processed. For *TP53* silencing two alternative siRNA sequences were used – marked p53 I (targeting p53 cds) and p53 II (targeting p53 mRNA 3'UTR). If number is not indicated – p53 I was used. siRNAs coding sequence used in this work are listed in the Tab. 2.

**Total RNA extraction and RT-qPCR of mRNA and miRNA**

Total RNA was extracted with QIAzol (Qiagen) following manufacturer's instructions. 1μg of total RNA was reverse-transcribed with QuantiTect Reverse Transcription (Qiagen). Real-time qPCR in technical duplicates from each biological replicate (for

cell lines at least 2 biological replicates were used) was performed using SsoAdvancedTMSYBR Green Master Mix (Biorad) on a CFX96 Real-Time PCR System (Biorad). Quantitative RT-PCR of miRNAs was performed starting from total RNA and using miScript kit (Qiagen) for retrotranscription to cDNA. Human mature forms of let-7a and miR-30c were analyzed in technical duplicates from each biological sample (3 biological replicates for the cell line experiments) by using QuantiTect SYBR Green Master Mix (Qiagen) and primer kits (MS00031220, MS00009366; Qiagen). The list of qPCR primers used is provided in the Tab. 2.

**Gene signatures, functional annotation and Gene Ontology term enrichment analysis**

Full transcriptome, proteomic or ChIPseq expression datasets were imported to Ingenuity Pathway Analysis (IPA) software (Qiagen, www.ingenuity.com). P-value and log fold-change cutoffs were applied in IPA as described in the Figures. IPA was used to overlap datasets, generate Venn diagrams, produce resulting signature gene/protein lists and pathway analysis. ClueGo and GeneMania plugins for Cytoscape were used for further pathway, GO-term and functional annotation.

**RNA-seq and low level analysis**

MDA-MB-231 mRNA-seq libraries were obtained by Illumina TruSeq library construction kit using total RNA from the cell line transfected with control siRNA or p53 siRNA I (three biological replicates for each condition). mRNA-seq libraries were sequenced using Illumina HiSeq2000 for 100bp paired-end sequencing. Quality control of mRNA-seq data was performed using Fatsqc (www.bioinformatics.babraham.ac.uk/projects/fastqc/). Read files were mapped to the human genome (hg19) and analyzed for differential expression using the Tuxedo software suite [3] implemented in the Galaxy workflow manager. The mapping was performed by Tophat2 and Cufflinks was used to find out differential expressed genes.

P-values are adjusted for multiple testing using the Benjamini–Hochberg correction with a false discovery rate (FDR) $\leq 0.05$. The full data set was submitted to Gene Expression Omnibus under accession number GSE68248.

**Microarray Hybridization and low level analysis**

For gene expression profiling in MDA-MB-468, BT-549, SUM-149PT and HCC1395 cell lines, we used the Illumina HumanHT-12-v4-BeadChip (Illumina). Total RNA isolated from the utilized cell lines expressing control siRNA and p53 siRNA I, were reverse transcribed and amplified according to standard protocols and *in vitro* transcription was then carried out to generate cRNA. cRNA was hybridized onto each array (three biological replicates for each cell line and condition) and then labeled with Cy3-streptavidin (Amersham Biosciences). The array was then scanned using a BeadStation 500 system (Illumina). The probe intensities were calculated and normalized using GenomeStudio Data Analysis Software's Gene Expression Module (GSGX) Version 1.9 (Illumina). Further data processing was performed in the R computing environment version 3.0 (http://www.r-project.org/), with BioConductor packages (http://www.bioconductor.org/). Statistical analysis for differentially expressed genes was performed with *limma*. P-values were adjusted for multiple testing using Benjamini and Hochberg's method to control the false discovery rate.

**Chromatin immunoprecipitation and ChIP-sequencing**

Chromatin immunoprecipitation has been performed essentially as described [1] with modification of cell lysis and sonication stage to produce DNA fragments suitable for ChIP-sequencing: Cells were lysed in Lysis Buffer - 50 mM HEPES pH 7.9, 140 mM NaCl, 1 mM EDTA, 10% glycerol, 0.5% NP-40, 0.25% Triton X-100, nuclei spun down, washed in 10 mM Tris-HCl, pH 7.5, 200 mM NaCl, 1mM EDTA and resuspended in Sheraing Buffer - 0.1% SDS, 1mM EDTA, 10 mM Tris, pH 7.5. Samples were sonicated using Bioruptor sonicator (Diagenode; medium power setting) for the total time of 30 min., to achieve average size of 250-300 bp of the sonicated chromatin fragments. The Shearing Buffer was then supplemented to RIPA buffer of composition described in (Javier E. Girardini et al. 2011) and the rest of the protocol followed. For the used mouse (anti- p53, p300) and rabbit (anti- NRF1, NRF2, Acetyl-H3K9, Histone H3) ChIP antibodies the species-matched IgG unspecific antibodies were used as controls. ChIP results are means of at least 2 biological replicates and 2 technical replicates for each cell line. List of used ChIP qPCR primers is provided in Tab. 2.

For the ChIP-sequencing, 2–10 ng DNA resulting from ChIP procedure described above, obtained from six 15 cm plates of MDA-MB-231 per IP, was prepared for HiSeq2000 sequencing with the TruSeq ChIP Sample Prep Kit (Illumina) following the manufacturer's instructions. The full ChIP-sequencing data sets were submitted to Gene Expression Omnibus under accession number GSE66543.

**ChIP-seq peak calling and artefact filtering**

ChIP-seq NGS reads were aligned to the hg19 genome through the BWA aligner using default settings. We identified significant peaks using the Model-based Analysis of ChIP-Seq (MACS, version 1.0.1) program, integrated in the Galaxy web-based platform. We considered the reads as reliable mut p53 binding sites if the *P*-value was ≤ 1.00e-05 and fold enrichment (FE) ≥ 10. As described in MACS manual, FDR is calculated by reversing the control and treatment data, calling peaks using the same strategy, then calculating p-values for these 'negative peaks'. After ranking 'positive' peaks and 'negative' peaks by p-values, the FDR in percentage for a certain p-value can be calculated. We used the Genomic Regions Enrichment of Annotations Tool (GREAT, version 2.0.2) to associate MACS peaks to nearby genes within a distance of +/-500 bp from peaks to gene TSS.

**Enriched Transcription Factor Binding Sites Discovery**

We selected the ChIP-seq peaks of 37 human proteasome genes and obtained the nucleotide sequences corresponding to the genomic regions +/-150bp around the centre of each peak using EnsEMBL BioMart (Homo sapiens assembly GRCh38).

We identified enriched Transcription Factor Binding Sites (TFBS) using the LASAGNA-Search web tool (version 2.0), using the JASPAR CORE Matrices (version 5.0_ALPHA) as the reference Matrix-Derived Model, and applied the following filtering parameters: Cutoff P-value: 0.001 and "Report top-5 scoring sites per promoter for each TF".

We adjusted P-values for multiple testing using the Benjamini-Hochberg's method to control the false discovery rate, retaining only sites with counts≥20 (i.e. sites occurring in at least 20 different positions, in at least 10 different promoters).

For all the sites with maximum similarity, we created consensus sequences using WebLogo (version 3.4). Finally, we re-aligned every consensus sequence to its original predicted TFBS using the TOMTOM Motif Comparison Tool (version 4.9.1, integrated in the MEME suite), keeping only the sites with a P-value<1.00e-04 (Pearson correlation coefficient) with respect to binding sites of the "Vertebrates (In vivo and in silico)" database.

**Proteomic Analysis**

MDA-MB-231 cell line transfected with control siRNA, p53 siRNA I or PSMA2 siRNA (4 biological replicates for each condition) were lysed in 50 mM Tris-HCl, pH 7.8 containing 2% (w/v) SDS and 0.1 M DTT and the lysates were processed by the MED FASP procedure with consecutive protein cleavages using LysC and trypsin. The released peptides were loaded on strong anion exchange microcolumns and were eluted with Britton-Robinson universal buffer at pH 5 and pH 2. The fractions were analyzed by LC-MS/MS using LTQ-Orbitrap instrument as described previously. Spectra were searched by MaxQuant software (www.maxquant.org) and the concentrations of proteins were assessed by the Total Protein Approach using the raw protein intensities T-test was used to assess p-value support of differences between protein concentrations in distinct experimental conditions. The mass spectrometry proteomics data have been deposited to the ProteomeXchange Consortium (http://proteomecentral.proteomexchange.org) via the PRIDE partner repository with the dataset identifier PXD001673.

**Gene signatures, functional annotation and pathway enrichment analysis**

Full transcriptomic, proteomic or ChIPseq expression datasets have been imported to Ingenuity Pathway Analysis (IPA) software (Qiagen, www.ingenuity.com). P-value and log fold-change cutoffs were applied in IPA as described in text and figures. IPA was used to overlap datasets, generate Venn diagrams and produce resulting signature gene/protein lists

Pathway analysis module of IPA was further used to associate analyzed signatures with molecular pathways – producing shown bar graphs. An independent, parallel method for analyzing the signatures was the pathway-related gene ontology term enrichment

analysis, using ClueGO plugin for Cytoscape environment (http://www.cytoscape.org/) – employing simultaneous association with KEGG, Reactome and WikiPathways with otherwise default settings (analysis using broader GO-terms categories yielded enrichment of general cellular processes).

For proteomic data functional analysis GeneMania plugin for Cytoscape [14] has been used, allowing to analyze cellular co-localization, interaction and pathway association simultaneously (otherwise default settings were employed). The network visualization has been generated in Cytoscape.

**Biostatistical analyses**

The statistical analysis of experiments carried out is described in figure legends (tests were performed and p-value thresholds were obtained using GraphPad 6.0) and appropriate Extended Experimental Procedures sections (number of biological/technical replicates).

To verify the correlation of the gene signatures and breast cancer clinical data, survival analysis was performed on a breast cancer meta-dataset composed by 3458 samples using the Km-plotter online analysis tool. In order to perform the analysis on the greatest possible number of patients, for each gene, we selected only HGU133A probe-sets. The samples were split into two groups according to quantile expressions of the proposed signatures. The two groups were then compared by survival analysis. The Kaplan-Maier curves of relapse free survival time (RFS), the hazard ratio with 95% confidence intervals and log-rank test p-values were calculated. Because we are investigating the effect of mutant p53 in cancer patients we inverted the signs of expression fold change coming from the mutant *TP53* silencing experiments. This way, a high expression of the signature means that the genes down-regulated after silencing of mutant *TP53* (hence induced by mutant p53) are highly expressed. In order to combine up-regulated and down-regulated genes in the same analysis, to the genes that are down-regulated in the signatures (up-regulated after silencing of mutant *TP53*) a negative weight has been assigned, so the less they are expressed, the more the signature is considered highly expressed.

Gene expression data, *TP53* mutation status and clinical annotation for Breast Invasive Carcinoma, (TCGA datasets) have been obtained from Cancer Genomics Data Server

using the cgdsr package for R (R Core Team, 2013). The datasets were chosen for analysis according to the wt *TP53* vs mutant *TP53* status availability, with *TP53*-null samples excluded. For each patient we defined the levels of a 37-gene signature expression as the mean of the expression values of all the genes included in the signature. The statistical differences between the distributions of expression values in the two molecular conditions (mutated *TP53* and wt *TP53*) were calculated by Mann–Whitney U test in R/Bioconductor environment (R Core Team, 2013).

Pearson's Chi-squared test with Yates' continuity correction has been performed to test independence between TP53 status and a signature expression. All statistical analysis has been performed using R statistical analysis environment.

**Mouse strains and animal care**

P53 R172H/R172H, p53 -/- and p53 +/+ genotypes were maintained on a C57BL/6 background and genotyping was performed polymerase chain reaction (PCR) analysis as described [1]. Animals showing signs of illness or evident tumor burden were sacrificed and organs frozen upon extraction in the liquid nitrogen for 80$^{o}$C storage until protein extraction for the proteasome activity assay and western blot.

For *in vivo* xenograft studies we used SCID CB17 female mice (Charles River Laboratories, Lecco, Italy) aged 7 weeks.

Procedures involving animals and their care were in conformity with institutional guidelines (D.L. 116/92 and subsequent complementing circulars), all experimental protocols were approved by the ethical Committee of the University of Padua (CEASA) and conducted according to the UK Coordinating Committee on Cancer Research (UKCCCR) guidelines of 1989 for the welfare of animals in experimental neoplasia. During *in vivo* experiments, animals in all experimental groups were examined daily for a decrease in physical activity and other signs of disease.

***In vivo* xenograft experiments**

For *in vivo* tumor growth and metastasis assays MDA-MB-231 cells were transduced with a lentiviral vector coding for the Firefly Luciferase reporter gene. The vector was

previously described (Breckpot et al. 2003). Cells were propagated *in vitro* before injections.

For MDA-MB-231 xenograft experiments, $1x10^6$ cells were resuspended in 100 µl of DMEM, and injected into the mammary fat pad of previously anesthetized (1-3% isoflurane, Merial Italia) SCID female mice. For MCF7 xenograft experiment $10x10^6$ cells were resuspended in 100 µl of DMEM, and injected into the mammary fat pad of SCID female mice anesthetized as above. To support the MCF7 ER+ xenograft growth mice were injected once a week I.M. with 1mg/kg estradiol cypionate in cottonseed oil (solution 1mg/ml prepared from Sigma reagents). Tumor growth at the injection sites was monitored by caliper measurements. Tumor volume was calculated using the formula: tumor volume ($mm^3$) = $D \times d^2/2$, where D and d are the longest and the shortest diameters, respectively.

We performed *in vivo* imaging at 9-37 days after the subcutaneous fat pad injection, in 7 day intervals. Anesthetized animals were given the substrate D-Luciferin (PerkinElmer, MA, USA) by intraperitoneal injection at 150 mg/Kg in PBS (Sigma). Imaging times ranged from 15 s to 5 min. The light emitted from the bioluminescent tumors or metastasis was detected using a cooled charge-coupled device camera mounted on a light-tight specimen box (IVIS Lumina II Imaging System; Caliper Life Sciences). Regions of interest from displayed images were identified around the tumor sites or lymph node metastasis region and were quantified as total photon counts or photon/s using Living Image® software (Xenogen). In lymph node metastasis detection, the lower portion of each animal was shielded before reimaging in order to minimize the bioluminescence from primary tumor so that the signals from metastatic regions could be observed *in vivo*.

Primary tumors were extracted at 5 weeks post treatment initiation for treatment controls and after reaching a comparable size in mice treated with drugs. Tumors were directly frozen in liquid nitrogen for molecular analyses. Lymph nodes and lungs were excised, formalin-fixed and paraffin-embedded for hematoxylin-eosin staining and human Cytokeratin 7 (Cell Marque, OV-TL12/30) immunohistochemistry.

**Animal groups and drug administration**

The animals were randomized both prior to cell injection and prior to treatment.

Experiment 1, MDA-MB-231: 36 SCID mice, 6 groups of 6 mice, 4 weeks, drugs administered 2x a week intravenously with 2 days interval, drugs mixed before administration (where needed) in final injection volume of 200µl PBS. Groups: DMSO (ctrl), CFZ (Carflilzomib, Selleckchem; 1.5mg/kg), PRIMA-1 (Tocris Biosiecnce; 50 mg/kg), CFZ (1.5 mg/kg) + PRIMA-1 (50 mg/kg), SAHA (Tocris Biosiecnce; 50 mg/kg) - 2 animals deceased at 2 weeks, CFZ (1.5 mg/kg) + SAHA (50 mg/kg) - 2 animals deceased at 2 weeks. 4 mice in each group were selected for the final result.

Experiment 2, MDA-MB-231: 36 SCID mice, 4 groups of 9 mice, 5-7 weeks, CFZ administered intravenously 2x a week with 2 days interval, APR-246 (PRIMA-1 MET, provided by Aprea, Karolinska Institutet Science Park, Solna, Sweden) administered intravenously 3x a week on days alternating the CFZ injection (drugs were not mixed on administration), injection in 200µl PBS. Groups: DMSO (ctrl), CFZ (1.5mg/kg), APR-246 (100 mg/kg), CFZ (1.5 mg/kg) + APR-246 (100 mg/kg). 8 mice in each group were selected for the final results, ex vivo molecular studies were performed in the biopsy material from 5 mice from the selected groups.

Experiment 3, MCF7: 14 SCID mice, 2 groups of 7 mice, 5 weeks, CFZ administered intravenously 2x a week with 2 days interval, APR-246 (PRIMA-1 MET, provided by Aprea, Karolinska Institutet Science Park, Solna, Sweden) administered intravenously 3x a week on days alternating the CFZ injection (drugs were not mixed on administration), injection in 200µl PBS: CFZ (1.5 mg/kg) + APR-246 (100 mg/kg). 6 mice in each group were selected for the final results.

# LITERATURE

Adorno, M. et al., 2009. A Mutant-p53/Smad complex opposes p63 to empower TGFbeta-induced metastasis. *Cell*, 137(1), pp.87–98. Available at: http://www.cell.com/article/S0092867409000877/fulltext [Accessed January 7, 2016].

Di Agostino, S. et al., 2006. Gain of function of mutant p53: The mutant p53/NF-Y protein complex reveals an aberrant transcriptional mechanism of cell cycle regulation. *Cancer Cell*, 10(3), pp.191–202.

Agostino, S. Di et al., 2008. The disruption of the protein complex mutantp53/p73 increases selectively the response of tumor cells to anticancer drugs. *Cell Cycle*. Available at: http://www.tandfonline.com/doi/abs/10.4161/cc.7.21.6995 [Accessed March 9, 2016].

Alexandrova, E.M. et al., 2015. Improving survival by exploiting tumour dependence on stabilized mutant p53 for treatment. *Nature*, 523(7560), pp.352–6. Available at: http://dx.doi.org/10.1038/nature14430 [Accessed February 22, 2016].

Ali, A. et al., 2013. Differential regulation of the REGγ-proteasome pathway by p53/TGF-β signalling and mutant p53 in cancer cells. *Nature communications*, 4(May), p.2667. Available at: http://www.pubmedcentral.nih.gov/articlerender.fcgi?artid=3876931&tool=pmcentrez&rendertype=abstract [Accessed March 13, 2016].

Allen, M.A. et al., 2014. Global analysis of p53-regulated transcription identifies its direct targets and unexpected regulatory mechanisms. *eLife*, 3, p.e02200. Available at: http://www.pubmedcentral.nih.gov/articlerender.fcgi?artid=4033189&tool=pmcentrez&rendertype=abstract [Accessed March 20, 2016].

Amelio, I. et al., 2014. Serine and glycine metabolism in cancer. *Trends in Biochemical Sciences*, 39(4), pp.191–198. Available at: http://linkinghub.elsevier.com/retrieve/pii/S0968000414000280.

Arlt, a et al., 2012. Inhibition of the Nrf2 transcription factor by the alkaloid

trigonelline renders pancreatic cancer cells more susceptible to apoptosis through decreased proteasomal gene expression and proteasome activity. *Oncogene*, 32(September), pp.1–11. Available at: http://www.ncbi.nlm.nih.gov/pubmed/23108405 [Accessed February 21, 2016].

Arlt, A. et al., 2009. Increased proteasome subunit protein expression and proteasome activity in colon cancer relate to an enhanced activation of nuclear factor E2-related factor 2 (Nrf2). *Oncogene*, 28(45), pp.3983–3996. Available at: http://www.ncbi.nlm.nih.gov/entrez/query.fcgi?cmd=Retrieve&db=PubMed&dopt=Citation&list_uids=19734940 [Accessed March 16, 2016].

Ben-Nissan, G. & Sharon, M., 2014. Regulating the 20S Proteasome Ubiquitin-Independent Degradation Pathway. *Biomolecules*, 4(3), pp.862–884. Available at: http://www.mdpi.com/2218-273X/4/3/862/.

Blagosklonny, M. V. et al., 1996. Mutant conformation of p53 translated in vitro or in vivo requires functional HSP90. *Proceedings of the National Academy of Sciences of the United States of America*, 93(16), pp.8379–8383. Available at: http://www.mendeley.com/catalog/mutant-conformation-p53-translated-vitro-vivo-requires-functional-hsp90/ [Accessed March 13, 2016].

Bossi, G. et al., 2006. Mutant p53 gain of function: reduction of tumor malignancy of human cancer cell lines through abrogation of mutant p53 expression. *Oncogene*, 25(2), pp.304–9. Available at: http://dx.doi.org/10.1038/sj.onc.1209026 [Accessed March 14, 2016].

Bui, C.-B. & Shin, J., 2011. Persistent expression of Nqo1 by p62-mediated Nrf2 activation facilitates p53-dependent mitotic catastrophe. *Biochemical and biophysical research communications*, 412(2), pp.347–52. Available at: http://www.ncbi.nlm.nih.gov/pubmed/21821009 [Accessed March 14, 2016].

Bullock, A.N. & Fersht, A.R., 2001. Rescuing the function of mutant p53. *Nature reviews. Cancer*, 1(1), pp.68–76. Available at: http://www.ncbi.nlm.nih.gov/pubmed/11900253 [Accessed February 26, 2016].

Bullock, A.N., Henckel, J. & Fersht, A.R., 2000. Quantitative analysis of residual

folding and DNA binding in mutant p53 core domain: definition of mutant states for rescue in cancer therapy. *Oncogene*, 19(10), pp.1245–56. Available at: http://www.nature.com/onc/journal/v19/n10/full/1203434a.html [Accessed March 9, 2016].

Bykov, V.J.N. et al., 2005. PRIMA-1(MET) synergizes with cisplatin to induce tumor cell apoptosis. *Oncogene*, 24(21), pp.3484–3491. Available at: http://www.ncbi.nlm.nih.gov/pubmed/15735745.

Bykov, V.J.N. et al., 2002. Restoration of the tumor suppressor function to mutant p53 by a low-molecular-weight compound. *Nature medicine*, 8(3), pp.282–8. Available at: http://dx.doi.org/10.1038/nm0302-282 [Accessed March 13, 2016].

Bykov, V.J.N. et al., 2016. Targeting of Mutant p53 and the Cellular Redox Balance by APR-246 as a Strategy for Efficient Cancer Therapy. *Frontiers in Oncology*, 6(February). Available at: http://journal.frontiersin.org/article/10.3389/fonc.2016.00021.

Bykov, V.J.N. & Wiman, K.G., 2014. Mutant p53 reactivation by small molecules makes its way to the clinic. *FEBS letters*, 588(16), pp.2622–7. Available at: http://www.sciencedirect.com/science/article/pii/S0014579314003032.

Canning, P., Sorrell, F.J. & Bullock, A.N., 2015. Structural Basis of KEAP1 Interactions with Nrf2. *Free Radical Biology and Medicine*, (in Press), pp.1–7. Available at: http://linkinghub.elsevier.com/retrieve/pii/S0891584915002579.

Chan, K. et al., 1996. NRF2, a member of the NFE2 family of transcription factors, is not essential for murine erythropoiesis, growth, and development. *Proceedings of the National Academy of Sciences of the United States of America*, 93(24), pp.13943–13948.

Chen, W. et al., 2009. Direct Interaction between Nrf2 and p21Cip1/WAF1 Upregulates the Nrf2-Mediated Antioxidant Response. *Molecular Cell*, 34(6), pp.663–673. Available at: http://linkinghub.elsevier.com/retrieve/pii/S1097276509003050.

Chevillard, G. & Blank, V., 2011. NFE2L3 (NRF3): The Cinderella of the Cap'n'Collar

transcription factors. *Cellular and Molecular Life Sciences*, 68(20), pp.3337–3348.

Cho, Y. et al., 1994. Crystal structure of a p53 tumor suppressor-DNA complex: understanding tumorigenic mutations. *Science*, 265(5170), pp.346–355. Available at: http://science.sciencemag.org/content/265/5170/346.abstract [Accessed January 14, 2016].

Chorley, B.N. et al., 2012. Identification of novel NRF2-regulated genes by ChIP-Seq: influence on retinoid X receptor alpha. *Nucleic Acids Research*, 40(15), pp.7416–7429. Available at: http://nar.oxfordjournals.org/lookup/doi/10.1093/nar/gks409.

Chowdhry, S. et al., 2013. Nrf2 is controlled by two distinct β-TrCP recognition motifs in its Neh6 domain, one of which can be modulated by GSK-3 activity. *Oncogene*, 32(32), pp.3765–81. Available at: http://www.pubmedcentral.nih.gov/articlerender.fcgi?artid=3522573&tool=pmcentrez&rendertype=abstract.

Chowdhury, P. et al., 2014. Targeting TopBP1 at a convergent point of multiple oncogenic pathways for cancer therapy. *Nature communications*, 5, p.5476. Available at: http://www.nature.com/ncomms/2014/141117/ncomms6476/full/ncomms6476.html [Accessed March 13, 2016].

Ciechanover, A., 2005. Proteolysis: from the lysosome to ubiquitin and the proteasome. *Nature reviews. Molecular cell biology*, 6(1), pp.79–87. Available at: http://www.ncbi.nlm.nih.gov/pubmed/15688069 [Accessed February 17, 2016].

Crawford, L.J., Walker, B. & Irvine, A.E., 2011. Proteasome inhibitors in cancer therapy. *Journal of Cell Communication and Signaling*, 5(2), pp.101–110. Available at: http://link.springer.com/10.1007/s12079-011-0121-7.

Cullinan, S.B. et al., 2004. The Keap1-BTB protein is an adaptor that bridges Nrf2 to a Cul3-based E3 ligase: oxidative stress sensing by a Cul3-Keap1 ligase. *Molecular and cellular biology*, 24(19), pp.8477–8486. Available at: http://www.pubmedcentral.nih.gov/articlerender.fcgi?artid=516753&tool=pmcentrez&rendertype=abstract [Accessed February 9, 2016].

Cullinan, S.B. & Diehl, J.A., 2004. PERK-dependent activation of Nrf2 contributes to redox homeostasis and cell survival following endoplasmic reticulum stress. *The Journal of biological chemistry*, 279(19), pp.20108–17. Available at: http://www.ncbi.nlm.nih.gov/pubmed/14978030 [Accessed February 23, 2016].

Curtis, C. et al., 2012. The genomic and transcriptomic architecture of 2,000 breast tumours reveals novel subgroups. *Nature*, 486(7403), pp.346–352. Available at: http://www.pubmedcentral.nih.gov/articlerender.fcgi?artid=3440846&tool=pmcentrez&rendertype=abstract.

Dasgupta, G. & Momand, J., 1997. Geldanamycin prevents nuclear translocation of mutant p53. *Experimental cell research*, 237(1), pp.29–37. Available at: http://www.sciencedirect.com/science/article/pii/S0014482797937666 [Accessed March 13, 2016].

DeNicola, G.M. et al., 2015. NRF2 regulates serine biosynthesis in non–small cell lung cancer. *Nature Genetics*, 47(12), pp.1475–1481. Available at: http://www.nature.com/doifinder/10.1038/ng.3421.

DeNicola, G.M. et al., 2012. Oncogene-induced Nrf2 transcription promotes ROS detoxification and tumorigenesis. *Nature*, 475(7354), pp.106–109.

DeNicola, G.M. & Cantley, L.C., 2015. Cancer's Fuel Choice: New Flavors for a Picky Eater. *Molecular Cell*, 60(4), pp.514–523. Available at: http://dx.doi.org/10.1016/j.molcel.2015.10.018.

Dittmer, D. et al., 1993. Gain of function mutations in p53. *Nature genetics*, 4(1), pp.42–6. Available at: http://dx.doi.org/10.1038/ng0593-42 [Accessed March 9, 2016].

Do, P.M. et al., 2012. Mutant p53 cooperates with ETS2 to promote etoposide resistance. *Genes & development*, 26(8), pp.830–45. Available at: http://www.pubmedcentral.nih.gov/articlerender.fcgi?artid=3337457&tool=pmcentrez&rendertype=abstract [Accessed March 21, 2016].

Drost, J. et al., 2010. BRD7 is a candidate tumour suppressor gene required for p53

function. *Nature cell biology*, 12(4), pp.380–9. Available at: http://www.ncbi.nlm.nih.gov/pubmed/20228809 [Accessed March 20, 2016].

Eades, G. et al., 2011. miR-200a regulates Nrf2 activation by targeting Keap1 mRNA in breast cancer cells. *The Journal of biological chemistry*, 286(47), pp.40725–33. Available at: http://www.pubmedcentral.nih.gov/articlerender.fcgi?artid=3220489&tool=pmcentrez&rendertype=abstract [Accessed March 4, 2016].

Eldridge, A.G. & O'Brien, T., 2010. Therapeutic strategies within the ubiquitin proteasome system. *Cell death and differentiation*, 17(1), pp.4–13. Available at: http://www.ncbi.nlm.nih.gov/pubmed/19557013 [Accessed March 20, 2016].

Foster, B.A., 1999. Pharmacological Rescue of Mutant p53 Conformation and Function. *Science*, 286(5449), pp.2507–2510. Available at: http://science.sciencemag.org/content/286/5449/2507.abstract [Accessed March 13, 2016].

Freed-Pastor, W.A. et al., 2012. Mutant p53 Disrupts Mammary Tissue Architecture via the Mevalonate Pathway. *Cell*, 148(1-2), pp.244–258. Available at: http://linkinghub.elsevier.com/retrieve/pii/S0092867411015698.

Freed-Pastor, W.A. & Prives, C., 2012. Mutant p53: one name, many proteins. *Genes & development*, 26(12), pp.1268–86. Available at: http://genesdev.cshlp.org/content/26/12/1268.full.

Friling, R.S., Bergelson, S. & Daniel, V., 1992. Two adjacent AP-1-like binding sites form the electrophile-responsive element of the murine glutathione S-transferase Ya subunit gene. *Proceedings of the National Academy of Sciences of the United States of America*, 89(2), pp.668–72. Available at: http://www.pubmedcentral.nih.gov/articlerender.fcgi?artid=48300&tool=pmcentrez&rendertype=abstract [Accessed February 9, 2016].

Garibaldi, F. et al., 2016. Mutant p53 inhibits miRNA biogenesis by interfering with the microprocessor complex. *Oncogene*. Available at: http://www.nature.com/onc/journal/vaop/ncurrent/pdf/onc201651a.pdf [Accessed

March 21, 2016].

Gillotin, S., Yap, D. & Lu, X., 2010. Mutation at Ser392 specifically sensitizes mutant p53H175 to mdm2-mediated degradation. *Cell cycle (Georgetown, Tex.)*, 9(7), pp.1390–8. Available at: http://www.ncbi.nlm.nih.gov/pubmed/20234175 [Accessed March 31, 2016].

Girardini, J.E. et al., 2011. A Pin1/mutant p53 axis promotes aggressiveness in breast cancer. *Cancer cell*, 20(1), pp.79–91. Available at: http://www.ncbi.nlm.nih.gov/pubmed/21741598.

Girardini, J.E. et al., 2011. A Pin1/Mutant p53 Axis Promotes Aggressiveness in Breast Cancer. *Cancer Cell*, 20(1), pp.79–91. Available at: http://linkinghub.elsevier.com/retrieve/pii/S1535610811002261.

Girardini, J.E., Marotta, C. & Del Sal, G., 2014. Disarming mutant p53 oncogenic function. *Pharmacological Research*, 79, pp.75–87. Available at: http://linkinghub.elsevier.com/retrieve/pii/S1043661813001783.

Gonyeau, M.J., 2014. The spectrum of statin therapy in cancer patients: is there a need for further investigation? *Current atherosclerosis reports*, 16(1), p.383. Available at: http://www.ncbi.nlm.nih.gov/pubmed/24306898 [Accessed March 14, 2016].

Gorrini, C., Harris, I.S. & Mak, T.W., 2013. Modulation of oxidative stress as an anticancer strategy. *Nature Reviews Drug Discovery*, 12(12), pp.931–947. Available at: http://www.nature.com/doifinder/10.1038/nrd4002.

Grigoreva, T.A. et al., 2015. The 26S proteasome is a multifaceted target for anti-cancer therapies. *Oncotarget*, 6(28), pp.24733–24749.

Gu, Z.C. & Enenkel, C., 2014. Proteasome assembly. *Cellular and molecular life sciences : CMLS*, 71(24), pp.4729–45. Available at: http://www.ncbi.nlm.nih.gov/pubmed/25107634 [Accessed March 20, 2016].

Guida, E. et al., 2008. Peptide aptamers targeting mutant p53 induce apoptosis in tumor cells. *Cancer research*, 68(16), pp.6550–8. Available at: http://cancerres.aacrjournals.org/content/68/16/6550.abstract [Accessed March 13,

2016].

Gusterson, B., 2009. Do “basal-like” breast cancers really exist? *Nature reviews. Cancer*, 9(2), pp.128–34. Available at: http://dx.doi.org/10.1038/nrc2571 [Accessed March 30, 2016].

Halevy, O., Michalovitz, D. & Oren, M., 1990. Different tumor-derived p53 mutants exhibit distinct biological activities. *Science*, 250(4977), pp.113–116. Available at: http://science.sciencemag.org/content/250/4977/113.abstract [Accessed March 9, 2016].

Hanahan, D. & Weinberg, R.A., 2011. Hallmarks of cancer: the next generation. *Cell*, 144(5), pp.646–74. Available at: http://www.ncbi.nlm.nih.gov/pubmed/21376230 [Accessed July 9, 2014].

Hanahan, D. & Weinberg, R.A., 2000. The hallmarks of cancer. *Cell*, 100(1), pp.57–70. Available at: http://www.ncbi.nlm.nih.gov/pubmed/10647931 [Accessed July 10, 2014].

Harris, I.S. et al., 2015. Glutathione and Thioredoxin Antioxidant Pathways Synergize to Drive Cancer Initiation and Progression. *Cancer Cell*, 27(2), pp.211–222. Available at: http://www.cell.com/article/S153561081400470X/fulltext [Accessed October 4, 2015].

Hayes, J.D. et al., 2010. Cancer chemoprevention mechanisms mediated through the Keap1-Nrf2 pathway. *Antioxidants & redox signaling*, 13(11), pp.1713–48. Available at: http://www.ncbi.nlm.nih.gov/pubmed/20446772 [Accessed January 7, 2016].

Hayes, J.D. & Dinkova-Kostova, A.T., 2014. The Nrf2 regulatory network provides an interface between redox and intermediary metabolism. *Trends in Biochemical Sciences*, 39(4), pp.199–218. Available at: http://linkinghub.elsevier.com/retrieve/pii/S0968000414000267.

He, X. et al., 2015. CP-31398 prevents the growth of p53-mutated colorectal cancer cells in vitro and in vivo. *Tumour biology : the journal of the International Society*

*for Oncodevelopmental Biology and Medicine*, 36(3), pp.1437–44. Available at: http://www.ncbi.nlm.nih.gov/pubmed/25663456 [Accessed March 13, 2016].

Hirotsu, Y. et al., 2012. Nrf2-MafG heterodimers contribute globally to antioxidant and metabolic networks. *Nucleic acids research*, 40(20), pp.10228–39. Available at: http://www.pubmedcentral.nih.gov/articlerender.fcgi?artid=3488259&tool=pmcentrez&rendertype=abstract [Accessed March 25, 2016].

Höhn, T.J.A. & Grune, T., 2014. The proteasome and the degradation of oxidized proteins: Part III-Redox regulation of the proteasomal system. *Redox Biology*, 2(1), pp.388–394. Available at: http://dx.doi.org/10.1016/j.redox.2013.12.029.

Huang, H.C., Nguyen, T. & Pickett, C.B., 2002. Phosphorylation of Nrf2 at Ser-40 by protein kinase C regulates antioxidant response element-mediated transcription. *Journal of Biological Chemistry*, 277(45), pp.42769–42774.

Huang, Y. et al., 2015. The complexity of the Nrf2 pathway: Beyond the antioxidant response. *Journal of Nutritional Biochemistry*, 26(12), pp.1401–1413. Available at: http://dx.doi.org/10.1016/j.jnutbio.2015.08.001.

Huang, Z. et al., 2014. Efficacy of therapy with bortezomib in solid tumors: a review based on 32 clinical trials. *Future oncology (London, England)*, 10(10), pp.1795–807. Available at: http://www.ncbi.nlm.nih.gov/pubmed/25303058 [Accessed March 24, 2016].

Irvin, W.J. et al., 2010. Phase II study of bortezomib and pegylated liposomal doxorubicin in the treatment of metastatic breast cancer. *Clinical breast cancer*, 10(6), pp.465–70. Available at: http://www.ncbi.nlm.nih.gov/pubmed/21147690 [Accessed March 24, 2016].

Itoh, K. et al., 1997. An Nrf2/Small Maf Heterodimer Mediates the Induction of Phase II Detoxifying Enzyme Genes through Antioxidant Response Elements. *Biochemical and Biophysical Research Communications*, 236(2), pp.313–322. Available at: http://www.sciencedirect.com/science/article/pii/S0006291X97969436 [Accessed November 12, 2015].

Jaramillo, M. & Zhang, D., 2013. The emerging role of the Nrf2–Keap1 signaling pathway in cancer. *Genes & development*, 27, pp.2179–2191. Available at: http://genesdev.cshlp.org/content/27/20/2179.short.

Joerger, A.C. et al., 2009. Structural evolution of p53, p63, and p73: implication for heterotetramer formation. *Proceedings of the National Academy of Sciences of the United States of America*, 106(42), pp.17705–17710.

Johnson, D.E., 2015. The ubiquitin-proteasome system: opportunities for therapeutic intervention in solid tumors. *Endocrine-related cancer*, 22(1), pp.T1–17. Available at: http://www.pubmedcentral.nih.gov/articlerender.fcgi?artid=4170053&tool=pmcentrez&rendertype=abstract [Accessed March 20, 2016].

Jung, T. & Grune, T., 2013. Redox Biology The proteasome and the degradation of oxidized proteins : Part I — structure of proteasomes $. *Redox Biology*, 1(1), pp.178–182. Available at: http://dx.doi.org/10.1016/j.redox.2013.01.004.

Kalo, E. et al., 2012. Mutant p53R273H attenuates the expression of phase 2 detoxifying enzymes and promotes the survival of cells with high levels of reactive oxygen species. *Journal of cell science*, 125(Pt 22), pp.5578–86. Available at: http://www.ncbi.nlm.nih.gov/pubmed/22899716.

Kandoth, C. et al., 2013. Mutational landscape and significance across 12 major cancer types. *Nature*, 502(7471), pp.333–9. Available at: http://www.pubmedcentral.nih.gov/articlerender.fcgi?artid=3927368&tool=pmcentrez&rendertype=abstract [Accessed July 10, 2014].

Kang, H.J. et al., 2014. HER2 confers drug resistance of human breast cancer cells through activation of NRF2 by direct interaction. *Scientific reports*, 4, p.7201. Available at: http://www.pubmedcentral.nih.gov/articlerender.fcgi?artid=4252900&tool=pmcentrez&rendertype=abstract.

Katoh, Y. et al., 2001. Two domains of Nrf2 cooperatively bind CBP, a CREB binding protein, and synergistically activate transcription. *Genes to Cells*, 6, pp.857–868.

Kawai, Y. et al., 2011. Acetylation-Deacetylation of the Transcription Factor Nrf2 (Nuclear Factor Erythroid 2-related Factor 2) Regulates Its Transcriptional Activity and Nucleocytoplasmic Localization. *Journal of Biological Chemistry*, 286(9), pp.7629–7640. Available at: http://www.jbc.org/cgi/doi/10.1074/jbc.M110.208173.

Kim, H. et al., 2010. Redox regulation of lipopolysaccharide-mediated sulfiredoxin induction, which depends on both AP-1 and Nrf2. *The Journal of biological chemistry*, 285(45), pp.34419–28. Available at: http://www.pubmedcentral.nih.gov/articlerender.fcgi?artid=2966056&tool=pmcentrez&rendertype=abstract [Accessed February 25, 2016].

Kim, J.-H. et al., 2013. The nuclear cofactor RAC3/AIB1/SRC-3 enhances Nrf2 signaling by interacting with transactivation domains. *Oncogene*, 32(4), pp.514–27. Available at: http://www.pubmedcentral.nih.gov/articlerender.fcgi?artid=3538952&tool=pmcentrez&rendertype=abstract [Accessed March 18, 2016].

Kobayashi, M. et al., 2009. The antioxidant defense system Keap1-Nrf2 comprises a multiple sensing mechanism for responding to a wide range of chemical compounds. *Molecular and cellular biology*, 29(2), pp.493–502. Available at: http://www.pubmedcentral.nih.gov/articlerender.fcgi?artid=2612520&tool=pmcentrez&rendertype=abstract [Accessed March 16, 2016].

Koch, A., Steffen, J. & Krüger, E., 2011. TCF11 at the crossroads of oxidative stress and the ubiquitin proteasome system. *Cell cycle (Georgetown, Tex.)*, 10(8), pp.1200–7. Available at: http://www.ncbi.nlm.nih.gov/pubmed/21412055 [Accessed March 16, 2016].

Kollareddy, M. et al., 2015. Regulation of nucleotide metabolism by mutant p53 contributes to its gain-of-function activities. *Nature communications*, 6, p.7389. Available at: http://www.nature.com/ncomms/2015/150612/ncomms8389/full/ncomms8389.html [Accessed March 13, 2016].

Komatsu, M. et al., 2010. The selective autophagy substrate p62 activates the stress responsive transcription factor Nrf2 through inactivation of Keap1. *Nature cell biology*, 12(3), pp.213–223. Available at: http://dx.doi.org/10.1038/ncb2021.

Kwak, M.-K. et al., 2003. Antioxidants enhance mammalian proteasome expression through the Keap1-Nrf2 signaling pathway. *Molecular and cellular biology*, 23(23), pp.8786–8794. Available at: http://www.pubmedcentral.nih.gov/articlerender.fcgi?artid=262680&tool=pmcentrez&rendertype=abstract [Accessed March 16, 2016].

Lacher, S.E. et al., 2015. Beyond antioxidant genes in the ancient NRF2 regulatory network. *Free radical biology & medicine*. Available at: http://www.ncbi.nlm.nih.gov/pubmed/26163000.

Lambert, J.M.R. et al., 2010. Mutant p53 reactivation by PRIMA-1MET induces multiple signaling pathways converging on apoptosis. *Oncogene*, 29(9), pp.1329–1338. Available at: http://dx.doi.org/10.1038/onc.2009.425.

Lambert, J.M.R. et al., 2009. PRIMA-1 Reactivates Mutant p53 by Covalent Binding to the Core Domain. *Cancer Cell*, 15(5), pp.376–388. Available at: http://linkinghub.elsevier.com/retrieve/pii/S1535610809000786.

Lang, G. a. et al., 2004. Gain of function of a p53 hot spot mutation in a mouse model of Li-Fraumeni syndrome. *Cell*, 119(6), pp.861–872.

Lau, A. et al., 2008. Dual roles of Nrf2 in cancer. *Pharmacological research*, 58(5-6), pp.262–70. Available at: http://www.sciencedirect.com/science/article/pii/S104366180800162X [Accessed January 28, 2016].

Lee, D.-F. et al., 2009. KEAP1 E3 ligase-mediated downregulation of NF-kappaB signaling by targeting IKKbeta. *Molecular cell*, 36(1), pp.131–40. Available at: http://www.pubmedcentral.nih.gov/articlerender.fcgi?artid=2770835&tool=pmcentrez&rendertype=abstract [Accessed March 14, 2016].

Lee, M.K. et al., 2012. Cell-type, Dose, and Mutation-type Specificity Dictate Mutant

p53 Functions In Vivo. *Cancer Cell*, 22(6), pp.751–764. Available at: http://dx.doi.org/10.1016/j.ccr.2012.10.022.

Lehmann, B.D.B. et al., 2011. Identification of human triple-negative breast cancer subtypes and preclinical models for selection of targeted therapies. *Journal of Clinical Investigation*, 121(7), pp.2750–2767. Available at: http://www.pubmedcentral.nih.gov/articlerender.fcgi?artid=3127435&tool=pmcentrez&rendertype=abstract\nhttp://www.ncbi.nlm.nih.gov/pmc/articles/pmc3127435/.

Lehmann, S. et al., 2012. Targeting p53 in vivo: a first-in-human study with p53-targeting compound APR-246 in refractory hematologic malignancies and prostate cancer. *Journal of clinical oncology : official journal of the American Society of Clinical Oncology*, 30(29), pp.3633–9. Available at: http://www.ncbi.nlm.nih.gov/pubmed/22965953 [Accessed March 20, 2016].

Li, D., Marchenko, N.D. & Moll, U.M., 2011. SAHA shows preferential cytotoxicity in mutant p53 cancer cells by destabilizing mutant p53 through inhibition of the HDAC6-Hsp90 chaperone axis. *Cell Death and Differentiation*, 18(12), pp.1904–13. Available at: http://dx.doi.org/10.1038/cdd.2011.71 [Accessed February 29, 2016].

Liu, K., Ling, S. & Lin, W.-C., 2011. TopBP1 mediates mutant p53 gain of function through NF-Y and p63/p73. *Molecular and cellular biology*, 31(22), pp.4464–81. Available at: http://mcb.asm.org/content/31/22/4464.abstract [Accessed March 13, 2016].

Lukashchuk, N. & Vousden, K.H., 2007. Ubiquitination and degradation of mutant p53. *Molecular and cellular biology*, 27(23), pp.8284–95. Available at: http://www.pubmedcentral.nih.gov/articlerender.fcgi?artid=2169174&tool=pmcentrez&rendertype=abstract [Accessed February 18, 2016].

Ma, C.X. et al., 2013. A phase II study of UCN-01 in combination with irinotecan in patients with metastatic triple negative breast cancer. *Breast cancer research and treatment*, 137(2), pp.483–92. Available at:

http://www.pubmedcentral.nih.gov/articlerender.fcgi?artid=3539064&tool=pmcentrez&rendertype=abstract [Accessed March 14, 2016].

Ma, C.X. et al., 2012. Targeting Chk1 in p53-deficient triple-negative breast cancer is therapeutically beneficial in human-in-mouse tumor models. *The Journal of clinical investigation*, 122(4), pp.1541–52. Available at: http://www.jci.org/articles/view/58765 [Accessed March 14, 2016].

Ma, Q., 2013. Role of Nrf2 in Oxidative Stress and Toxicity. *Annu. Rev. Pharmacol. Toxicol*, 53, pp.401–26.

MacLeod, A.K. et al., 2009. Characterization of the cancer chemopreventive NRF2-dependent gene battery in human keratinocytes: demonstration that the KEAP1-NRF2 pathway, and not the BACH1-NRF2 pathway, controls cytoprotection against electrophiles as well as redox-cycling compounds. *Carcinogenesis*, 30(9), pp.1571–80. Available at: http://www.pubmedcentral.nih.gov/articlerender.fcgi?artid=3656619&tool=pmcentrez&rendertype=abstract [Accessed February 9, 2016].

Malhotra, D. et al., 2010. Global mapping of binding sites for Nrf2 identifies novel targets in cell survival response through chip-seq profiling and network analysis. *Nucleic Acids Research*, 38(17), pp.5718–5734.

Malkin, D., 2011. Li-fraumeni syndrome. *Genes & cancer*, 2(4), pp.475–84. Available at: http://www.pubmedcentral.nih.gov/articlerender.fcgi?artid=3135649&tool=pmcentrez&rendertype=abstract [Accessed November 3, 2015].

Mantovani, A., 2009. Cancer: Inflaming metastasis. *Nature*, 457(7225), pp.36–7. Available at: http://dx.doi.org/10.1038/457036b [Accessed February 29, 2016].

Martinez, L.A., 2016. Mutant p53 and ETS2, a tale of reciprocity. *Frontiers in Oncology*.

Martynova, E. et al., 2012. Gain-of-function p53 mutants have widespread genomic locations partially overlapping with p63. *Oncotarget*, 3(2), pp.132–43. Available

at:
http://www.pubmedcentral.nih.gov/articlerender.fcgi?artid=3326644&tool=pmcentrez&rendertype=abstract [Accessed March 21, 2016].

McMahon, M. et al., 2006. Dimerization of substrate adaptors can facilitate Cullin-mediated ubiquitylation of proteins by a "tethering" mechanism: A two-site interaction model for the Nrf2-Keap1 complex. *Journal of Biological Chemistry*, 281(34), pp.24756–24768.

McMahon, M. et al., 2004. Redox-regulated turnover of Nrf2 is determined by at least two separate protein domains, the redox-sensitive Neh2 degron and the redox-insensitive Neh6 degron. *Journal of Biological Chemistry*, 279(30), pp.31556–31567.

McMahon, M. et al., 2001. The cap "n" collar basic leucine zipper transcription factor Nrf2 (NF-E2 p45-related factor 2) controls both constitutive and inducible expression of intestinal detoxification and glutathione biosynthetic enzymes. *Cancer Research*, 61, pp.3299–3307.

Meister, A., 1983. Selective modification of glutathione metabolism. *Science (New York, N.Y.)*, 220(4596), pp.472–7. Available at: http://www.ncbi.nlm.nih.gov/pubmed/6836290 [Accessed March 9, 2016].

Di Minin, G. et al., 2014. Mutant p53 reprograms TNF signaling in cancer cells through interaction with the tumor suppressor DAB2IP. *Molecular cell*, 56(5), pp.617–29. Available at: http://www.ncbi.nlm.nih.gov/pubmed/25454946 [Accessed February 23, 2016].

Mitsuishi, Y. et al., 2012. Nrf2 Redirects Glucose and Glutamine into Anabolic Pathways in Metabolic Reprogramming. *Cancer Cell*, 22(1), pp.66–79. Available at: http://dx.doi.org/10.1016/j.ccr.2012.05.016.

Mohell, N. et al., 2015. APR-246 overcomes resistance to cisplatin and doxorubicin in ovarian cancer cells. *Cell Death and Disease*, 6(6), p.e1794. Available at: http://www.nature.com/doifinder/10.1038/cddis.2015.143.

Moi, P. et al., 1994. Isolation of NF-E2-related factor 2 (Nrf2), a NF-E2-like basic leucine zipper transcriptional activator that binds to the tandem NF-E2/AP1 repeat of the beta-globin locus control region. *Proceedings of the National Academy of Sciences of the United States of America*, 91(21), pp.9926–9930.

Moschonas, A. et al., 2008. CD40 induces antigen transporter and immunoproteasome gene expression in carcinomas via the coordinated action of NF-kappaB and of NF-kappaB-mediated de novo synthesis of IRF-1. *Molecular and cellular biology*, 28(20), pp.6208–22. Available at: http://www.pubmedcentral.nih.gov/articlerender.fcgi?artid=2577429&tool=pmcentrez&rendertype=abstract [Accessed March 20, 2016].

Motohashi, H. et al., 2004. Small Maf proteins serve as transcriptional cofactors for keratinocyte differentiation in the Keap1-Nrf2 regulatory pathway. *Proceedings of the National Academy of Sciences of the United States of America*, 101(17), pp.6379–84. Available at: http://www.pnas.org/content/101/17/6379 [Accessed March 20, 2016].

Mullarky, E. et al., 2016. Identification of a small molecule inhibitor of 3-phosphoglycerate dehydrogenase to target serine biosynthesis in cancers. *Proceedings of the National Academy of Sciences*, 113(11), p.201602228. Available at: http://www.pnas.org/lookup/doi/10.1073/pnas.1602228113.

Muller, P. et al., 2008. Chaperone-dependent stabilization and degradation of p53 mutants. *Oncogene*, 27(24), pp.3371–83. Available at: http://www.ncbi.nlm.nih.gov/pubmed/18223694 [Accessed March 12, 2016].

Muller, P.A.J. et al., 2009. Mutant p53 Drives Invasion by Promoting Integrin Recycling. *Cell*, 139(7), pp.1327–41. Available at: http://www.cell.com/article/S009286740901438X/fulltext [Accessed February 17, 2016].

Muller, P.A.J. & Vousden, K.H., 2013. P53 Mutations in Cancer. *Nature Cell Biology*, 15(1), pp.2–8. Available at: http://www.nature.com/doifinder/10.1038/ncb2641.

Murray-Zmijewski, F., Slee, E. a & Lu, X., 2008. A complex barcode underlies the

heterogeneous response of p53 to stress. *Nature reviews. Molecular cell biology*, 9(9), pp.702–712. Available at: papers3://publication/doi/10.1038/nrm2451.

Muscarella, L.A. et al., 2011. Regulation of KEAP1 expression by promoter methylation in malignant gliomas and association with patient's outcome. *Epigenetics*, 6(3), pp.317–25. Available at: http://www.pubmedcentral.nih.gov/articlerender.fcgi?artid=3092680&tool=pmcentrez&rendertype=abstract [Accessed March 15, 2016].

Neilsen, P.M. et al., 2011. Mutant p53 uses p63 as a molecular chaperone to alter gene expression and induce a pro-invasive secretome. *Oncotarget*, 2(12), pp.1203–1217. Available at: http://www.impactjournals.com/oncotarget/index.php?journal=oncotarget&page=article&op=view&path%5B%5D=382&path%5B%5D=660 [Accessed March 21, 2016].

Nijhawan, D. et al., 2012. Cancer vulnerabilities unveiled by genomic loss. *Cell*, 150(4), pp.842–54. Available at: http://www.pubmedcentral.nih.gov/articlerender.fcgi?artid=3429351&tool=pmcentrez&rendertype=abstract [Accessed December 2, 2015].

Nioi, P. et al., 2005. The carboxy-terminal Neh3 domain of Nrf2 is required for transcriptional activation. *Molecular and cellular biology*, 25(24), pp.10895–10906.

Oakman, C., Viale, G. & Di Leo, A., 2010. Management of triple negative breast cancer. *Breast (Edinburgh, Scotland)*, 19(5), pp.312–21. Available at: http://www.sciencedirect.com/science/article/pii/S0960977610000949.

Ogrunc, M. et al., 2014. Oncogene-induced reactive oxygen species fuel hyperproliferation and DNA damage response activation. *Cell death and differentiation*, 21(6), pp.998–1012. Available at: http://dx.doi.org/10.1038/cdd.2014.16 [Accessed January 22, 2016].

Olive, K.P. et al., 2004. Mutant p53 gain of function in two mouse models of Li-Fraumeni syndrome. *Cell*, 119(6), pp.847–860.

Ooi, A. et al., 2011. An antioxidant response phenotype shared between hereditary and sporadic type 2 papillary renal cell carcinoma. *Cancer cell*, 20(4), pp.511–23. Available at: http://www.ncbi.nlm.nih.gov/pubmed/22014576 [Accessed March 15, 2016].

Ooi, A. et al., 2013. CUL3 and NRF2 mutations confer an NRF2 activation phenotype in a sporadic form of papillary renal cell carcinoma. *Cancer Research*, 73(7), pp.2044–2051. Available at: http://www.ncbi.nlm.nih.gov/pubmed/23365135 [Accessed February 19, 2016].

Origanti, S. et al., 2013. Synthetic lethality of Chk1 inhibition combined with p53 and/or p21 loss during a DNA damage response in normal and tumor cells. *Oncogene*, 32(5), pp.577–88. Available at: http://dx.doi.org/10.1038/onc.2012.84 [Accessed March 14, 2016].

Padmanabhan, B. et al., 2006. Structural basis for defects of Keap1 activity provoked by its point mutations in lung cancer. *Molecular Cell*, 21(5), pp.689–700.

Parrales, A. & Iwakuma, T., 2015. Targeting Oncogenic Mutant p53 for Cancer Therapy. *Frontiers in Oncology*, 5(December), pp.1–13. Available at: http://journal.frontiersin.org/article/10.3389/fonc.2015.00288.

Perou, C.M. et al., 2000. Molecular portraits of human breast tumours. *Nature*, 406(6797), pp.747–752.

Petitjean, A. et al., 2007. Impact of mutant p53 functional properties on TP53 mutation patterns and tumor phenotype: lessons from recent developments in the IARC TP53 database. *Human mutation*, 28(6), pp.622–9. Available at: http://www.ncbi.nlm.nih.gov/pubmed/17311302 [Accessed December 8, 2015].

Petrocca, F. et al., 2013. A Genome-wide siRNA Screen Identifies Proteasome Addiction as a Vulnerability of Basal-like Triple-Negative Breast Cancer Cells. *Cancer Cell*, 24(2), pp.182–196. Available at: http://dx.doi.org/10.1016/j.ccr.2013.07.008.

Pi, J. et al., 2007. Molecular mechanism of human Nrf2 activation and degradation: role

of sequential phosphorylation by protein kinase CK2. *Free radical biology & medicine*, 42(12), pp.1797–1806. Available at: http://www.ncbi.nlm.nih.gov/pubmed/17512459.

Pickering, a. M. et al., 2012. A conserved role for the 20S proteasome and Nrf2 transcription factor in oxidative-stress adaptation in mammals, C. elegans and D. melanogaster. *Journal of Experimental Biology*, (October), pp.543–553.

Pickering, A.M. et al., 2012. Nrf2-dependent induction of proteasome and Pa28???? regulator are required for adaptation to oxidative stress. *Journal of Biological Chemistry*, 287(13), pp.10021–10031. Available at: http://www.pubmedcentral.nih.gov/articlerender.fcgi?artid=3323025&tool=pmcentrez&rendertype=abstract [Accessed January 25, 2016].

Plafker, K.S. et al., 2010. The ubiquitin-conjugating enzyme UbcM2 can regulate the stability and activity of the antioxidant transcription factor Nrf2. *Journal of Biological Chemistry*, 285(30), pp.23064–23074.

Polotskaia, A. et al., 2015. Proteome-wide analysis of mutant p53 targets in breast cancer identifies new levels of gain-of-function that influence PARP, PCNA, and MCM4. *Proceedings of the National Academy of Sciences of the United States of America*, 112(11), pp.E1220–9. Available at: http://www.pubmedcentral.nih.gov/articlerender.fcgi?artid=4371979&tool=pmcentrez&rendertype=abstract [Accessed February 15, 2016].

Prat, A. et al., 2010. Phenotypic and molecular characterization of the claudin-low intrinsic subtype of breast cancer. *Breast cancer research : BCR*, 12(5), p.R68. Available at: http://breast-cancer-research.biomedcentral.com/articles/10.1186/bcr2635 [Accessed December 8, 2015].

Radhakrishnan, S.K. et al., 2010. Transcription Factor Nrf1 Mediates the Proteasome Recovery Pathway after Proteasome Inhibition in Mammalian Cells. *Molecular Cell*, 38(1), pp.17–28.

Ren, D. et al., 2011. Brusatol enhances the efficacy of chemotherapy by inhibiting the

Nrf2-mediated defense mechanism. *Proceedings of the National Academy of Sciences*, 108(4), pp.1433–1438. Available at: http://www.pnas.org/cgi/doi/10.1073/pnas.1014275108.

Rivlin, N. et al., 2011. Mutations in the p53 Tumor Suppressor Gene: Important Milestones at the Various Steps of Tumorigenesis. *Genes & cancer*, 2(4), pp.466–474. Available at: papers3://publication/doi/10.1177/1947601911408889.

Rushmore, T.H., Morton, M.R. & Pickett, C.B., 1991. The antioxidant responsive element. Activation by oxidative stress and identification of the DNA consensus sequence required for functional activity. *The Journal of biological chemistry*, 266(18), pp.11632–9. Available at: http://www.ncbi.nlm.nih.gov/pubmed/1646813 [Accessed February 9, 2016].

Rushworth, S. a., Bowles, K.M. & MacEwan, D.J., 2011. High basal nuclear levels of Nrf2 in acute myeloid leukemia reduces sensitivity to proteasome inhibitors. *Cancer research*, 71(5), pp.1999–2009. Available at: http://www.ncbi.nlm.nih.gov/pubmed/21212410 [Accessed March 16, 2016].

Rustighi, A. et al., 2009. The prolyl-isomerase Pin1 is a Notch1 target that enhances Notch1 activation in cancer. *Nature cell biology*, 11(2), pp.133–42. Available at: http://dx.doi.org/10.1038/ncb1822 [Accessed March 20, 2016].

Sasaki, H. et al., 2013. Genotype analysis of the NRF2 gene mutation in lung cancer. *International journal of molecular medicine*, 31(5), pp.1135–8. Available at: http://www.ncbi.nlm.nih.gov/pubmed/23545629 [Accessed March 15, 2016].

Schmid, P. et al., 2008. A phase I/II study of bortezomib and capecitabine in patients with metastatic breast cancer previously treated with taxanes and/or anthracyclines. *Annals of oncology : official journal of the European Society for Medical Oncology / ESMO*, 19(5), pp.871–6. Available at: http://www.ncbi.nlm.nih.gov/pubmed/18209010 [Accessed March 24, 2016].

Scian, M.J. et al., 2005. Tumor-derived p53 mutants induce NF-kappaB2 gene expression. *Molecular and cellular biology*, 25(22), pp.10097–110. Available at: http://mcb.asm.org/content/25/22/10097 [Accessed March 21, 2016].

Selivanova, G. et al., 1997. Restoration of the growth suppression function of mutant p53 by a synthetic peptide derived from the p53 C-terminal domain. *Nature Medicine*, 3(6), pp.632–638. Available at: http://dx.doi.org/10.1038/nm0697-632 [Accessed March 13, 2016].

Shah, S.P. et al., 2012. The clonal and mutational evolution spectrum of primary triple-negative breast cancers. *Nature*, 486(7403), pp.395–399. Available at: http://dx.doi.org/10.1038/nature10933.

Shetzer, Y. et al., 2014. The onset of p53 loss of heterozygosity is differentially induced in various stem cell types and may involve the loss of either allele. *Cell death and differentiation*, 21(9), pp.1419–31. Available at: http://dx.doi.org/10.1038/cdd.2014.57 [Accessed March 9, 2016].

Shibata, T. et al., 2008. Cancer related mutations in NRF2 impair its recognition by Keap1-Cul3 E3 ligase and promote malignancy. *Proceedings of the National Academy of Sciences of the United States of America*, 105(36), pp.13568–73. Available at: http://www.pubmedcentral.nih.gov/articlerender.fcgi?artid=2533230&tool=pmcentrez&rendertype=abstract [Accessed January 27, 2016].

Shibata, T. et al., 2010. Global downstream pathway analysis reveals a dependence of oncogenic NF-E2-related factor 2 mutation on the mTOR growth signaling pathway. *Cancer research*, 70(22), pp.9095–105. Available at: http://www.ncbi.nlm.nih.gov/pubmed/21062981 [Accessed March 14, 2016].

Shirozu, R., Yashiroda, H. & Murata, S., 2015. Identification of minimum Rpn4-responsive elements in genes related to proteasome functions. *FEBS letters*, 589(8), pp.933–40. Available at: http://www.ncbi.nlm.nih.gov/pubmed/25747386 [Accessed March 21, 2016].

Sidera, K. & Patsavoudi, E., 2014. HSP90 inhibitors: current development and potential in cancer therapy. *Recent patents on anti-cancer drug discovery*, 9(1), pp.1–20. Available at: http://www.eurekaselect.com/108016/article [Accessed March 14, 2016].

Singh, A. et al., 2010. Gain of Nrf2 function in non-small-cell lung cancer cells confers radioresistance. *Antioxidants & redox signaling*, 13(11), pp.1627–37. Available at: http://www.pubmedcentral.nih.gov/articlerender.fcgi?artid=3541552&tool=pmcentrez&rendertype=abstract [Accessed March 15, 2016].

Sjöblom, T. et al., 2006. The consensus coding sequences of human breast and colorectal cancers. *Science (New York, N.Y.)*, 314(5797), pp.268–74. Available at: http://www.ncbi.nlm.nih.gov/pubmed/16959974 [Accessed July 19, 2014].

Solomon, H. et al., 2012. Various p53 mutant proteins differently regulate the Ras circuit to induce a cancer-related gene signature. *Journal of cell science*, 125(Pt 13), pp.3144–52. Available at: http://www.ncbi.nlm.nih.gov/pubmed/22427690 [Accessed March 3, 2016].

Song, H., Hollstein, M. & Xu, Y., 2007. p53 gain-of-function cancer mutants induce genetic instability by inactivating ATM. *Nature cell biology*, 9(5), pp.573–80. Available at: http://dx.doi.org/10.1038/ncb1571 [Accessed March 9, 2016].

Sorrentino, G. et al., 2014. Metabolic control of YAP and TAZ by the mevalonate pathway. *Nature Cell Biology*, 16(4), pp.357–366. Available at: http://eutils.ncbi.nlm.nih.gov/entrez/eutils/elink.fcgi?dbfrom=pubmed&id=24658687&retmode=ref&cmd=prlinks\npapers2://publication/doi/10.1038/ncb2936.

Soussi, T., 2011. TP53 mutations in human cancer: database reassessment and prospects for the next decade. *Advances in cancer research*, 110, pp.107–39. Available at: http://www.sciencedirect.com/science/article/pii/B9780123864697000050 [Accessed March 9, 2016].

Sporn, M.B., Liby, K.T. & Michael B. Sporn and Karen T. Liby, 2012. NRF2 and cancer: the good, the bad and the importance of context. *Nature reviews. Cancer*, 12(8), pp.564–71. Available at: http://www.pubmedcentral.nih.gov/articlerender.fcgi?artid=3836441&tool=pmcentrez&rendertype=abstract.

Stambolsky, P. et al., 2010. Modulation of the Vitamin D3 Response by Cancer-Associated Mutant p53. *Cancer Cell*, 17(3), pp.273–285. Available at:

http://dx.doi.org/10.1016/j.ccr.2009.11.025.

Steffen, J. et al., 2010. Proteasomal degradation is transcriptionally controlled by TCF11 via an ERAD-dependent feedback loop. *Molecular Cell*, 40(1), pp.147–158.

Stiewe, T., 2007. The p53 family in differentiation and tumorigenesis. *Nature reviews. Cancer*, 7(3), pp.165–8. Available at: http://www.ncbi.nlm.nih.gov/pubmed/17332760 [Accessed March 31, 2016].

Sun, Z., Chin, Y.E. & Zhang, D.D., 2009. Acetylation of Nrf2 by p300/CBP Augments Promoter-Specific DNA Binding of Nrf2 during the Antioxidant Response. *Molecular and Cellular Biology*, 29(10), pp.2658–2672. Available at: http://mcb.asm.org/cgi/doi/10.1128/MCB.01639-08.

Sun, Z., Huang, Z. & Zhang, D.D., 2009. Phosphorylation of Nrf2 at multiple sites by MAP kinases has a limited contribution in modulating the Nrf2-dependent antioxidant response. *PLoS ONE*, 4(8).

Syu, J., Chi, J. & Kung, H., 2016. Nrf2 is the key to chemotherapy resistance in MCF7 breast cancer cells under hypoxia.

Tal, P. et al., 2016. Cancer therapeutic approach based on conformational stabilization of mutant p53 protein by small peptides. , 7(11).

Tan, K.P. et al., 2008. NRF2 as a determinant of cellular resistance in retinoic acid cytotoxicity. *Free Radical Biology and Medicine*, 45(12), pp.1663–1673. Available at: http://dx.doi.org/10.1016/j.freeradbiomed.2008.09.010.

Terzian, T. et al., 2008. The inherent instability of mutant p53 is alleviated by Mdm2 or p16 INK4a loss. *Genes and Development*, 22(10), pp.1337–1344.

Toledo, F. & Wahl, G.M., 2006. Regulating the p53 pathway: in vitro hypotheses, in vivo veritas. *Nature reviews. Cancer*, 6(12), pp.909–23.

Tonelli, C. et al., 2015. Genome-wide analysis of p53 transcriptional programs in B cells upon exposure to genotoxic stress in vivo. *Oncotarget*, 6(28), pp.24611–26.

Available at: http://www.pubmedcentral.nih.gov/articlerender.fcgi?artid=4694782&tool=pmcentrez&rendertype=abstract [Accessed March 20, 2016].

Tong, K.I. et al., 2007. Different electrostatic potentials define ETGE and DLG motifs as hinge and latch in oxidative stress response. *Molecular and cellular biology*, 27(21), pp.7511–21. Available at: http://www.pubmedcentral.nih.gov/articlerender.fcgi?artid=2169061&tool=pmcentrez&rendertype=abstract [Accessed March 16, 2016].

Turner, N. et al., 2013. Targeting triple negative breast cancer: Is p53 the answer? *Cancer Treatment Reviews*, 39(5), pp.541–550. Available at: http://dx.doi.org/10.1016/j.ctrv.2012.12.001.

Valenti, F. et al., 2011. Mutant p53 oncogenic functions are sustained by Plk2 kinase through an autoregulatory feedback loop. *Cell cycle (Georgetown, Tex.)*, 10(24), pp.4330–40. Available at: http://www.ncbi.nlm.nih.gov/pubmed/22134238 [Accessed March 31, 2016].

Vangala, J.R. et al., 2014. Regulation of PSMB5 protein and β subunits of mammalian proteasome by constitutively activated signal transducer and activator of transcription 3 (STAT3): potential role in bortezomib-mediated anticancer therapy. *The Journal of biological chemistry*, 289(18), pp.12612–22. Available at: http://www.pubmedcentral.nih.gov/articlerender.fcgi?artid=4007451&tool=pmcentrez&rendertype=abstract [Accessed March 20, 2016].

Varley, J.M., 2003. Germline TP53 mutations and Li-Fraumeni syndrome. *Human mutation*, 21(3), pp.313–20. Available at: http://www.ncbi.nlm.nih.gov/pubmed/12619118 [Accessed March 9, 2016].

Vousden, K.H. & Prives, C., 2009. Blinded by the Light: The Growing Complexity of p53. *Cell*, 137(3), pp.413–431. Available at: http://linkinghub.elsevier.com/retrieve/pii/S0092867409004590.

Wakabayashi, N. et al., 2014. Notch-Nrf2 axis: regulation of Nrf2 gene expression and cytoprotection by notch signaling. *Molecular and cellular biology*, 34(4), pp.653–

63. Available at: http://www.pubmedcentral.nih.gov/articlerender.fcgi?artid=3911489&tool=pmcentrez&rendertype=abstract [Accessed March 14, 2016].

Wakabayashi, N. et al., 2010. When NRF2 talks, who's listening? *Antioxidants & redox signaling*, 13(11), pp.1649–1663.

Walerych, D. et al., 2012. The rebel angel: mutant p53 as the driving oncogene in breast cancer. *Carcinogenesis*, 33(11), pp.2007–2017. Available at: http://www.carcin.oxfordjournals.org/cgi/doi/10.1093/carcin/bgs232.

Walerych, D., Lisek, K. & Del Sal, G., 2015. Mutant p53: One, No One, and One Hundred Thousand. *Frontiers in Oncology*, 5(December), p.289. Available at: http://www.pubmedcentral.nih.gov/articlerender.fcgi?artid=4685664&tool=pmcentrez&rendertype=abstract.

Wang, H. et al., 2013. RXRα inhibits the NRF2-ARE signaling pathway through a direct interaction with the Neh7 domain of NRF2. *Cancer Research*, 73(10), pp.3097–3108.

Wang, Q. et al., 2013. Nrf2 is associated with the regulation of basal transcription activity of the BRCA1 gene. *Acta Biochimica et Biophysica Sinica*, 45(3), pp.179–187.

Wang, X.J. et al., 2008. Nrf2 enhances resistance of cancer cells to chemotherapeutic drugs, the dark side of Nrf2. *Carcinogenesis*, 29(6), pp.1235–1243.

Wei, S. et al., 2015. Active Pin1 is a key target of all-trans retinoic acid in acute promyelocytic leukemia and breast cancer. *Nature medicine*, 21(5), pp.457–66. Available at: http://www.ncbi.nlm.nih.gov/pubmed/25849135 [Accessed March 13, 2016].

Weissmueller, S. et al., 2014. Mutant p53 Drives Pancreatic Cancer Metastasis through Cell-Autonomous PDGF Receptor β Signaling. *Cell*, 157(2), pp.382–394. Available at: http://www.cell.com/article/S0092867414002141/fulltext [Accessed March 14, 2016].

Weisz, L. et al., 2007. Mutant p53 enhances nuclear factor kappaB activation by tumor necrosis factor alpha in cancer cells. *Cancer research*, 67(6), pp.2396–401. Available at: http://www.ncbi.nlm.nih.gov/pubmed/17363555 [Accessed March 20, 2016].

West, A.C. & Johnstone, R.W., 2014. New and emerging HDAC inhibitors for cancer treatment. *The Journal of clinical investigation*, 124(1), pp.30–9. Available at: http://www.jci.org/articles/view/69738 [Accessed May 25, 2015].

Xiong, S. et al., 2014. Pla2g16 phospholipase mediates gain-of-function activities of mutant p53. *Proceedings of the National Academy of Sciences of the United States of America*, 111(30), pp.11145–50. Available at: http://www.pnas.org/content/111/30/11145 [Accessed March 21, 2016].

Xu, H. et al., 2012. The CCAAT box-binding transcription factor NF-Y regulates basal expression of human proteasome genes. *Biochimica et biophysica acta*, 1823(4), pp.818–25. Available at: http://www.ncbi.nlm.nih.gov/pubmed/22285817 [Accessed March 20, 2016].

Yamamoto, S. et al., 2014. The impact of miRNA-based molecular diagnostics and treatment of NRF2-stabilized tumors. *Molecular cancer research : MCR*, 12(1), pp.58–68. Available at: http://www.ncbi.nlm.nih.gov/pubmed/24307696.

Yan, W. et al., 2014. Arsenic trioxide reactivates proteasome-dependent degradation of mutant p53 protein in cancer cells in part via enhanced expression of Pirh2 E3 ligase. *PLoS ONE*, 9(8), pp.3–10.

Yan, W. et al., 2013. Histone deacetylase inhibitors suppress mutant p53 transcription via histone deacetylase 8. *Oncogene*, 32(5), pp.599–609. Available at: http://dx.doi.org/10.1038/onc.2012.81 [Accessed March 13, 2016].

Yan, W. & Chen, X., 2010. Characterization of functional domains necessary for mutant p53 gain of function. *The Journal of biological chemistry*, 285(19), pp.14229–38. Available at: http://www.jbc.org/content/285/19/14229 [Accessed March 7, 2016].

Yap, D.B.S. et al., 2004. Ser392 phosphorylation regulates the oncogenic function of mutant p53. *Cancer research*, 64(14), pp.4749–54. Available at: http://www.ncbi.nlm.nih.gov/pubmed/15256442 [Accessed March 31, 2016].

Ye, P. et al., 2014. Nrf2- and ATF4-dependent upregulation of xCT modulates the sensitivity of T24 bladder carcinoma cells to proteasome inhibition. *Molecular and cellular biology*, 34(18), pp.3421–34. Available at: http://www.pubmedcentral.nih.gov/articlerender.fcgi?artid=4135628&tool=pmcentrez&rendertype=abstract [Accessed March 15, 2016].

You, A. et al., 2011. Transcription factor Nrf2 maintains the basal expression of Mdm2: An implication of the regulation of p53 signaling by Nrf2. *Archives of biochemistry and biophysics*, 507(2), pp.356–64. Available at: http://www.ncbi.nlm.nih.gov/pubmed/21211512 [Accessed February 17, 2016].

Younger, S.T. et al., 2015. Integrative genomic analysis reveals widespread enhancer regulation by p53 in response to DNA damage. *Nucleic acids research*, 43(9), pp.4447–62. Available at: http://www.pubmedcentral.nih.gov/articlerender.fcgi?artid=4482066&tool=pmcentrez&rendertype=abstract [Accessed March 21, 2016].

Zache, N. et al., 2008. PRIMA-1MET inhibits growth of mouse tumors carrying mutant p53. *Cellular oncology : the official journal of the International Society for Cellular Oncology*, 30(5), pp.411–8. Available at: http://www.pubmedcentral.nih.gov/articlerender.fcgi?artid=4618963&tool=pmcentrez&rendertype=abstract [Accessed March 13, 2016].

Zhang, C. et al., 2013. Tumour-associated mutant p53 drives the Warburg effect. *Nature Communications*, 4. Available at: http://www.nature.com/ncomms/2013/131217/ncomms3935/full/ncomms3935.html [Accessed January 11, 2016].

Zhang, D.D. et al., 2004. Keap1 is a redox-regulated substrate adaptor protein for a Cul3-dependent ubiquitin ligase complex. *Molecular and cellular biology*, 24(24), pp.10941–10953. Available at: http://www.ncbi.nlm.nih.gov/pubmed/15572695.

Zhang, J. et al., 2006. p16INK4a modulates p53 in primary human mammary epithelial cells. *Cancer research*, 66(21), pp.10325–31. Available at: http://www.ncbi.nlm.nih.gov/pubmed/17079452 [Accessed March 12, 2016].

Zhang, Y., Yan, W. & Chen, X., 2011. Mutant p53 disrupts MCF-10A cell polarity in three-dimensional culture via epithelial-to-mesenchymal transitions. *Journal of Biological Chemistry*, 286(18), pp.16218–16228.

Zhu, J. et al., 2015. Gain-of-function p53 mutants co-opt chromatin pathways to drive cancer growth. *Nature*, 525(7568), pp.206–11. Available at: http://www.ncbi.nlm.nih.gov/pubmed/26331536\nhttp://www.pubmedcentral.nih.gov/articlerender.fcgi?artid=PMC4568559 [Accessed February 12, 2016].

Zucker, S.N. et al., 2014. Nrf2 amplifies oxidative stress via induction of Klf9. *Molecular Cell*, 53(6), pp.916–928. Available at: http://dx.doi.org/10.1016/j.molcel.2014.01.033.

# FIGURES

# FIGURE 1

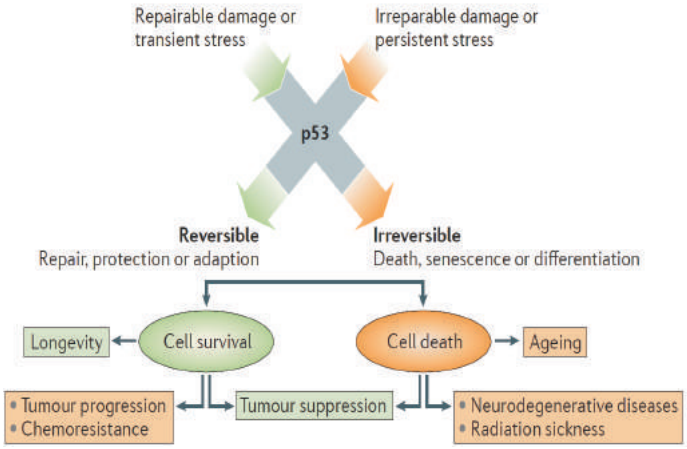


**Figure 1. p53 as an integrator of cellular stress.**

p53 functions to integrate signals from different types of cellular stress and subsequently promotes the appropriate biological response, which can lead to cell survival or cell death. In the case of repairable damage or transient stress, a reversible process is activated that allows for damage repair and/or adaptation in response to the change in environment. However, when the stress stimulus is persistent and irreparable, the affected cell is permanently removed from the pool of proliferating cells through cell death, senescence or the induction of terminal differentiation. Although both responses can promote tumour suppression, uncoupled or deregulated survival functions can contribute to tumour progression and chemoresistance.

(Kruiswijk et al., 2015)

# FIGURE 2

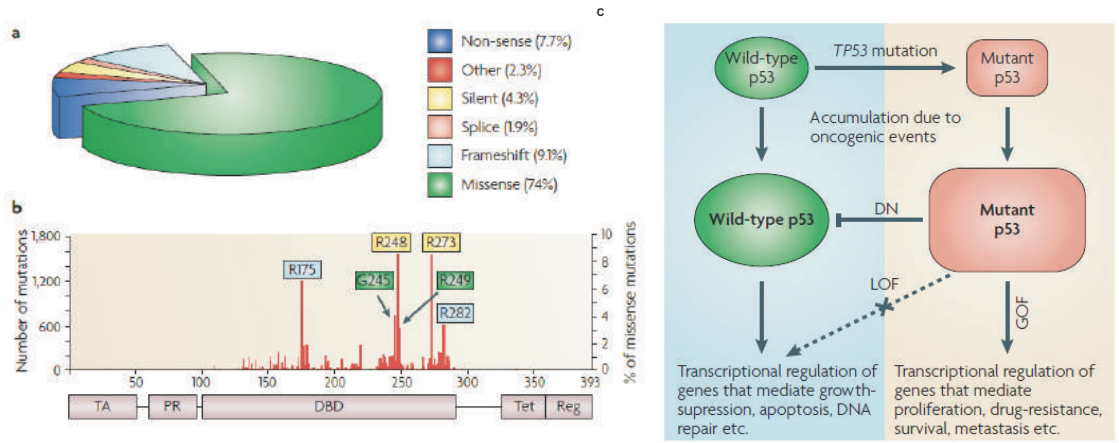


**Figure 2. Mutations in p53**

A: the different tumor-derived mutation types. B: the distribution of reported missense mutations along 393 amino-acid sequence of p53. The six most common hotspot mutations are highlighted in yellow for DNA-contact mutations, green for locally distorted mutants and blue for globally denatured mutants. C: phenotypic effects of *TP53* mutations.

Ab: LOF (loss-of-function); DN (dominant-negative effects); GOF (gain-of-function).

(Brosh & Rotter, 2009)

## FIGURE 3

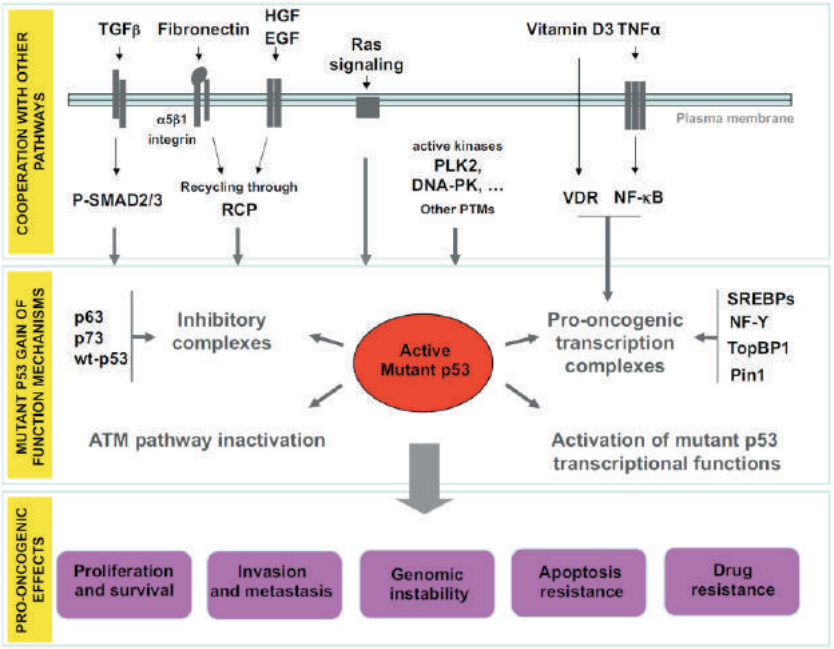


**Figure 3. Summary of the proposed mechanisms for mutant p53 oncogenic function.**

The upper panel shows the pathways that cooperate with mutant p53 pro-oncogenicmechanisms and signals or interactors that are required for its activation. The middle panel shows a schematic representation of the proposed molecular mechanisms ofmutant p53 gain of function (GOF). In the bottom panel the biological effects of mutant p53 function are indicated (see text for details). Membrane receptors for the indicatedsignaling molecules are depicted in dark gray; a double line represents the plasma membrane. PTMs: posttranslational modifications; P-SMAD2/3: phosphorylated SMAD2o SMAD3.

(Girrardini et al., 2014)

## FIGURE 4

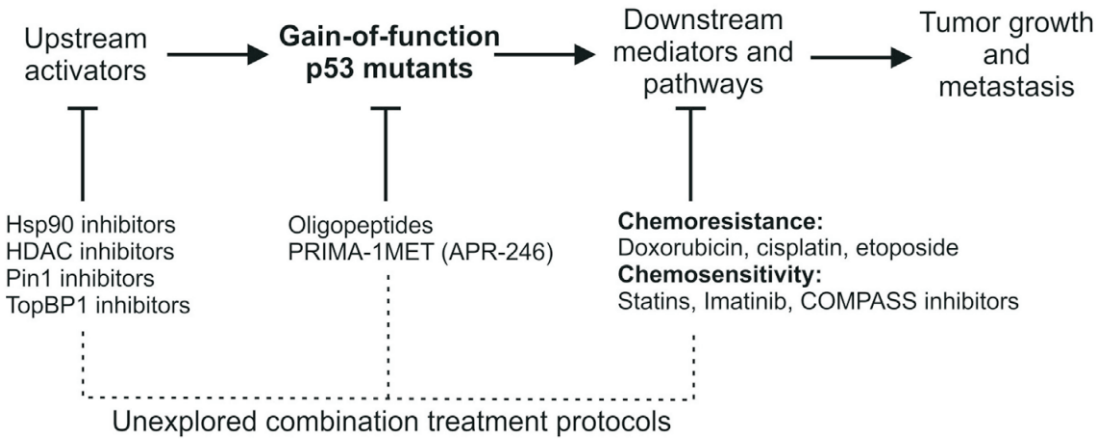


**Figure 4. Therapeutic strategies to target mtp53 bearing tumors.**

A schematic view of gain-of-function mutant p53 activation, mutant p53 downstream effectors/pathways, and therapeutic opportunities of targeting each of the processes. Below the largely unexplored possibilities of mutant p53-related combinational anti-cancer therapies are suggested.

(Walerych, Lisek, Del Sal, 2015)

## FIGURE 5

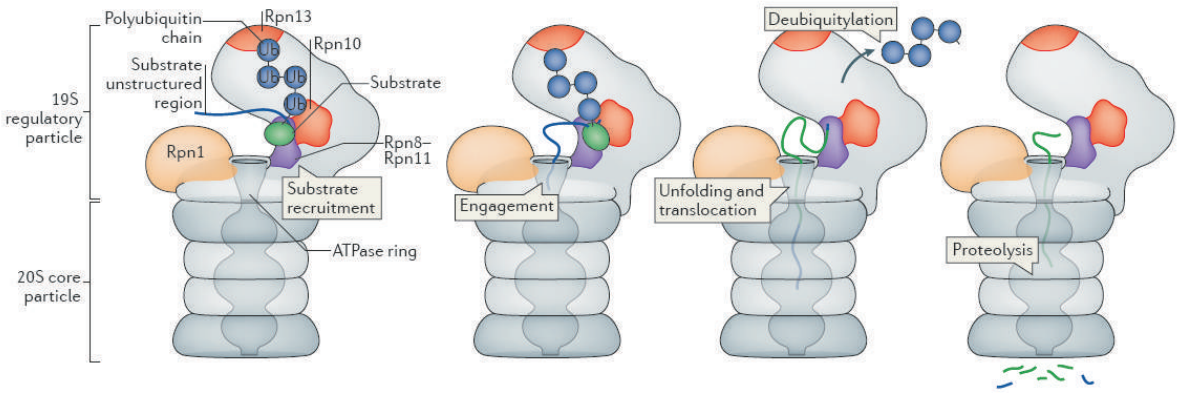


**Figure 5. Steps of proteasomal degradation.**

The proteasome recognizes ubiquitin tags in substrates through its receptors (here regulatory particle non-ATPase 10 (Rpn10) and (Rpn13) and then initiates degradation at an unstructured region in the substrate. As the ATPase motors pull the substrate into the degradation channel, the ubiquitin chain is cleaved off, the substrate unfolds and is finally cleaved into peptides.

(Bhattacharyya et al., 2014)

## FIGURE 6

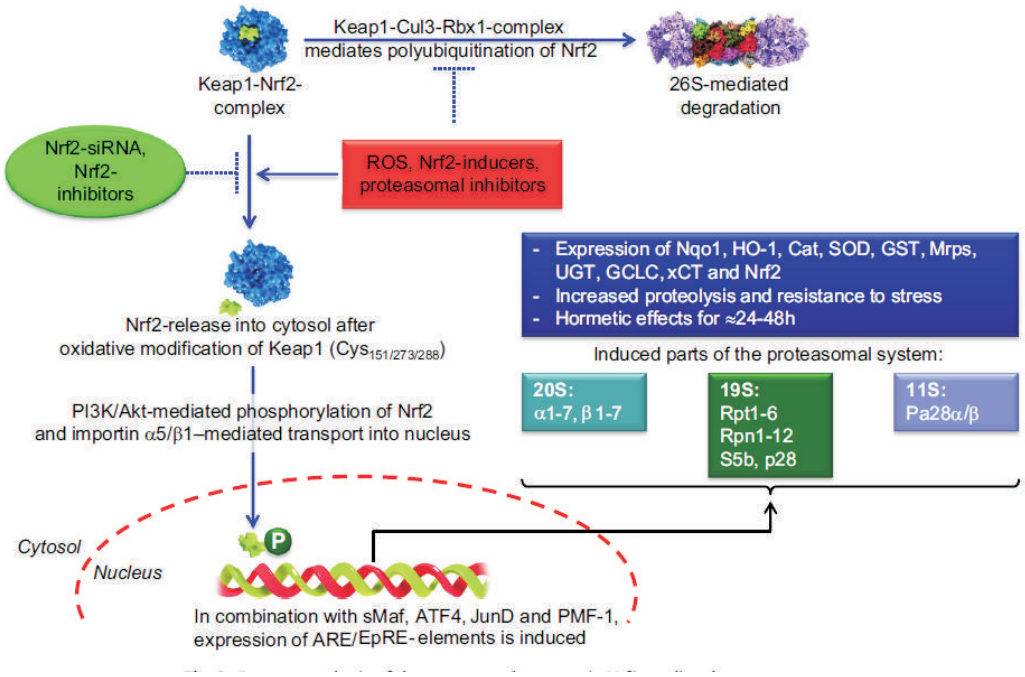


**Figure 6. *De novo* synthesis of the proteasomal system via Nrf2-mediated stress-response.**

NRF2 controls a battery of genes encoding for proteasomal subunits of both the 20S core and the 19S regulatory particle are targets direct targets of NRF2. Both 20S and 19S proteasome encoding genes possess the ARE-like sequence in their promoters. When present in nucleus NRF2 my play its TF role in transacticating the PSM encoding genes together with other targets including the oxidative stress response genes like MRPs, NQO1, HO-1, GCLC etc.

(Jung et al., 2013)

# FIGURE 7

Basal:

Induced:

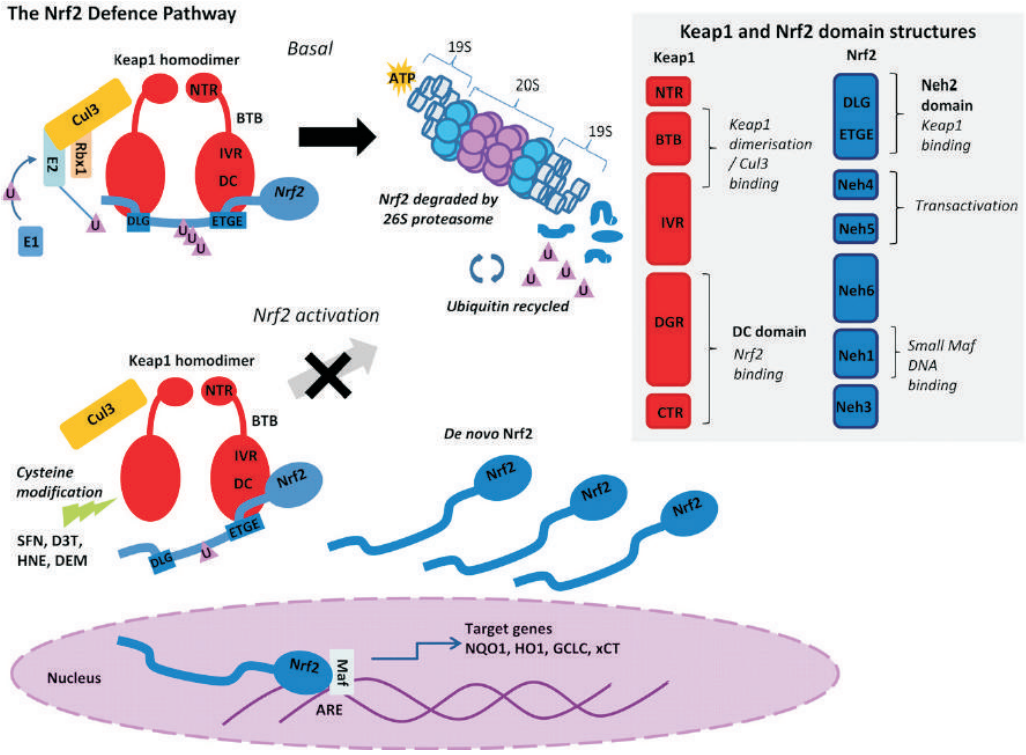


**Fiugre 7. The Nrf2–Keap1 defense pathway.**

Under basal conditions, Nrf2 binds to the adaptor protein Keap1 present in the cytosol and becomes polyubiquitinated by a Cullin E3 ubiquitin ligase complex, targeting Nrf2 for degradation by the 26S proteasome. Ubiquitin requires activation by an E1 activating enzyme, with ubiquitin transferred by an E2 conjugating enzyme to the E3 ligase complex (consisting of Nrf2, Keap1, Cullin3 and Rbx1). Stress agents (e.g. HNE, SFN, DEM, D3T) induce Nrf2 activation through the oxidation of specific redox-sensitive cysteine residues on Keap1. This disrupts Keap1–Nrf2 interactions, preventing Nrf2 ubiquitination and subsequent degradation and thereby depletes the 'free' Keap1 pool. De novo synthesis of Nrf2 then leads to accumulation and translocation of Nrf2 to the nucleus, where it heterodimerises with other transcription factors such as small Maf proteins and binds the ARE/EpRE consensus sequence to initiate transcription of protective phase II and antioxidant genes. Key domain structures of Nrf2 and Keap1 are shown in the inset panel (right). Abbreviations: N-terminal region (NTR); broad complex, tramtrack and bric a brac domain (BTB); intervening region (IVR); DGR and CTR domain (DC); double glycine repeat or Kelch repeat (DGR); C-terminal region (CTR); Nrf2 ECH homology (Neh); Cullin E3 ubiquitin ligase complex (Cul3); ubiquitin (U); 4-hydroxynonenal (HNE); sulforaphane (SFN); diethylmaleate (DEM); dithiolethione 3-H-1,2-dithiole-3-thione (D3T).

(Chapple et al. 2012)

# FIGURE 8

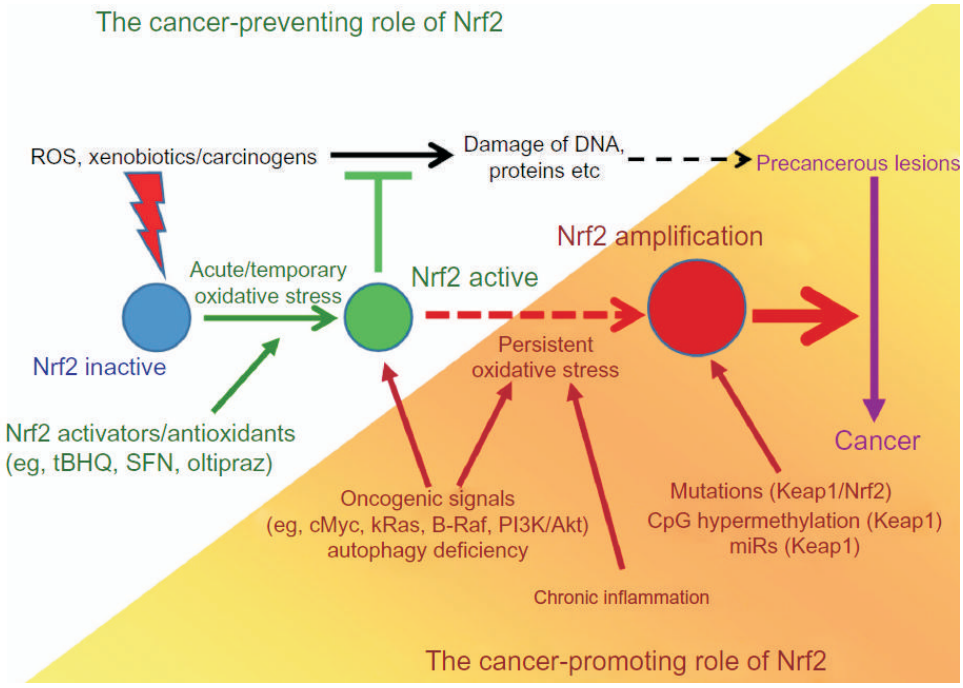


**Figure 8. Two modes of action of Nrf2**

As long as it is kept under homeostatic control, Nrf2 activation protects cellular components like DNA from damaging insults arising from acute/temporary oxidative and xenobiotic stress. In this way, Nrf2 prevents tumor development. When deregulated by 1) epigenetic and genetic alterations affecting the Keap1–Nrf2 pathway, 2) persistent stress conditions, and/or 3) oncogenic pathways, Nrf2 activation facilitates the growth and survival of transformed cells, thus promoting tumorigenesis. Abbreviations: ROS, reactive oxygen species; DNA, deoxyribonucleic acid; tBHQ, tert-butylhydroquinone; SFN, sulforaphane

(Geisman et al., 2014)

# FIGURE 9

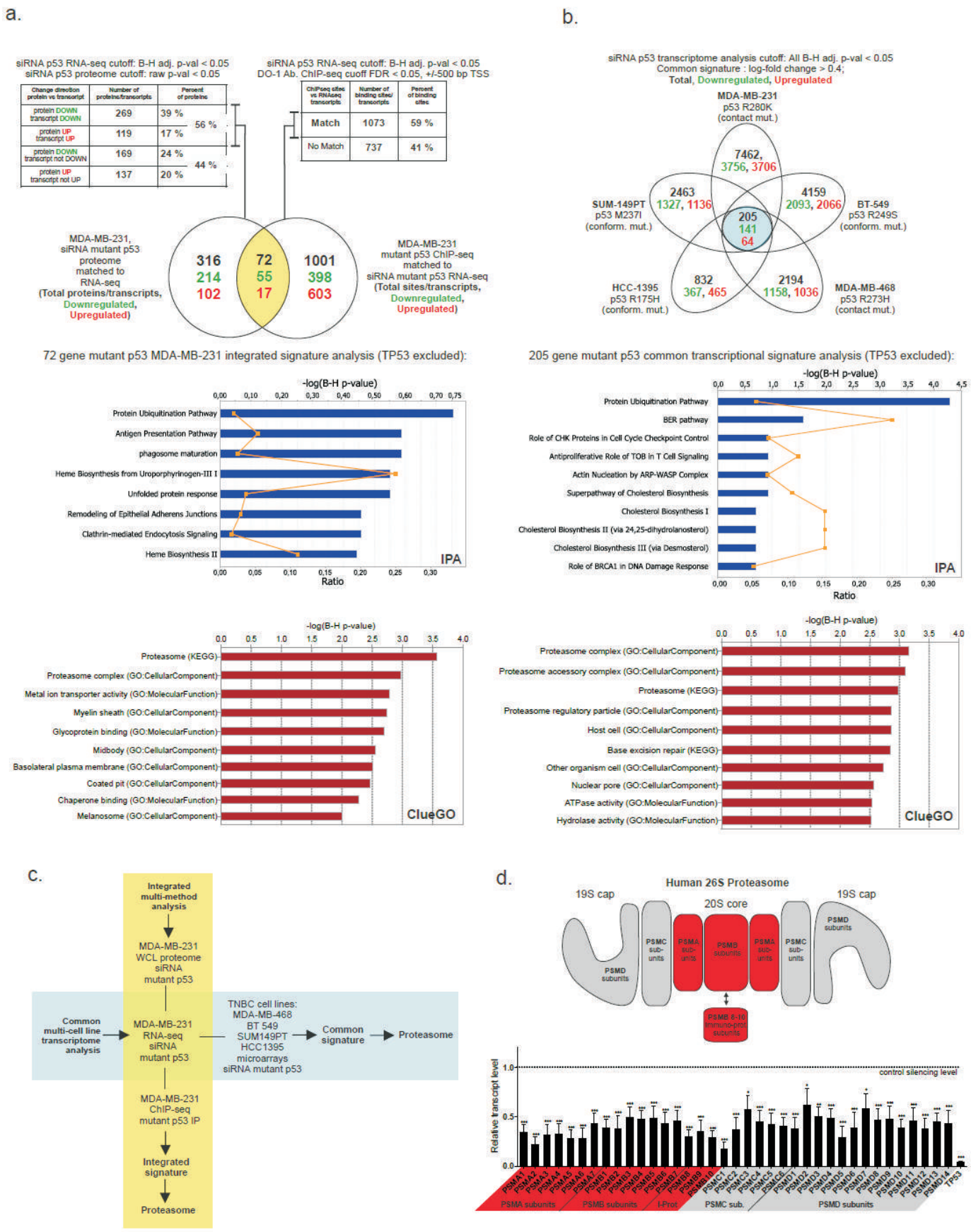
a.
siRNA p53 RNA-seq cutoff: B-H adj. p-val < 0.05
siRNA p53 proteome cutoff: raw p-val < 0.05
Change direction protein vs transcript
Number of proteins/transcripts
Percent of proteins
protein DOWN transcript DOWN
269
39 %
56 %
protein UP transcript UP
119
17 %
protein DOWN transcript not DOWN
169
24 %
44 %
protein UP transcript not UP
137
20 %
siRNA p53 RNA-seq cutoff: B-H adj. p-val < 0.05
DO-1 Ab. ChIP-seq cuoff FDR < 0.05, +/-500 bp TSS
ChIPseq sites vs RNAseq transcripts
Number of binding sites/ transcripts
Percent of binding sites
Match
1073
59 %
No Match
737
41 %
MDA-MB-231, siRNA mutant p53 proteome matched to RNA-seq (Total proteins/transcripts, Downregulated, Upregulated)
316
214
102
72
55
17
1001
398
603
MDA-MB-231 mutant p53 ChIP-seq matched to siRNA mutant p53 RNA-seq (Total sites/transcripts, Downregulated, Upregulated)
b.
siRNA p53 transcriptome analysis cutoff: All B-H adj. p-val < 0.05
Common signature : log-fold change > 0.4;
Total, Downregulated, Upregulated
MDA-MB-231
p53 R280K
(contact mut.)
7462,
3756, 3706
SUM-149PT
p53 M237I
(conform. mut.)
2463
1327, 1136
BT-549
p53 R249S
(conform. mut.)
4159
2093, 2066
205
141
64
HCC-1395
p53 R175H
(conform. mut.)
832
367, 465
MDA-MB-468
p53 R273H
(contact mut.)
2194
1158, 1036
72 gene mutant p53 MDA-MB-231 integrated signature analysis (TP53 excluded):
-log(B-H p-value)
Protein Ubiquitination Pathway
Antigen Presentation Pathway
phagosome maturation
Heme Biosynthesis from Uroporphyrinogen-III I
Unfolded protein response
Remodeling of Epithelial Adherens Junctions
Clathrin-mediated Endocytosis Signaling
Heme Biosynthesis II
IPA
Ratio
-log(B-H p-value)
Proteasome (KEGG)
Proteasome complex (GO:CellularComponent)
Metal ion transporter activity (GO:MolecularFunction)
Myelin sheath (GO:CellularComponent)
Glycoprotein binding (GO:MolecularFunction)
Midbody (GO:CellularComponent)
Basolateral plasma membrane (GO:CellularComponent)
Coated pit (GO:CellularComponent)
Chaperone binding (GO:MolecularFunction)
Melanosome (GO:CellularComponent)
ClueGO
205 gene mutant p53 common transcriptional signature analysis (TP53 excluded):
-log(B-H p-value)
Protein Ubiquitination Pathway
BER pathway
Role of CHK Proteins in Cell Cycle Checkpoint Control
Antiproliferative Role of TOB in T Cell Signaling
Actin Nucleation by ARP-WASP Complex
Superpathway of Cholesterol Biosynthesis
Cholesterol Biosynthesis I
Cholesterol Biosynthesis II (via 24,25-dihydrolanosterol)
Cholesterol Biosynthesis III (via Desmosterol)
Role of BRCA1 in DNA Damage Response
IPA
Ratio
-log(B-H p-value)
Proteasome complex (GO:CellularComponent)
Proteasome accessory complex (GO:CellularComponent)
Proteasome (KEGG)
Proteasome regulatory particle (GO:CellularComponent)
Host cell (GO:CellularComponent)
Base excision repair (KEGG)
Other organism cell (GO:CellularComponent)
Nuclear pore (GO:CellularComponent)
ATPase activity (GO:MolecularFunction)
Hydrolase activity (GO:MolecularFunction)
ClueGO
c.
Integrated multi-method analysis
MDA-MB-231 WCL proteome siRNA mutant p53
Common multi-cell line transcriptome analysis
MDA-MB-231 RNA-seq siRNA mutant p53
TNBC cell lines: MDA-MB-468 BT 549 SUM149PT HCC1395 microarrays siRNA mutant p53
Common signature
Proteasome
MDA-MB-231 ChIP-seq mutant p53 IP
Integrated signature
Proteasome
d.
Human 26S Proteasome
19S cap
20S core
19S cap
PSMD subunits
PSMC sub-units
PSMA sub-units
PSMB subunits
PSMA sub-units
PSMC sub-units
PSMD subunits
PSMB 8-10 immuno-prot subunits
Relative transcript level
control silencing level
PSMA1 PSMA2 PSMA3 PSMA4 PSMA5 PSMA6 PSMA7 PSMB1 PSMB2 PSMB3 PSMB4 PSMB5 PSMB6 PSMB7 PSMB8 PSMB9 PSMB10 PSMC1 PSMC2 PSMC3 PSMC4 PSMC5 PSMC6 PSMD1 PSMD2 PSMD3 PSMD4 PSMD5 PSMD6 PSMD7 PSMD8 PSMD9 PSMD10 PSMD11 PSMD12 PSMD13 PSMD14 TP53
PSMA subunits
PSMB subunits
I-Prot
PSMC sub.
PSMD subunits

**Figure 9. Proteasome is the most affected and conserved pathway controlled by missense mutant p53 variants in TNBC cell lines**

a. An integrated analysis of the mutant p53 program muti-omic data from MDA-MB-231 cell line with indicated cutoffs used. The top left table shows matching of the proteomic and RNA-seq transcriptomic data upon mutant *TP53* silencing (proteomics: n=4 for each condition, raw p-value $p<0.05$; RNA-seq: n=3 for each condition, B-H adj. p-value $p<0.05$). The top right table shows matching of ChIP-seq peaks (DO-1 immunoprecipitation, cutoff for called peaks: FDR<0.05, +/- 500bp of the adjacent TSS) to RNA-seq transcriptomic data upon mutant *TP53* silencing (n=3 for each condition, B-H adj. p-value $p<0.05$). Transcripts in agreement with protein level changes (corresponding to a majority of significantly changing proteins) and ChIP-seq peaks (corresponding to a majority of significant peaks +/- 500bp of the adjacent TSSes) are overlapped in the Venn diagram, resulting in the integrated 72-gene signature. The signature is further analyzed by the pathway association: IPA pathways (upper graph; bars – log (B-H adjusted p-values of the pathway association), line – ratios of the number of found genes to the total number of genes in the pathways) and ClueGO top enriched KEGG pathways/GO-terms (lower table; bars –log (B-H adjusted p-values of the pathway association)).

b. Venn diagram of the multi-transcriptome analysis in the indicated 5 TNBC cell lines with the silenced listed *TP53* mutants (n=3 for each cell line and condition, B-H adj. p-value $p<0.05$) and the 205-gene common signature pathway association results, as in a. c. Scheme of the used multi-omic mutant p53 gain-of-function high-throughput analyses in the TNBC cell lines presented in a and b;

d. Human 26S proteasome and immunoproteasome (shown schematically in the top picture) subunit gene transcript means levels from 5 TNBC cell lines (as in b) upon two mutant *TP53* silencings (bar graph, means of results in 5 cell lines with s.e.m. are shown, ANOVA test with Bonferroni correction: * $p<0.05$, ** $p<0.01$, *** $p<0.001$).

# FIGURE 10

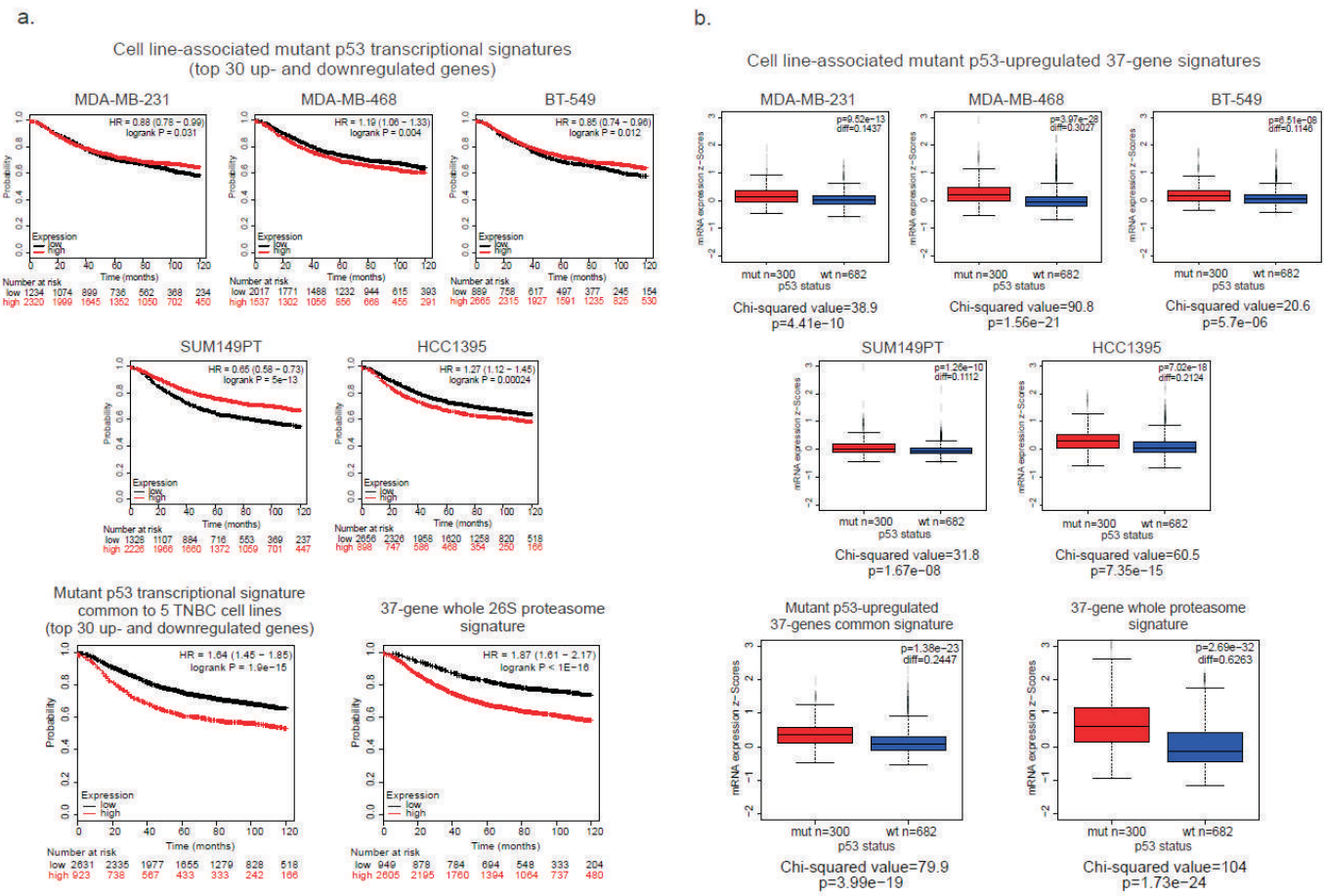
a.
Cell line-associated mutant p53 transcriptional signatures
(top 30 up- and downregulated genes)
MDA-MB-231
HR = 0.68 (0.78 − 0.99)
logrank P = 0.031
MDA-MB-468
HR = 1.19 (1.06 − 1.33)
logrank P = 0.004
BT-549
HR = 0.85 (0.74 − 0.96)
logrank P = 0.012
SUM149PT
HR = 0.65 (0.58 − 0.73)
logrank P = 5e−13
HCC1395
HR = 1.27 (1.12 − 1.45)
logrank P = 0.00024
Mutant p53 transcriptional signature
common to 5 TNBC cell lines
(top 30 up- and downregulated genes)
HR = 1.64 (1.45 − 1.85)
logrank P = 1.9e−15
37-gene whole 26S proteasome
signature
HR = 1.87 (1.61 − 2.17)
logrank P < 1E−16
Probability
Expression
low
high
Time (months)
Number at risk
b.
Cell line-associated mutant p53-upregulated 37-gene signatures
MDA-MB-231
p=9.52e−13
diff=0.1437
MDA-MB-468
p=3.97e−29
diff=0.3027
BT-549
p=6.51e−08
diff=0.1146
mRNA expression z-Scores
mut n=300
wt n=682
p53 status
Chi-squared value=38.9
p=4.41e−10
Chi-squared value=90.8
p=1.56e−21
Chi-squared value=20.6
p=5.7e−06
SUM149PT
p=1.26e−10
diff=0.1112
HCC1395
p=7.02e−18
diff=0.2124
Chi-squared value=31.8
p=1.67e−08
Chi-squared value=60.5
p=7.35e−15
Mutant p53-upregulated
37-genes common signature
p=1.38e−23
diff=0.2447
37-gene whole proteasome
signature
p=2.69e−32
diff=0.6263
Chi-squared value=79.9
p=3.99e−19
Chi-squared value=104
p=1.73e−24

**Figure 10. The proteasome signature is associated with a poor patient prognosis and a mutant *TP53* status in breast cancer**

a. Association of the mutant p53-related signatures derived from 5 indicated TNBC cell lines, the mutant p53-related 205-gene common signature and the 37 genes, "whole proteasome signature" with the survival of breast cancer patients. The red curve ("high") represents the transcript levels in patients matching the level in the presence of mutant p53 in cell line-derived signature, black curve ("low") – expression level not matching the presence of mutant p53 (for cell line and common signatures top 30 genes downregualted and top 30 genes upregulated were used; see Extended Experimental Procedures for analysis details). HR – hazard ratio; log-rank P – log-rank test p-value for the curves comparison. Numbers below graphs indicate number of patients at risk – total and at consecutive time points;

b. Association of the mutant/wt *TP53* status and expression of the indicated 37-gene signatures in breast carcinoma – derived form each cell line individually (upper plots), derived from the common 205-gene transcriptional signature or the 37-gene whole proteasome signature (lower plots). The signatures used were all 37 genes and contain only genes upregulated by mutant p53 to allow a direct comparison with the 37-gene whole proteasome signature - composed of proteasome subunit genes upregulated by mutant p53. Box plots: diff – difference in mean gene expression in mutant vs wt p53 status samples; p-value is derived from Mann–Whitney U test). Below each plot the independence chi-squared ($\chi 2$) test value (for df=1) along with the supporting p-value is shown. The chi-squared test indicates if the mutant p53 status is independent of a high expression of a signature – the higher the value and the lower p-value the less probable the independence.

# FIGURE 11

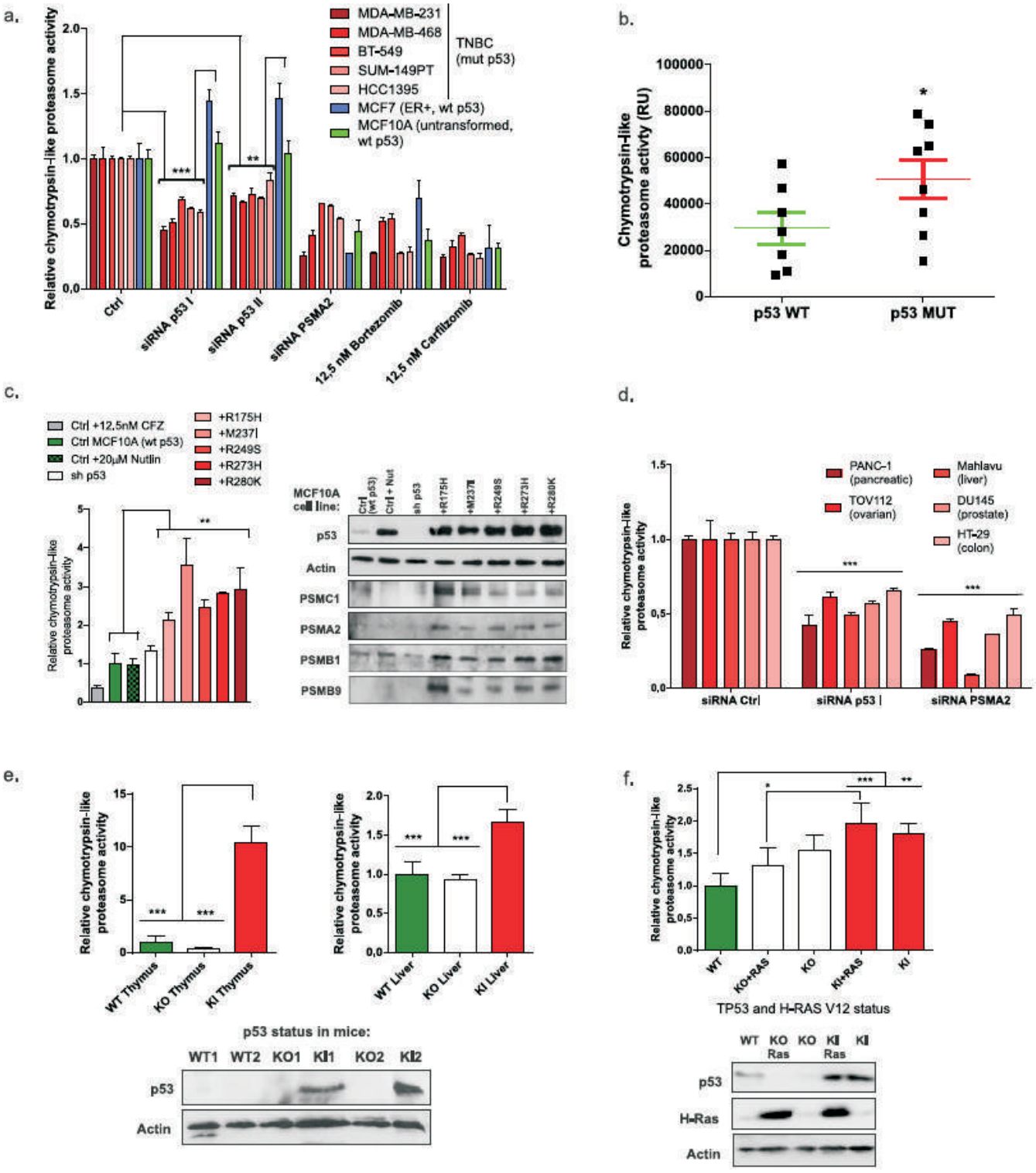
a.
Relative chymotrypsin-like proteasome activity
MDA-MB-231
MDA-MB-468
BT-549
SUM-149PT
HCC1395
TNBC (mut p53)
MCF7 (ER+, wt p53)
MCF10A (untransformed, wt p53)
Ctrl
siRNA p53 I
siRNA p53 II
siRNA PSMA2
12,5 nM Bortezomib
12,5 nM Carfilzomib
b.
Chymotrypsin-like proteasome activty (RU)
p53 WT
p53 MUT
c.
Ctrl +12,5nM CFZ
Ctrl MCF10A (wt p53)
Ctrl +20μM Nutlin
sh p53
+R175H
+M237I
+R249S
+R273H
+R280K
Relative chymotrypsin-like proteasome activity
MCF10A cell line:
p53
Actin
PSMC1
PSMA2
PSMB1
PSMB9
d.
PANC-1 (pancreatic)
TOV112 (ovarian)
Mahlavu (liver)
DU145 (prostate)
HT-29 (colon)
Relative chymotrypsin-like proteasome activity
siRNA Ctrl
siRNA p53 I
siRNA PSMA2
e.
Relative chymotrypsin-like proteasome activity
WT Thymus
KO Thymus
KI Thymus
WT Liver
KO Liver
KI Liver
p53 status in mice:
WT1 WT2 KO1 KI1 KO2 KI2
p53
Actin
f.
Relative chymotrypsin-like proteasome activity
WT
KO+RAS
KO
KI+RAS
KI
TP53 and H-RAS V12 status
WT KO Ras KO KI Ras KI
p53
H-Ras
Actin

**Figure 11. The proteasome activity is elevated in the presence of the GOF p53 mutants in various cancer models**

a. Chymotrypsin-like proteasome activity in 5 mutant p53 TNBC cell lines versus 2 wt p53 cell lines (MCF10A and MCF7) upon silencing of mutant *TP53* or *PSMA2* (48h post silencing) or proteasome inhibitor treatment (24h; Carfilzomib, Bortezomib);

b. Chymotrypsin-like proteasome activity in human basal-like breast cancer primary tumors is on average significantly elevated in association with the with the missense mutant *TP53* status as opposed to the wild-type status. Means with s.e.m are shown; t-test, * $p<0.05$ (see Supplementary Fig. 3d for mutant p53 status and IHC);

c. Chymotrypsin-like proteasome activity in MCF10A cell lines stably transfected with empty retroviral vector (Ctrl), vector encoding shRNA targeting *TP53* transcript (sh p53) and indicated mutant p53 cds shRNA-resistant HA-tagged variants, stably introduced into the MCF10A sh p53 cell line (+p53 changed residue). Ctrl MCF10A cells were also treated as indicated with 20μM Nutlin for 24h to induce wt p53 accumulation to a level similar to stably overexpressed *TP53* mutants. Right panel: western blot with p53 and indicated proteasome subunit levels in the MCF10A-derived cell lines;

d. Chymotrypsin-like proteasome activity in indicated non-breast cancer cell lines with p53 missense mutants is decreased upon mutant *TP53* expression silencing or *PSMA2* proteasome subunit expression silencing;

e. Chymotrypsin-like proteasome activity is elevated in protein extracts from thymi (enlarged with lymphomas in KO/KI mice) and livers (enlarged and infiltrated with lymphoma cells in KO/KI mice) mice with KI R172H p53 genotype as compared to the WT/KO genotype mice (two animals per each genotype, 3 technical replicates of the assay per animal were used). Lower panel: p53 protein levels in liver extracts (western blot). Means with s.e.m. are shown, ANOVA test with Bonferroni correction: * $p<0.05$, ** $p<0.01$, *** $p<0.001$.

f. Chymotrypsin-like proteasome activity is elevated in Mouse Embryo Fibroblast cells (MEFs) from mice with KI R172H *TP53* genotype as compared to the MEFs from WT/KO genotype mice, with or without a stable overexpression of the *RAS* V12 oncogenic variant. Lower panel: corresponding western blot with p53 and Ras level detection.

a, c-d, f: Means with s.d. are shown, ANOVA test with Bonferroni correction: * $p<0.05$, ** $p<0.01$, *** $p<0.001$.

# FIGURE 12

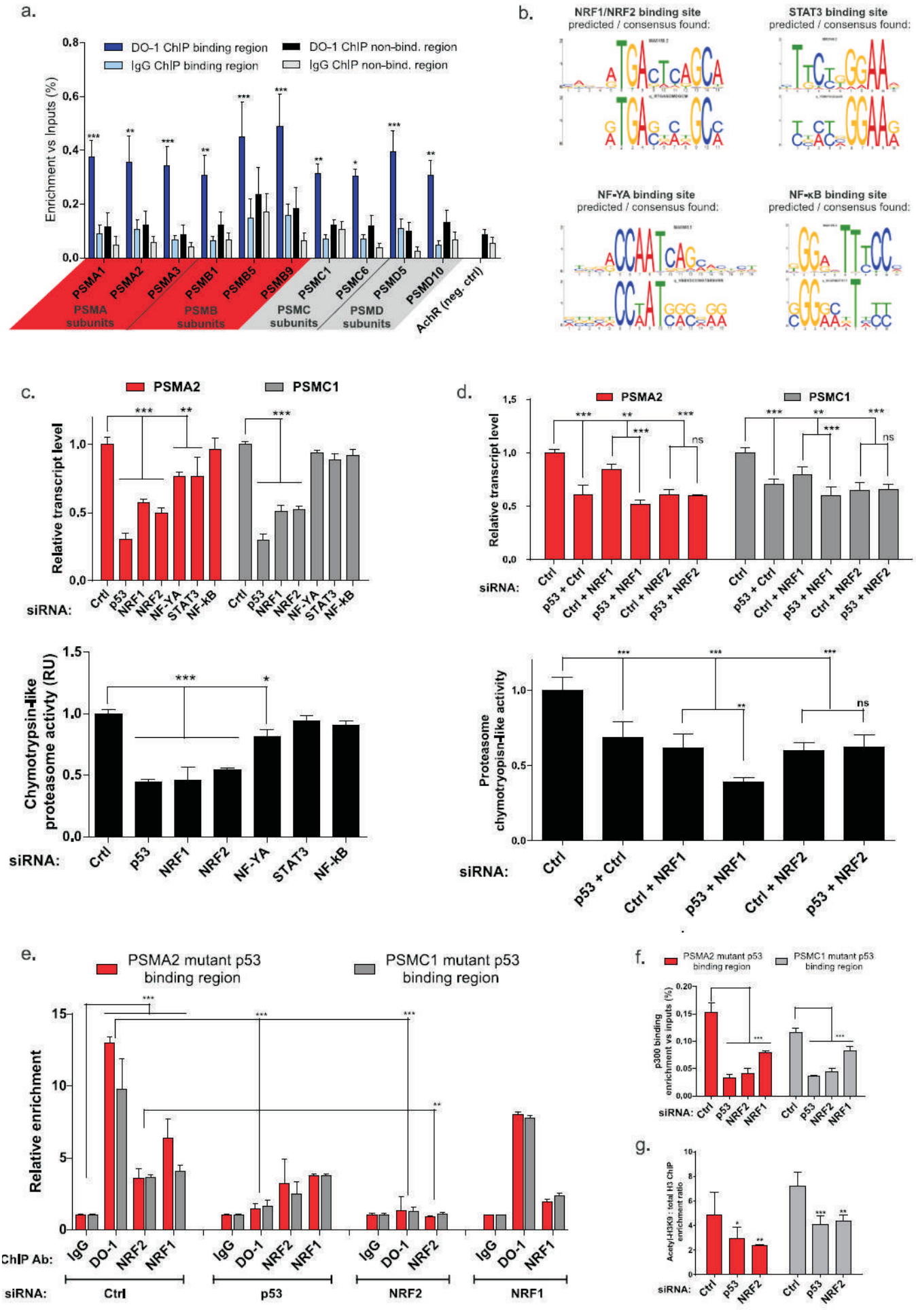
a.
DO-1 ChIP binding region
DO-1 ChIP non-bind. region
IgG ChIP binding region
IgG ChIP non-bind. region
Enrichment vs Inputs (%)
PSMA1
PSMA2
PSMA3
PSMB1
PSMB5
PSMB9
PSMC1
PSMC6
PSMD5
PSMD10
AchR (neg. ctrl)
PSMA subunits
PSMB subunits
PSMC subunits
PSMD subunits
b.
NRF1/NRF2 binding site
predicted / consensus found:
STAT3 binding site
predicted / consensus found:
NF-YA binding site
predicted / consensus found:
NF-κB binding site
predicted / consensus found:
c.
PSMA2
PSMC1
Relative transcript level
siRNA:
Crtl
p53
NRF1
NRF2
NF-YA
STAT3
NF-kB
d.
PSMA2
PSMC1
Relative transcript level
siRNA:
Ctrl
p53 + Ctrl
Ctrl + NRF1
p53 + NRF1
Ctrl + NRF2
p53 + NRF2
ns
Chymotrypsin-like proteasome activity (RU)
siRNA:
Crtl
p53
NRF1
NRF2
NF-YA
STAT3
NF-kB
Proteasome chymotrypsin-like activity
siRNA:
Ctrl
p53 + Ctrl
Ctrl + NRF1
p53 + NRF1
Ctrl + NRF2
p53 + NRF2
ns
e.
PSMA2 mutant p53 binding region
PSMC1 mutant p53 binding region
Relative enrichment
ChIP Ab:
IgG
DO-1
NRF2
NRF1
siRNA:
Ctrl
p53
NRF2
NRF1
f.
PSMA2 mutant p53 binding region
PSMC1 mutant p53 binding region
p300 binding enrichment vs inputs (%)
siRNA:
Ctrl
p53
NRF2
NRF1
g.
Acetyl-H3K9 : total H3 ChIP enrichment ratio
siRNA:
Ctrl
p53
NRF2

**Figure 12. Mutant p53 cooperates with NRF2 in binding and activating promoters of the 26S proteasome subunit genes**

a. Chromatin immunoprecipitation is significantly enriched in anti-p53 DO-1 antibody IP in the mutant p53 binding regions, but not in the p53 non-binding ChIP-seq regions or the IP with a control IgG antibody. A heterochromatic *AchR* locus was used as a ChIP negative control. Mean result with s.e.m. for the panel of the 5 TNBC cell lines is shown – each cell line result is a mean of 2 technical replicates; ANOVA test with Bonferroni correction: * $p<0.05$, ** $p<0.01$, *** $p<0.001$;;

b. Predicted (upper) and derived (lower) consensus sequences found by motif analysis in the mutant p53 binding regions of the proteasome genes, corresponding to the transcription factors involved in the regulation of proteasome gene expression: NRF1/2, NFYA, STAT3, NF-κB

c. Transcription levels of *PSMA2* and *PSMC1* proteasome genes (upper graph) and chymotrypsin-like proteasome activity (lower graph) upon silencing of mutant *TP53* and candidate mutant p53 transcription co-factors (*NRF1/2, NFYA, STAT3, NFKB1*);

d. As in c, upon double silencing of mutant p53 together with *NRF1/2* transcription factors;

e. ChIP of mutant p53 binding regions of the *PSMA2* and *PSMC1* genes with the indicated antibodies (Ab) upon siRNA-mediated silencing of mutant *TP53*, *NRF2* or *NRF1*;

f. Chromatin immunoprecipitation enrichments obtained with anti-p300 antibody at mutant p53 binding regions of *PSMA2* and *PSMC1* genes in MDA-MB-231 cells upon the treatment with the indicated siRNAs;

g. Ratios of chromatin immunoprecipitation enrichments obtained with anti-acetyl-histone H3K9 (Lys9) antibody and anti-histone H3 antibody, indicating proportion of histone H3 acetylation at *PSMA2* and *PSMC1* mutant p53 binding regions in MDA-MB-231 cells upon treatment with the indicated siRNAs;

c-g: Means with s.d. are shown, ANOVA test with Bonferroni correction: * $p<0.05$, ** $p<0.01$, *** $p<0.001$;

# FIGURE 13

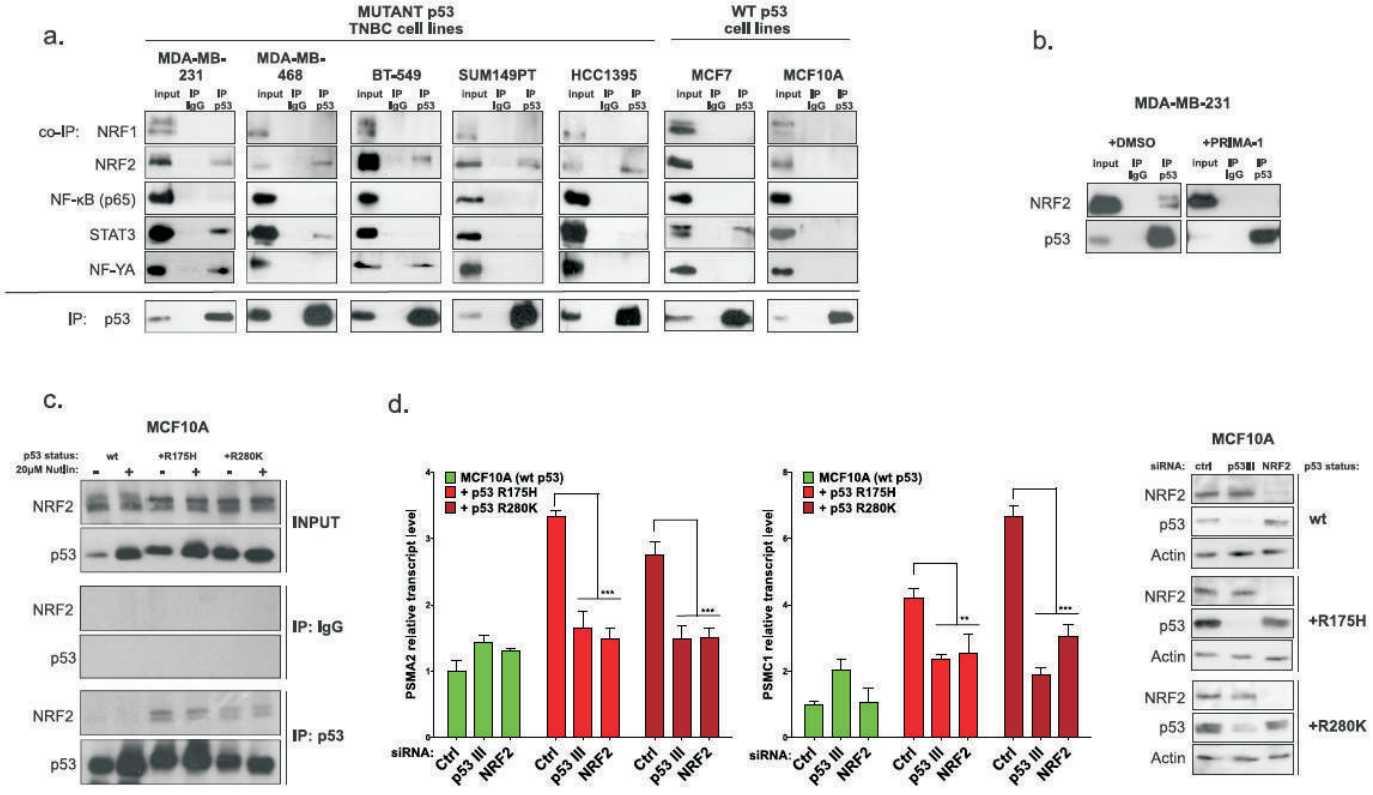


**Figure 13. The GOF p53 mutants interact with NRF2 and are functionally sensitive to *NRF2* silencing**

a. Western blot result of co-immunoprecipitation (co-IP) of mutant p53 (DO-1 antibody) with the candidate mutant p53 transcription co-factors (NRF1, NRF2, NFYA, STAT3, NFκB-p65) in lysates from indicated 5 TNBC mutant p53 cell lines and two wt p53 cell lines;

b. Western blot result of co-immunoprecipitation (co-IP) of mutant p53 (DO-1 antibody) with NRF2 post 24h treatment of MDA-MB-231 cells with DMSO or 1μM PRIMA-1;

c. Co-immunoprecipitation (co-IP; DO-1 or IgG antibody) of p53 and NRF2 is shown in control or p53 stabilizing conditions (24h 20 μM Nutlin treatment) for normal MCF10A cells with endogenous wt p53 (wt) and in the mutant p53 overexpresssing MCF10A cells with stably silenced endogenous wt p53 (+p53 R175H and +p53 R280K);

d. *PSMA2* or *PSMC1* gene expression in MCF10A cells (control or with stably silenced endogenous wt p53 and introduced mutant p53 variants +p53 R175H or +p53 R280K) upon indicated silencing (ctrl, NRF2, p53 III; for TP53 silencing siRNA was used that targets cds outside the residues used to produce siRNA resistance for the p53 I sequence in the *TP53* cds overexpressed ectopically in MCF10A). Means with s.d. are shown, ANOVA test with Bonferroni correction: ** $p<0.01$, *** $p<0.001$. The protein levels were controlled in the western blot (right panel);

# FIGURE 14

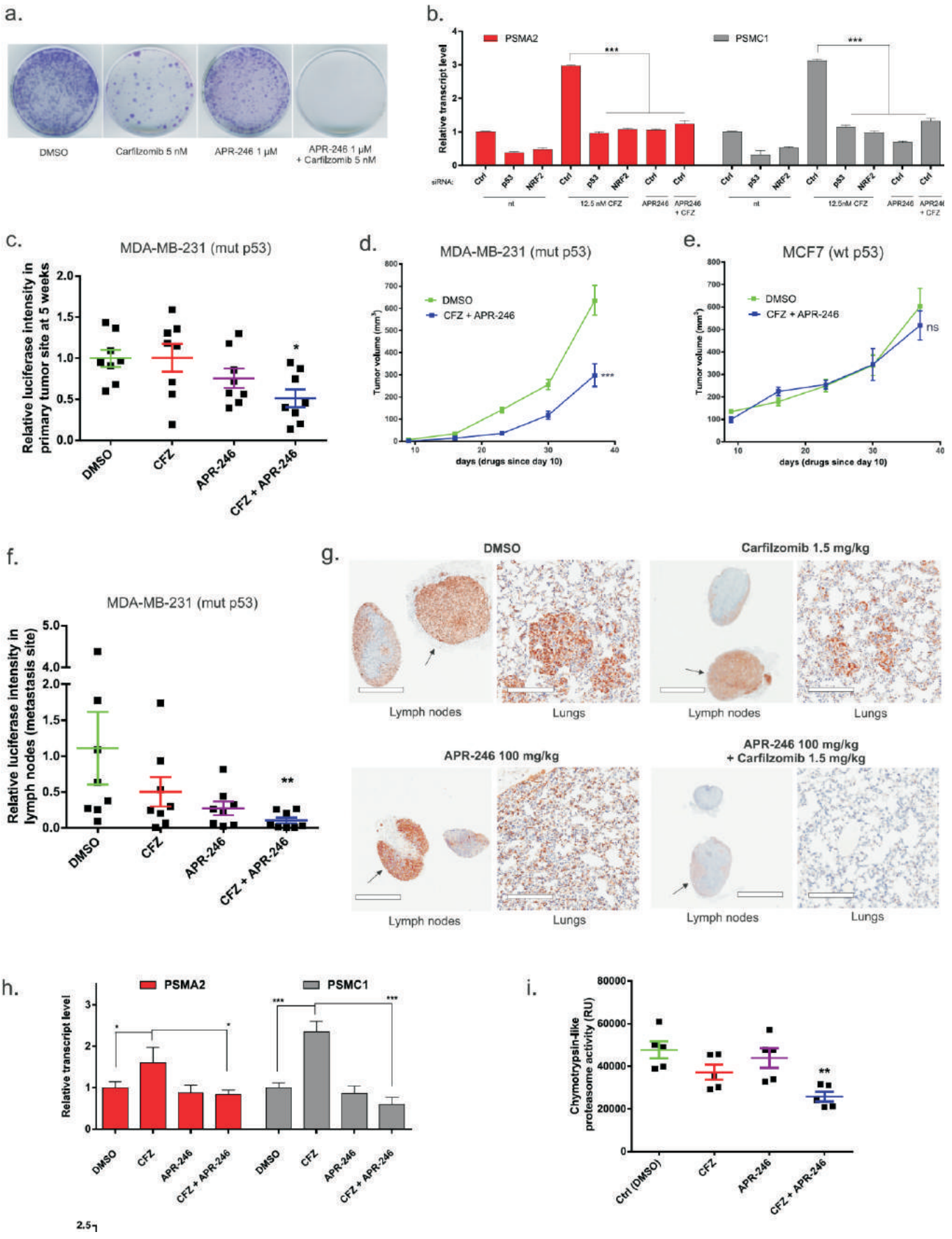
a.
DMSO
Carfilzomib 5 nM
APR-246 1 µM
APR-246 1 µM + Carfilzomib 5 nM
b.
PSMA2
PSMC1
Relative transcript level
siRNA:
Ctrl
p53
NRF2
nt
12.5 nM CFZ
APR246
APR246 + CFZ
c.
MDA-MB-231 (mut p53)
Relative luciferase intensity in primary tumor site at 5 weeks
DMSO
CFZ
APR-246
CFZ + APR-246
d.
MDA-MB-231 (mut p53)
DMSO
CFZ + APR-246
Tumor volume (mm³)
days (drugs since day 10)
e.
MCF7 (wt p53)
DMSO
CFZ + APR-246
ns
Tumor volume (mm³)
days (drugs since day 10)
f.
MDA-MB-231 (mut p53)
Relative luciferase intensity in lymph nodes (metastasis site)
DMSO
CFZ
APR-246
CFZ + APR-246
g.
DMSO
Carfilzomib 1.5 mg/kg
APR-246 100 mg/kg
APR-246 100 mg/kg + Carfilzomib 1.5 mg/kg
Lymph nodes
Lungs
h.
PSMA2
PSMC1
Relative transcript level
DMSO
CFZ
APR-246
CFZ + APR-246
i.
Chymotrypsin-like proteasome activity (RU)
Ctrl (DMSO)
CFZ
APR-246
CFZ + APR-246

**Figure 14. Mutant p53 targeting by APR-246 eliminates resistance to the proteasome inhibitor Carfilzomib in TNBC cells *in vitro* and in *in vivo* xenografts**

a. Colony formation assay in the MDA-MB-231 cells under treatment with the indicated drugs (representative picture of 3 independent experiments,);

b. Reducing effect of mutant *TP53*, *NRF2* silencing or APR-246 (PRIMA-1MET) treatment on transcription of the representative proteasome genes. *PSMA2* and *PSMC1* transcript levels are elevated due to a bounce-back effect post treatment with Carfilzomib (CFZ) in MDA-MB-231. Means with s.d. are shown, ANOVA test with Bonferroni correction; * $p<0.05$, ** $p<0.01$, *** $p<0.001$;

c. Luciferase *in vivo* intensity at 5 weeks at primary tumor sites at 5 weeks of the MDA-MB-231-Luc (cells stably overexpressing luciferase) mammary fat pad xenograft growth in SCID mice intravenously treated with DMSO, CFZ, APR-246 or combination of CFZ and APR-246;

d. Primary MDA-MB-231-Luc (mutant p53, TNBC) mammary fat pad xenograft growth in SCID mice intravenously treated with DMSO or combination of CFZ and APR-246 (caliper measurements with s.e.m., significance for the time-course is indicated - Friedman nonparametric matched pairs test with Dunn's correction; *** $p<0.001$);

e. Primary MCF7 (wt p53, ER+) mammary fat pad xenograft growth in SCID mice intravenously treated with DMSO or combination of CFZ and APR-246 (caliper measurement, statistical test as in d., difference not significant);

f. Lymph node area (metastasis) luciferase intensity in the mice treated as indicated in the MDA-MB-231-Luc xenograft experiment in c and d. Data refer to 5 weeks for the DMSO control group, and to later time-points for the treated groups, i.e. when the primary tumors reached sizes comparable to the controls;

g. Representative photos of lymph nodes (homolateral to the xenograft - indicated by arrows; bar size – 2 mm) and lung tissue (bar size – 200 μm) with IHC staining of the MDA-MB-231 metastasis (human cytokeratin, brown) in mice from c,d,f. As reported in f, the IHC analyses were carried out on samples collected when the primary tumor sizes were comparable in all groups.

h. *PSMA2* and *PSMC1* transcript levels in primary tumors extracted from mice in c-d under the indicated treatment;

i. Chymotrypsin-like proteasome activity in primary tumors, extracted from mice as in h;

# FIGURE 15

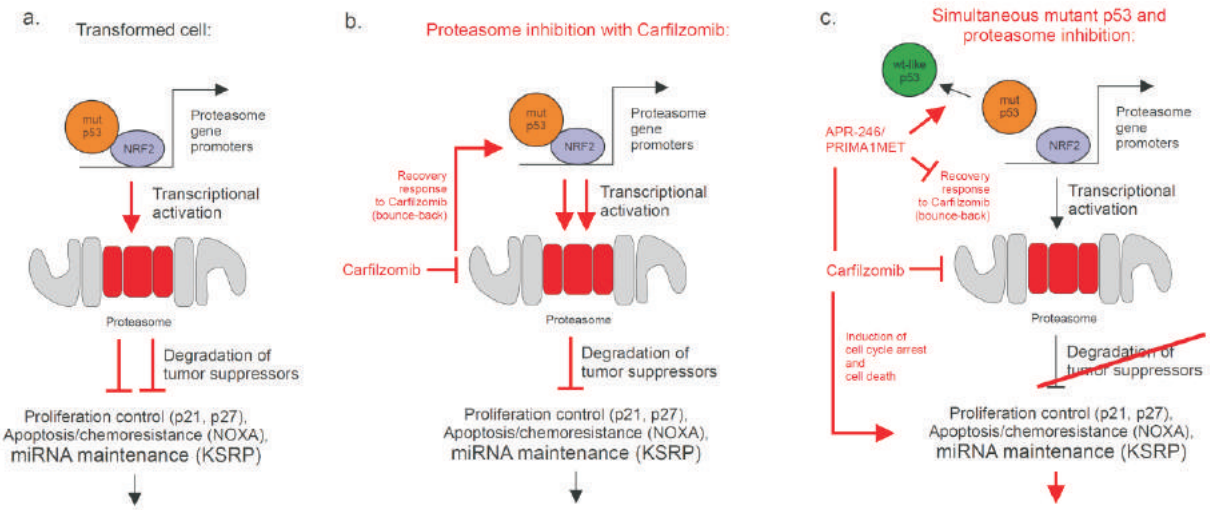


**Figure 15. Model representation of mutant p53 regulation of the proteasome machinery and its therapeutic implication**

a. Mutant p53 activates proteasome gene transcription by controlling NRF2 transcription factor that results in upregulation of proteasome activity and degradation of tumor suppressor proteins;

b. Inhibition of the proteasome with Carfilzomib results in the mutant p53 and NRF2-mediated bounce-back response of the increased proteasome transcription;

c. Proteasome activity can be efficiently decreased by the simultaneous treatment of cells with Carfilzomib and APR-246/PRIMA-1MET a drug which converts mutant p53 to the wild-type-like form and reduces the interaction of mutant p53 with NRF2.

# FIGURE 16

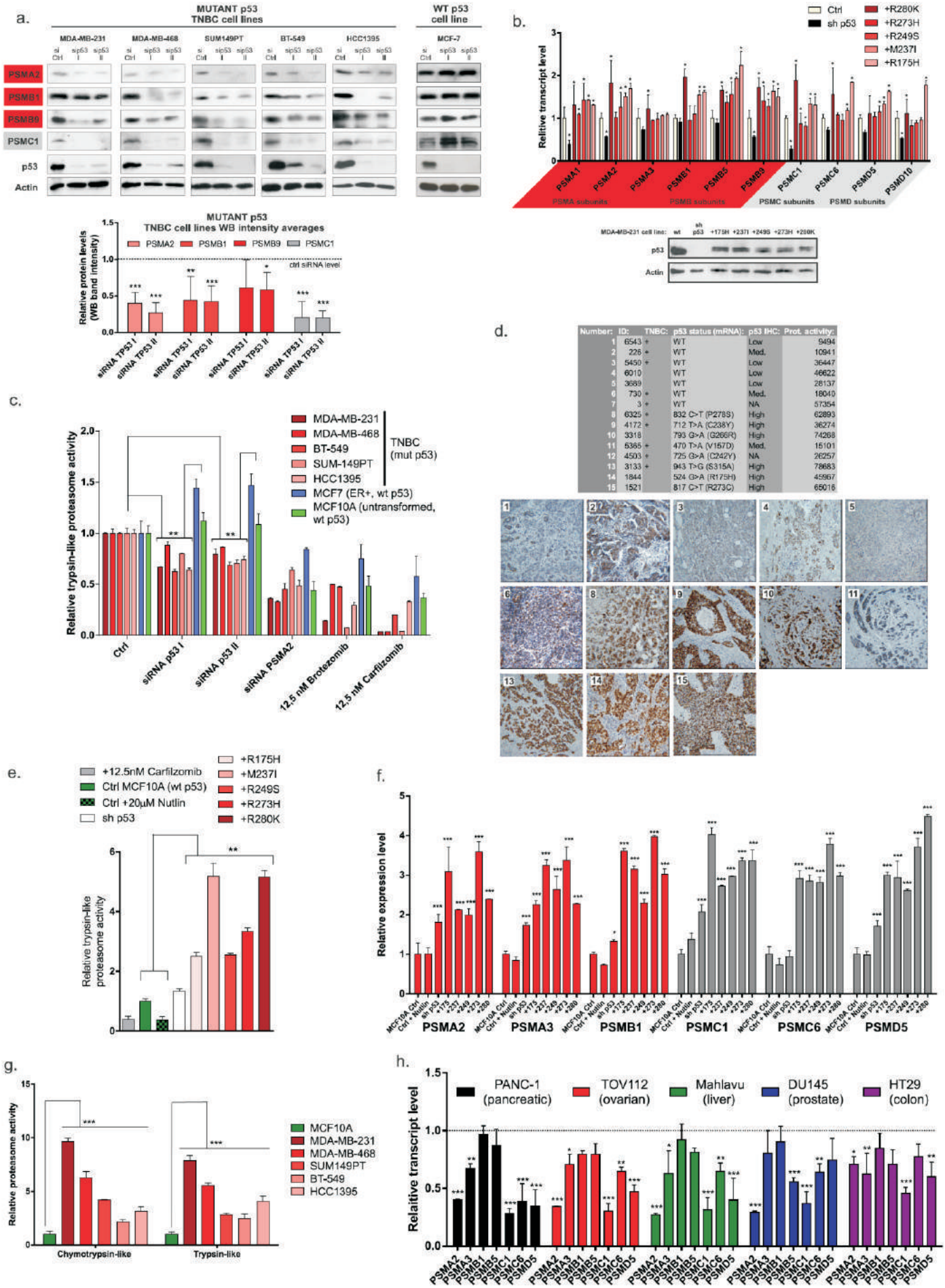
a.
MUTANT p53
TNBC cell lines
WT p53
cell line
MDA-MB-231
MDA-MB-468
SUM149PT
BT-549
HCC1395
MCF-7
si Ctrl
sip53 I
sip53 II
PSMA2
PSMB1
PSMB9
PSMC1
p53
Actin
MUTANT p53
TNBC cell lines WB intensity averages
Relative protein levels (WB band intensity)
ctrl siRNA level
siRNA TP53 I
siRNA TP53 II
b.
Ctrl
sh p53
+R280K
+R273H
+R249S
+M237I
+R175H
Relitive transcript level
PSMA1
PSMA2
PSMA3
PSME1
PSMB5
PSMB9
PSMC1
PSMC6
PSMD5
PSMD10
PSMA subunits
PSMB subunits
PSMC subunits
PSMD subunits
MDA-MB-231 cell line:
wt
sh p53
+175H
+237I
+249S
+273H
+280K
p53
Actin
c.
MDA-MB-231
MDA-MB-468
BT-549
SUM-149PT
HCC1395
TNBC (mut p53)
MCF7 (ER+, wt p53)
MCF10A (untransformed, wt p53)
Relative trypsin-like proteasome activity
Ctrl
siRNA p53 I
siRNA p53 II
siRNA PSMA2
12.5 nM Brotezomib
12.5 nM Carfilzomib
d.
Number: ID: TNBC: p53 status (mRNA): p53 IHC: Prot. activity:
1 6543 + WT Low 9494
2 226 + WT Med. 10941
3 5450 + WT Low 36447
4 6010 WT Low 46622
5 3689 WT Low 28137
6 730 + WT Med. 18040
7 3 + WT NA 57354
8 6325 + 832 C>T (P278S) High 62893
9 4172 + 712 T>A (C238Y) High 36274
10 3318 793 G>A (G266R) High 74268
11 6365 + 470 T>A (V157D) Med. 16101
12 4503 + 725 G>A (C242Y) NA 26257
13 3133 + 943 T>G (S315A) High 78683
14 1844 524 G>A (R175H) High 45967
15 1521 817 C>T (R273C) High 65016
e.
+12.5nM Carfilzomib
Ctrl MCF10A (wt p53)
Ctrl +20μM Nutlin
sh p53
+R175H
+M237I
+R249S
+R273H
+R280K
Relative trypsin-like proteasome activity
f.
Relative expression level
PSMA2
PSMA3
PSMB1
PSMC1
PSMC6
PSMD5
g.
MCF10A
MDA-MB-231
MDA-MB-468
SUM149PT
BT-549
HCC1395
Relative proteasome activity
Chymotrypsin-like
Trypsin-like
h.
PANC-1 (pancreatic)
TOV112 (ovarian)
Mahlavu (liver)
DU145 (prostate)
HT29 (colon)
Relative transcript level

**Figure 16. Mutant p53 upregulates the proteasome genes transcription, subunits protein levels and activity**

a. Levels of selected 26 proteasome (PSMA2, PSMB1, PSMC1) and immunoproteasome (PSMB9) subunits are lowered as determined by the western blot upon *TP53* expression silencing in the indicated 5 TNBC cell lines with mutant p53 and MCF7 ER+ breast cancer cell line with wt p53, using 2 alternative *TP53* siRNAs; Below – a bar graph demonstrating average protein levels of proteasome subunits measured by densitometry in 5 TNBC cell lines with mutant p53 (2 western blot results per each cell line were averaged then means of n=5 were obtained, bars indicate means with s.e.m., ANOVA test with Bonferroni correction: * $p<0.05$, ** $p<0.01$, *** $p<0.001$; normalized control silencing level shown as the dashed line);

b. Overexpressed mutant p53 variants from the studied TNBC cell lines rescue the proteasome genes transcription in the stably silenced endogenous mutant *TP53* background of MDA-MB-231 cells. Transcript levels of ten representative proteasome subunits in MDA-MB-231 cells stably transfected with: empty retroviral vector (Ctrl), vector encoding shRNA targeting *TP53* transcript (sh p53) and indicated mutant p53 cds shRNA-resistant HA-tagged variants, stably introduced into the MDA-MB-231 sh p53 cell line (+p53 changed residue). Lower panel: western blot demonstrating effect of the stable silencing of mutant *TP53* and the expression of the indicated HA-tagged mutant p53 variants. Means with s.d. are shown; ANOVA test with Bonferroni correction: * $p<0.05$. The p-value is marked with * for the sh p53 difference from Ctrl and for each of the introduced variants difference from sh p53;

c. Trypsin-like proteasome activity is decreased in mutant p53 TNBC cell lines versus wt p53 cell lines (MCF10A and MCF7) upon silencing of mutant *TP53* or *PSMA2* or proteasome inhibitor treatment (24h; Carfilzomib, Bortezomib). Means with s.d. are shown, ANOVA test with Bonferroni correction: * $p<0.05$, ** $p<0.01$, *** $p<0.001$;

d. Table listing the basal-like primary breast cancer tumor samples from patients, used to determine correlation between the p53 status and the proteasome activity. Mutations found by sequencing of the *TP53* mRNA expressed in samples are indicated along with the TNBC status, immunohistochemical p53 staining intensity assessment and proteasome chymotrypsin activity measurement result (mean of 3 technical replicates each). Lower panel - IHC staining of p53 (brown) in representative samples with indicated numbers corresponding to the table above;

e. Trypsin-like proteasome activity in MCF10A cell lines stably transfected with empty retroviral vector (Ctrl), Ctrl treated with 20μM Nutlin for 24h, stably transfected with vector encoding shRNA targeting *TP53* transcript (sh p53) and indicated mutant p53 cds shRNA-resistant HA-tagged variants, stably introduced into the MCF10A sh p53 cell line (+p53 changed residue; the proteasome activity is increased). Means with s.d. are shown, ANOVA test with Bonferroni correction: * $p<0.05$, ** $p<0.01$, *** $p<0.001$;

f. Transcript levels of four indicated proteasome subunits in MCF10A cell lines transfected with empty retroviral vector (Ctrl), vector encoding shRNA targeting p53 transcript (sh p53) and indicated mutant p53 cds shRNA-resistant HA-tagged variants, stably introduced into MCF10A sh p53 cell line (+p53 changed residue; increased proteasome transcript levels). Means with s.d. are shown, ANOVA test with Bonferroni correction: * $p<0.05$, ** $p<0.01$, *** $p<0.001$;

g. Basal chymotrypsin-like and trypsin-like proteasome activities are elevated in the five indicated TNBC cell lines (mutant p53), as compared to the MCF10A cell line (wt p53). Means with s.d. are shown, ANOVA test with Bonferroni correction: * $p<0.05$, ** $p<0.01$, *** $p<0.001$;

h. Transcript levels of seven proteasome subunits are decreased in the indicated non-breast cancer cell lines upon mutant *TP53* expression silencing. Control level is marked with the dashed line. Means with s.d. are shown, ANOVA test with Bonferroni correction: * $p<0.05$, ** $p<0.01$, *** $p<0.001$.

# FIGURE 17

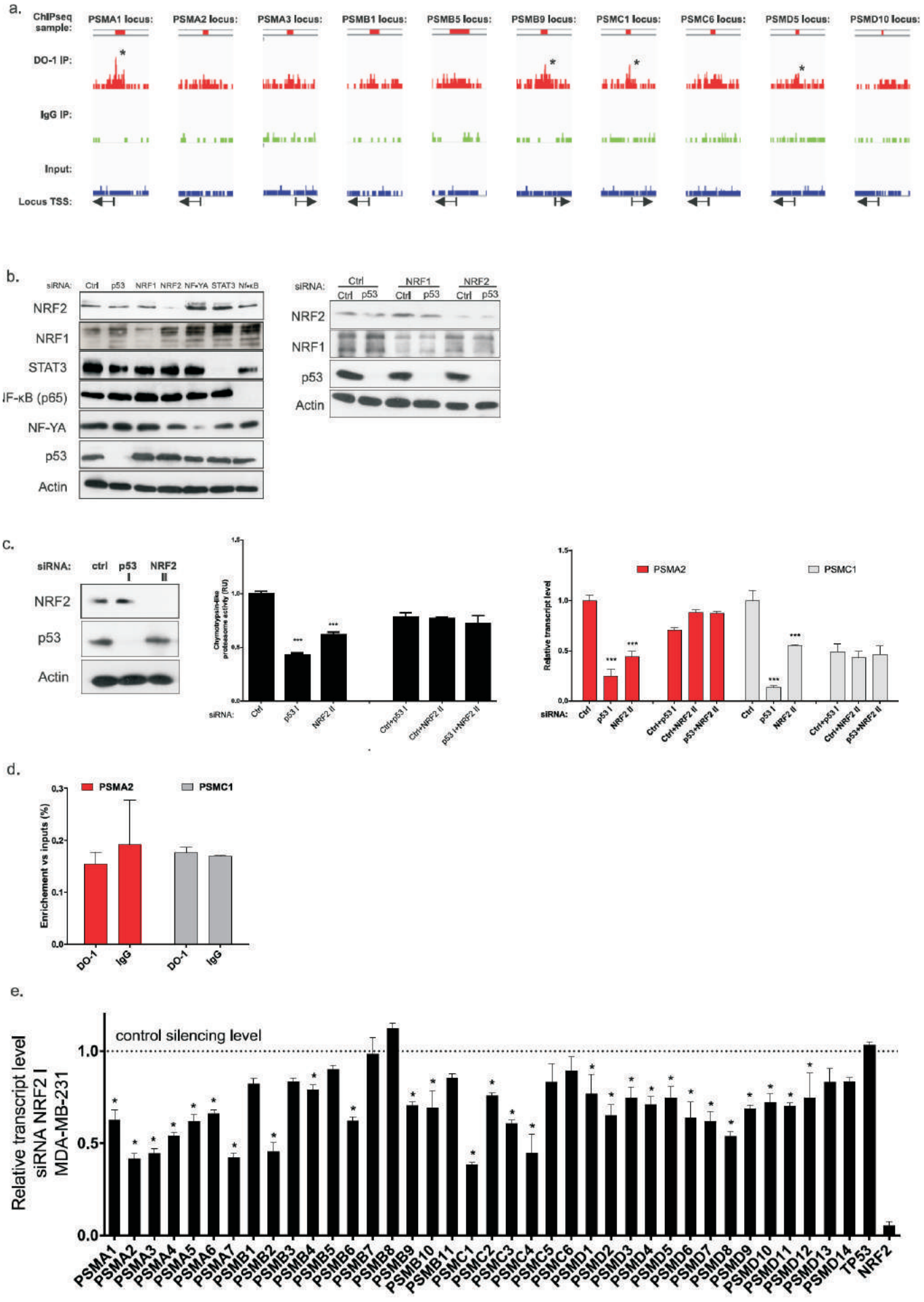
a.
ChIPseq sample:
PSMA1 locus:
PSMA2 locus:
PSMA3 locus:
PSMB1 locus:
PSMB5 locus:
PSMB9 locus:
PSMC1 locus:
PSMC6 locus:
PSMD5 locus:
PSMD10 locus:
DO-1 IP:
IgG IP:
Input:
Locus TSS:
b.
siRNA: Ctrl p53 NRF1 NRF2 NF-YA STAT3 Nf-κB
NRF2
NRF1
STAT3
IF-κB (p65)
NF-YA
p53
Actin
siRNA: Ctrl NRF1 NRF2
Ctrl p53 Ctrl p53 Ctrl p53
NRF2
NRF1
p53
Actin
c.
siRNA: ctrl p53 I NRF2 II
NRF2
p53
Actin
Chymotrypsin-like proteasome activity (RLU)
siRNA: Ctrl p53 I NRF2 II Ctrl+p53 I Ctrl+NRF2 II p53 I+NRF2 II
Relative transcript level
PSMA2
PSMC1
siRNA: Ctrl p53 I NRF2 II Ctrl+p53 I Ctrl+NRF2 II p53+NRF2 II Ctrl p53 I NRF2 II Ctrl+p53 I Ctrl+NRF2 II p53+NRF2 II
d.
PSMA2
PSMC1
Enrichement vs inputs (%)
DO-1 IgG DO-1 IgG
e.
Relative transcript level siRNA NRF2 I MDA-MB-231
control silencing level
PSMA1 PSMA2 PSMA3 PSMA4 PSMA5 PSMA6 PSMA7 PSMB1 PSMB2 PSMB3 PSMB4 PSMB5 PSMB6 PSMB7 PSMB8 PSMB9 PSMB10 PSMB11 PSMC1 PSMC2 PSMC3 PSMC4 PSMC5 PSMC6 PSMD1 PSMD2 PSMD3 PSMD4 PSMD5 PSMD6 PSMD7 PSMD8 PSMD9 PSMD10 PSMD11 PSMD12 PSMD13 PSMD14 TP53 NRF2

**Figure 17. NRF2 is required for the regulation of proteasome genes transcription and activity**

a. Integrative Genomics Viewer (IGV) snapshots at the selected proteasome subunit gene loci with shown ChIP-sequencing enrichment readouts for the indicated samples in the MDA-MB-231 cells – DO-1 p53 ChIP (red), IgG ChIP (green), ChIP input (blue). (*) indicate significant peaks called in range -+500 bp of proteasome gene TSSes (Supplementary Tab. 4), other peak regions were hand-picked in IGV. Regions highlighted in red were used to design mutant p53 binding-region region primers for ChIP validation shown in Figure 4a (primers listed in the Supplemetary Tab. 7);

b. Western blot related to Figure 4c (left panel) and Figure 4d (right panel) showing protein levels of the transcription factors whose expression has been silenced in the indicated samples;

c. Effects of transfection of alternative siRNA for *NRF2* (NRF2 II) and siRNA for *TP53* on proteasome activity (middle panel) and transcription (right panel) are coparable with siRNA NRF2 I treatment shown in Figure 4c and 4d. Means with s.d. are shown, ANOVA test with Bonferroni correction: * $p<0.05$, ** $p<0.01$, *** $p<0.001$.;

d. Chromatin immunoprecipitation enrichment obtained with the indicated antibodies at *PSMA2* and *PSMC1* mutant p53 binding regions in the wt p53 MCF7 cells. Means are shown, differences are insignificant - ANOVA test with Bonferroni correction;

e. Transcript levels of all human 26S proteasome and immunoproteasome subunits determined in MDA-MB-231 cells upon *NRF2* expression silencing (normalized control level shown as the dashed line, means with s.d. are shown, t-test: * $p<0.05$).

# FIGURE 18

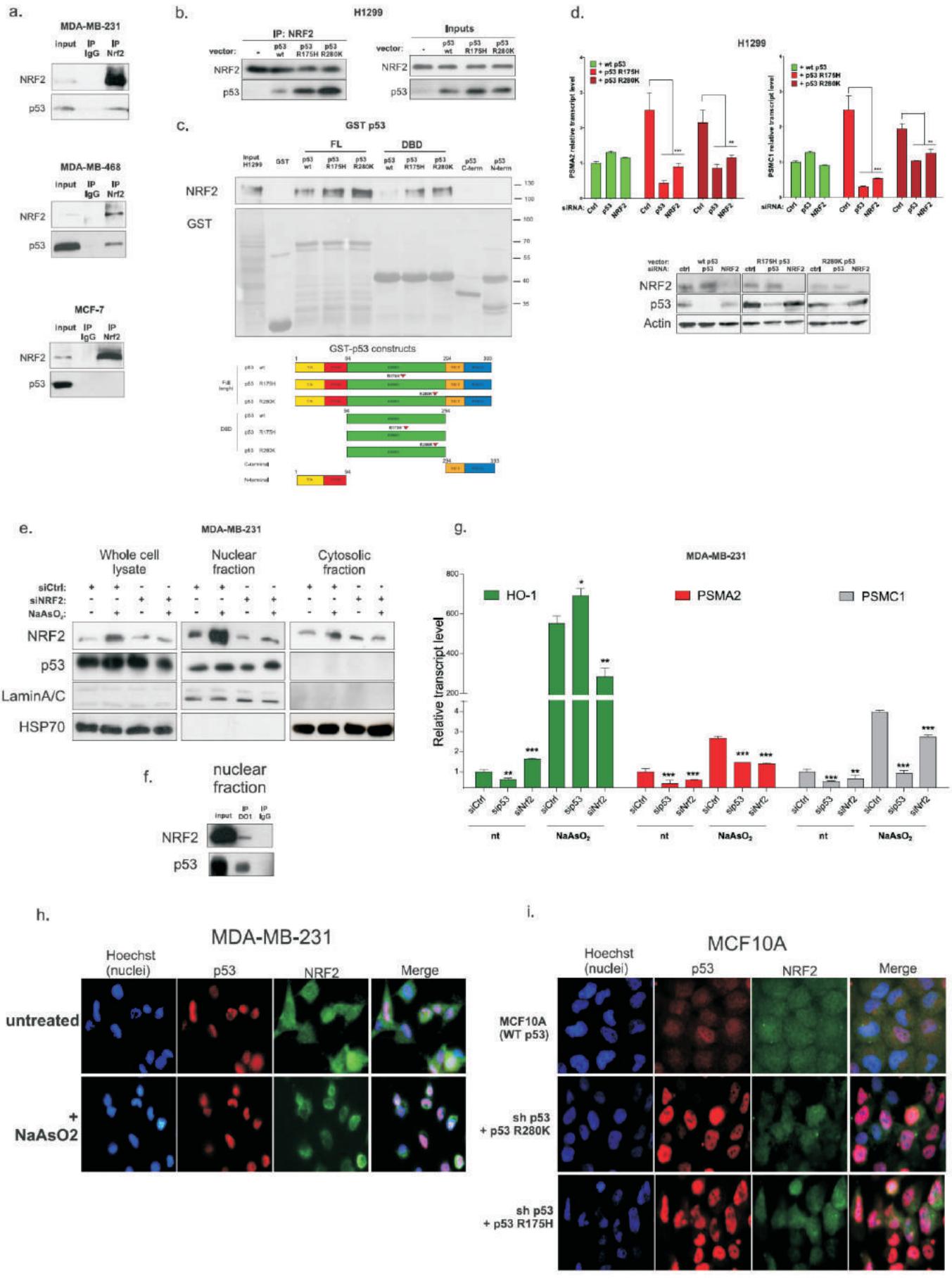
a.
MDA-MB-231
Input
IP IgG
IP Nrf2
NRF2
p53
MDA-MB-468
MCF-7
b.
H1299
IP: NRF2
Inputs
vector:
p53 wt
p53 R175H
p53 R280K
c.
GST p53
FL
DBD
GST
GST-p53 constructs
d.
H1299
PSMA2 relative transcript level
PSMC1 relative transcript level
+ wt p53
+ p53 R175H
+ p53 R280K
siRNA: Ctrl p53 NRF2
Actin
e.
MDA-MB-231
Whole cell lysate
Nuclear fraction
Cytosolic fraction
siCtrl:
siNRF2:
NaAsO2:
LaminA/C
HSP70
f.
nuclear fraction
IP DO1
IP IgG
g.
MDA-MB-231
HO-1
PSMA2
PSMC1
Relative transcript level
siCtrl
sip53
siNrf2
nt
NaAsO2
h.
MDA-MB-231
Hoechst (nuclei)
p53
NRF2
Merge
untreated
+ NaAsO2
i.
MCF10A
MCF10A (WT p53)
sh p53 + p53 R280K
sh p53 + p53 R175H

**Figure 18. Direct interaction between NRF2 and mutant p53 drives proteasome genes transcription upregulation**

a. Mutant p53 co-immunoprecipitates (co-IP) with NRF2 in MDA-MB-231 and MDA-MB-468 cell lysates (anti-NRF2 antibody). In MCF-7 cell lysate endogenous wt p53 does not co-immunoprecipitate with NRF2 (anti-NRF2 antibody);

b. NRF2 interacts stronger with the overexpressed mutant p53 than with wt p53 in the p53-null H1299 cell lysates. Co-immunoprecipitation (co-IP) of NRF2 (anti-NRF2 antibody) and overexpressed wt or mutant (R175H and R280K) p53 in p53-null H1299 cells;

c. GST tagged mutant p53 variants interact via DNA binding domain with overexpressed full length NRF2 in the p53-null H1299 cell lysates. Western blot results are shown of the GST pull-down of overexpressed full length NRF2 from H1299 lysates with the *E.coli* overexpressed, Sepharose-GSH-bound p53 variants fused with GST – wt, R175H and R280K (FL- full length protein; DBD – DNA binding domain; N-term – amino terminal domain; C-term – carboxy terminal domain of p53).

Scheme of the p53 constructs used for the experiment: All constructs were N-terminally GST-tagged. p53 domains and sub-domains are indicated – TA (trans-activation), PRD (proline-rich domain), DBD (DNA-binding domain), TET (tetramerization domain), REG (regulatory domain);

d. The increased expression of *PSMA2* and *PSMC1* proteasome genes is blunted by silencing of *TP53* or *NRF2* in the presence of the overexpressed mutant p53 variants (R175H and R280K) in p53-null H1299 cells. The effect is absent in the wt p53 overexpressing cells;

e. NRF2 and p53 are present in the nuclei of MDA-MB-231 cells with or without oxidative stress. Western blot results of cells fractionation to nuclear and cytosolic fractions (and whole cell lysate control) are shown. Cells optionally treated with NRF2-targeting siRNA and/or for 6h with 50 μM of oxidative stress-inducing sodium arsenite ($NaAsO_2$);

f. Mutant p53 co-immunoprecipitates with NRF2 in the nuclear fraction of MDA-MB-231. Western blot result is shown of the co-immunoprecipitation (co-IP) with the indicated antibodies after obtaining the nuclear fraction as in c.;

g. Mutant p53 regulates transcription of NRF2-dependent oxidative stress induced gene *HO-1* in the opposite manner to the proteasome genes. Transcription of *HO-1*, *PSMA2* and *PSMC1* genes is shown in MDA-MB-231 cells upon treatment with control silencing and silencing targeting *NRF2* or *TP53*, with or without 6h treatment with 50 μM of oxidative stress-inducing sodium arsenite ($NaAsO_2$). Oxidative stress strongly induces *HO-1* and moderately *PSMA2*/*PSMA2* expression – upon which *NRF2* silencing inhibits both, while mutant p53 silencing further induces *HO-1* expression and reduces proteasome genes' expression.

h. NRF2 and p53 co-localize in the nuclei of MDA-MB-231 with or without oxidative stress. Cells optionally treated for 6h with 50 μM of oxidative stress-inducing sodium arsenite ($NaAsO_2$). Upon oxidative stress NRF2 increases its presence in the nucleus;

i. NRF2 and p53 co-localize in the nuclei of MCF10A control cells (wt p53) and MCF10A cells with silenced endogenous wt *TP53* (sh p53) plus overexpressed mutant p53 variants (+p53 R280K. +p53 R175H).

# FIGURE 19

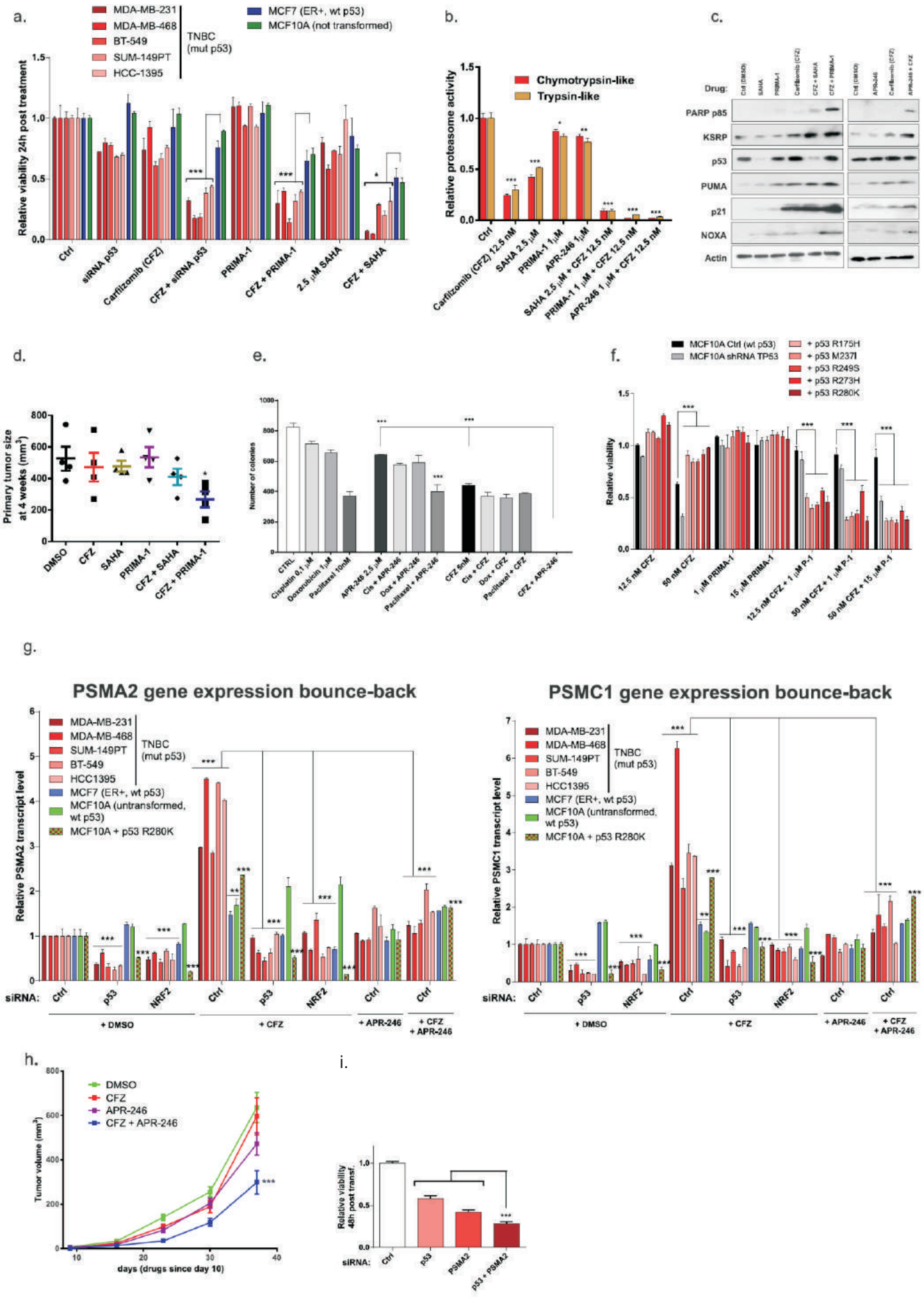
a.
MDA-MB-231
MDA-MB-468
BT-549
SUM-149PT
HCC-1395
TNBC (mut p53)
MCF7 (ER+, wt p53)
MCF10A (not transformed)
Relative viability 24h post treatment
Ctrl
siRNA p53
Carfilzomib (CFZ)
CFZ + siRNA p53
PRIMA-1
CFZ + PRIMA-1
2.5 μM SAHA
CFZ + SAHA
b.
Chymotrypsin-like
Trypsin-like
Relative proteasome activity
Ctrl
Carfilzomib (CFZ) 12.5 nM
SAHA 2.5 μM
PRIMA-1 1 μM
APR-246 1 μM
SAHA 2.5 μM + CFZ 12.5 nM
PRIMA-1 1 μM + CFZ 12.5 nM
APR-246 1 μM + CFZ 12.5 nM
c.
Drug:
PARP p85
KSRP
p53
PUMA
p21
NOXA
Actin
d.
Primary tumor size at 4 weeks (mm³)
DMSO
CFZ
SAHA
PRIMA-1
CFZ + SAHA
CFZ + PRIMA-1
e.
Number of colonies
CTRL
Cisplatin 0.1 μM
Doxorubicin 1μM
Paclitaxel 10nM
APR-246 2.5 μM
Cis + APR-246
Dox + APR-246
Paclitaxel + APR-246
CFZ 5nM
Cis + CFZ
Dox + CFZ
Paclitaxel + CFZ
CFZ + APR-246
f.
MCF10A Ctrl (wt p53)
MCF10A shRNA TP53
+ p53 R175H
+ p53 M237I
+ p53 R249S
+ p53 R273H
+ p53 R280K
Relative viability
12.5 nM CFZ
50 nM CFZ
1 μM PRIMA-1
15 μM PRIMA-1
12.5 nM CFZ + 1 μM P-1
50 nM CFZ + 1 μM P-1
50 nM CFZ + 15 μM P-1
g.
PSMA2 gene expression bounce-back
MDA-MB-231
MDA-MB-468
SUM-149PT
BT-549
HCC1395
TNBC (mut p53)
MCF7 (ER+, wt p53)
MCF10A (untransformed, wt p53)
MCF10A + p53 R280K
Relative PSMA2 transcript level
siRNA:
Ctrl
p53
NRF2
+ DMSO
+ CFZ
+ APR-246
+ CFZ + APR-246
PSMC1 gene expression bounce-back
Relative PSMC1 transcript level
h.
DMSO
CFZ
APR-246
CFZ + APR-246
Tumor volume (mm³)
days (drugs since day 10)
i.
Relative viability 48h post transf.
siRNA:
Ctrl
p53
PSMA2
p53 + PSMA2

**Figure 19. APR-246 and mtp53 targeting agents synergistically kill TNBC cells *in vivo* and *in vitro***

a. *TP53* silencing or targeting with SAHA (Vorinostat) or PRIMA-1 sensitizes TNBC but not wt p53 cell lines to the proteasome inhibitor Carfilzomib (CFZ). Viability is shown of indicated TNBC (mutant p53) and wt p53 cell lines (MCF7 and MCF10A) post 24h treatment with the proteasome inhibitor Carfilzomib (CFZ, 12.5 nM; for MDA-MB-468 cell line 5 nM CFZ was used due to a higher sensitivity of this cell line to proteasome inhibitors) with or without p53 silencing or treatment with SAHA (2,5 μM) / PRIMA-1 (1 μM). Means with s.d. are shown, ANOVA test with Bonferroni correction: * $p<0.05$, ** $p<0.01$, *** $p<0.001$;

b. Drug-mediated inhibition of proteasome and mutant p53 synergistically decreases the proteasome activity in MDA-MB-231 cells. Chymotrypsin-like and trypsin-like proteasome activities in MDA-MB-231 cell line post 24h treatment with the proteasome inhibitor Carfilzomib (CFZ), SAHA, PRIMA-1 or APR-246 (PRIMA-1MET) and their combinations. Means with s.d. are shown, ANOVA test with Bonferroni correction: * $p<0.05$, ** $p<0.01$, *** $p<0.001$;

c. Treatment of MDA-MB-231 cells with SAHA (2,5 μM), PRIMA-1 (1 μM) or APR-246 (1 μM) plus the proteasome inhibitor Carfilzomib (CFZ; 12.5 nM) induces tumor suppressive proteins KSRP, PUMA, p21 and NOXA and the apoptosis marker PARP p85 increase. Western blots are shown for the indicated proteins upon treatment with the listed drugs for 24h. PRIMA-1 and APR-246 treatments alone induce protein level increase of the wt p53 transcriptional targets – PUMA, p21 and NOXA;

d. Simultaneous administration of PRIMA-1 and the proteasome inhibitor Carfilzomib (CFZ) inhibits the growth of primary xenograft tumors more effectively than a combination of SAHA and CFZ. Average (bars) and individual (dots) primary tumor sizes of the MDA-MB-231-Luc subcutaneous xenografts in SCID mice post 4 weeks of treatment intravenously with the indicated drugs and their combinations are shown. 4 animals out of 6 originally involved in the test were selected for display in each treatment protocol – in each SAHA and SAHA+CFZ group 2 animals out of 6 died post 2 weeks of treatment, possibly due to SAHA toxicity (for details of the treatment protocol see Extended Experimental Procedures);

e. Concomitant treatment of MDA-MB-231 cells with Carfilzomib (CFZ) and APR-246 eliminates Carfilzomib resistant clones while the combining CFZ or APR-246 Cisplatin, Doxorubicin or Paclitaxel does not increase their toxicity. Colony formation assay average colony numbers are shown in 3 biological replicates of the treatment experiment with the indicated drugs and their combinations. Means with s.d. are shown, ANOVA test with Bonferroni correction: * $p<0.05$, ** $p<0.01$, *** $p<0.001$;

f. Introduction of mutant p53 variants to MCF10A cells with stably silenced wt p53 increases their resistance to proteasome inhibitor Carfilzomib (CFZ) but sensitizes them to CFZ+APR-246 combination. Mean viability of MCF10A cell lines is shown - treated for 24h with the different concentrations of CFZ or/and APR-246 - stably transfected with empty retroviral vector (Ctrl), vector encoding shRNA targeting *TP53* transcript (sh p53) and indicated mutant p53 cds shRNA-resistant HA-tagged variants, stably introduced into MCF10A sh p53 cell line (+p53 changed residue number). Means with s.d. are shown, ANOVA test with Bonferroni correction: * $p<0.05$, ** $p<0.01$, *** $p<0.001$

48 hours post silencing of mutant *TP53*, *PSMA2* or both. Means of 3 technical replicates are shown with s.d., ANOVA test with Bonferroni correction: *** $p<0.001$. Lower panel: western blot showing the silencing effects on p53/PSMA2 and induction of apoptosis markers: PARP p85 fragment and cleaved Caspase 3. *TP53* silencing does not induce apoptosis markers, viability decrease is due to cell cycle arrest

g. Mutant *TP53*, *NRF2* silencing or APR-246 (PRIMA-1MET) treatment reduces the proteasome genes *PSMA2* (left graph) and *PSMC1* (right graph) transcript elevation due to the bounce-back effect post treatment with Carfilzomib (CFZ) in indicated, four TNBC cell line. Both the bounce-back effect and its reduction due to the *TP53*, *NRF2* silencing or APR-246 treatment are less pronounced in the wt p53 MCF7 and MCF10A cell lines, unless mutant p53 (R280K) is introduced to the MCF10A the cell line – that significantly boosts the bounce-back effect;

h. Primary MDA-MB-231-Luc (mutant p53, TNBC) subcutaneous xenograft growth in SCID mice is significantly reduced compared with the DMSO treated controls in the mice intravenously treated with the combination of Carfilzomib (CFZ) and APR-246, but not in mice with the drugs administered alone (caliper measurement, means with s.e.m. are shown, significance for the time-course is indicated - Friedman nonparametric matched pairs test with Dunn's correction; *** $p<0.001$)

i. Simultaneous silencing of mutant *TP53* and essential proteasome subunit *PSMA2* concomitantly decreases MDA-MB-231 cells viability and induces apoptosis markers. Bar graph represents cell viability

## TABLE 1

| Entrez Gene Name | Gene symbol | 5TNBC Average Fold Change | General biochemical function |
|---|---|---|---|
| aldo-keto reductase family 1, member B1 | AKR1B1 | 1,26 | Detoxication: Phase I drug oxidation, reduction and hydrolysis |
| aldo-keto reductase family 1, member C2 | AKR1C1 | 1,56 | |
| aldehyde dehydrogenase 7 family, member A1 | ALDH7A1 | -1,17 | |
| carbonyl reductase 1 | CBR1 | 1,07 | |
| epoxide hydrolase 1, microsomal (xenobiotic) | EPHX1 | 1,21 | |
| NAD(P)H dehydrogenase, quinone 1 | NQO1 | 1,23 | |
| prostaglandin reductase 1 | PTGR1 | -1,37 | |
| ATP-binding cassette, sub-family B (MDR/TAP), member 6 | ABCB6 | -1,03 | Detoxication: Phase III drug transport |
| ATP-binding cassette, sub-family C (CFTR/MRP), member 1 | ABCC1 | 1,03 | |
| ATP-binding cassette, sub-family C (CFTR/MRP), member 3 | ABCC3 | 1,31 | |
| ATP-binding cassette, sub-family C (CFTR/MRP), member 4 | ABCC4 | 1,17 | |
| ATP-binding cassette, sub-family C (CFTR/MRP), member 5 | ABCC5 | 1,33 | |
| glutathione S-transferase mu 1 | GSTM1 | -1,19 | Detoxication: Phase II drug conjugation/ GSH system |
| glutathione S-transferase pi 1 | GSTP1 | -1,17 | |
| microsomal glutathione S-transferase 1 | MGST1 | -1,09 | |
| glutamate-cysteine ligase, catalytic subunit | GCLC | -1,01 | Antioxidant: GSH-based system |
| glutamate-cysteine ligase, modifier subunit | GCLM | -1,49 | |
| gamma-glutamyltransferase 1 | GGT1 | -1,01 | |
| glutaredoxin (thioltransferase) | GLRX | -1,20 | |
| glutaminase | GLS | 1,02 | |
| glutathione peroxidase 4 | GPX4 | 1,04 | |
| glutathione reductase | GSR | -1,03 | |
| solute carrier family 6, member 9 | SLC6A9 | 1,39 | |
| solute carrier family 7, member 11 | SLC7A11/x-CT | 1,04 | |
| peroxiredoxin 1 | PRDX1 | 1,09 | Antioxidant: TXN-based system |
| peroxiredoxin 6 | PRDX6 | -1,04 | |
| sulfiredoxin 1 | SRXN1 | 1,12 | |
| thioredoxin | TXN | 1,08 | |
| thioredoxin reductase 1 | TXNRD1 | 1,29 | |
| biliverdin reductase A | BLVRA | -1,14 | Heme and iron metabolism |
| biliverdin reductase B (flavin reductase (NADPH)) | BLVRB | 1,02 | |
| ferrochelatase | FECH | -1,01 | |
| ferritin, heavy polypeptide 1 | FTH1 | 1,00 | |
| ferritin, light polypeptide | FTL | 1,02 | |
| heme oxygenase (decycling) 1 | HMOX1 | 1,57 | |
| acyl-CoA thioesterase 7 | ACOT7 | 1,01 | Lipid metabolism: fatty acid oxidation |
| acyl-CoA thioesterase 8 | ACOT8 | -1,00 | |
| acyl-CoA oxidase 1, palmitoyl | ACOX1 | -1,24 | |
| acyl-CoA oxidase 2, branched chain | ACOX2 | -1,24 | |
| glucose-6-phosphate dehydrogenase | G6PD | 1,10 | Carbohydrate metabolism and NADPH regeneration |
| hexokinase 1 | HK1 | 1,02 | |
| malic enzyme 1, NADP(+)-dependent, cytosolic | ME1 | 1,10 | |
| phosphogluconate dehydrogenase | PGD | 1,15 | |
| transaldolase 1 | TALDO1 | 1,02 | |
| transketolase | TKT | 1,18 | |
| UDP-glucose 6-dehydrogenase | UGDH | -1,03 | |
| lipase, member H | LIPH | 1,01 | Lipid metabolism: lipases |
| patatin-like phospholipase domain containing 2 | PNPLA2 | 1,05 | |
| thromboxane A synthase 1 (platelet) | TBXAS1 | 1,12 | |
| P450 (cytochrome) oxidoreductase | POR | 1,05 | |
| ELOVL fatty acid elongase 1 | ELOVL1 | -1,01 | |
| prosaposin | PSAP | 1,27 | |
| lipin 1 | LPIN1 | 1,56 | |
| pyruvate carboxylase | PC | 1,00 | |
| aldehyde dehydrogenase 3 family, member A1 | ALDH3A1 | 1,01 | |
| serine hydroxymethyltransferase 1 (soluble) | SHMT1 | -1,20 | Serine biosynthesis |
| serine hydroxymethyltransferase 2 (mitochondrial) | SHMT2 | -1,00 | |
| phosphoserine aminotransferase 1 | PSAT1 | -1,74 | |
| phosphoglycerate dehydrogenase | PHGDH | 1,08 | |

**Table 1. NRF2 target genes and their regulation upon mutant p53 silencing in 5 TNBC cell lines (result FD on average)**

## TABLE 1

| Entrez Gene Name | Gene symbol | 5TNBC Average Fold Change | General biochemical function |
|---|---|---|---|
| proteasome (prosome, macropain) subunit, alpha type, 1 | PSMA1 | -1,45 | Proteasome machinery |
| proteasome (prosome, macropain) subunit, alpha type, 2 | PSMA2 | -1,57 | |
| proteasome (prosome, macropain) subunit, alpha type, 3 | PSMA3 | -1,21 | |
| proteasome (prosome, macropain) subunit, alpha type, 4 | PSMA4 | -1,20 | |
| proteasome (prosome, macropain) subunit, alpha type, 5 | PSMA5 | -1,21 | |
| proteasome (prosome, macropain) subunit, alpha type, 6 | PSMA6 | -1,24 | |
| proteasome (prosome, macropain) subunit, alpha type, 7 | PSMA7 | -1,04 | |
| proteasome (prosome, macropain) subunit, beta type, 1 | PSMB1 | -1,02 | |
| proteasome (prosome, macropain) subunit, beta type, 2 | PSMB2 | -1,17 | |
| proteasome (prosome, macropain) subunit, beta type, 3 | PSMB3 | -1,08 | |
| proteasome (prosome, macropain) subunit, beta type, 4 | PSMB4 | -1,06 | |
| proteasome (prosome, macropain) subunit, beta type, 5 | PSMB5 | -1,07 | |
| proteasome (prosome, macropain) subunit, beta type, 6 | PSMB6 | -1,11 | |
| proteasome (prosome, macropain) subunit, beta type, 7 | PSMB7 | -1,01 | |
| proteasome (prosome, macropain) 26S subunit, ATPase, 1 | PSMC1 | -1,68 | |
| proteasome (prosome, macropain) 26S subunit, ATPase, 2 | PSMC2 | -1,03 | |
| proteasome (prosome, macropain) 26S subunit, ATPase, 3 | PSMC3 | -1,10 | |
| proteasome (prosome, macropain) 26S subunit, ATPase, 4 | PSMC4 | -1,07 | |
| proteasome (prosome, macropain) 26S subunit, ATPase, 5 | PSMC5 | -1,12 | |
| proteasome (prosome, macropain) 26S subunit, ATPase, 6 | PSMC6 | -1,15 | |
| proteasome (prosome, macropain) 26S subunit, non-ATPase, 1 | PSMD1 | -1,06 | |
| proteasome (prosome, macropain) 26S subunit, non-ATPase, 2 | PSMD2 | -1,13 | |
| proteasome (prosome, macropain) 26S subunit, non-ATPase, 3 | PSMD3 | -1,10 | |
| proteasome (prosome, macropain) 26S subunit, non-ATPase, 4 | PSMD4 | -1,12 | |
| proteasome (prosome, macropain) 26S subunit, non-ATPase, 5 | PSMD5 | 1,00 | |
| proteasome (prosome, macropain) 26S subunit, non-ATPase, 6 | PSMD6 | -1,02 | |
| proteasome (prosome, macropain) 26S subunit, non-ATPase, 8 | PSMD8 | -1,04 | |
| proteasome (prosome, macropain) 26S subunit, non-ATPase, 9 | PSMD9 | 1,04 | |
| proteasome (prosome, macropain) 26S subunit, non-ATPase, 10 | PSMD10 | -1,44 | |
| proteasome (prosome, macropain) 26S subunit, non-ATPase, 11 | PSMD11 | -1,09 | |
| proteasome (prosome, macropain) 26S subunit, non-ATPase, 12 | PSMD12 | -1,32 | |
| proteasome (prosome, macropain) 26S subunit, non-ATPase, 13 | PSMD13 | -1,13 | |
| proteasome (prosome, macropain) 26S subunit, non-ATPase, 14 | PSMD14 | -1,06 | |
| peroxisome proliferator-activated receptor gamma | PPARG | 1,03 | various novel NRF2 targets (validated targets) |
| peroxisome proliferator-activated receptor gamma, coactivator 1 beta | PPARGC1B | 1,08 | |
| retinoid X receptor, alpha | RXRA | 1,03 | |
| Mdm2, p53 E3 ubiquitin protein ligase homolog (mouse) | MDM2 | -1,06 | |
| hypoxia up-regulated 1 | HYOU1/ORP150 | -1,16 | |
| zinc finger protein 143 | ZNF143 | -1,13 | |
| CUGBP, Elav-like family member 2 | CELF2 | 1,02 | |
| nuclear receptor corepressor 2 | NCOR2 | 1,02 | |
| RAB10, member RAS oncogene family | RAB10 | 1,28 | |
| activating transcription factor 4 | ATF4 | 1,16 | |
| Kruppel-like factor 9 | KLF9 | 1,04 | |
| CCAAT/enhancer binding protein (C/EBP), beta | CEBPB | -1,05 | NRF2-KEAP1 pathway |
| kelch-like ECH-associated protein 1 | KEAP1 | -1,14 | |
| v-maf musculoaponeurotic fibrosarcoma oncogene homolog G | MAFG | 1,06 | |
| nuclear factor (erythroid-derived 2)-like 1 | NFE2L1 | -1,06 | |
| nuclear factor (erythroid-derived 2)-like 2 | NFE2L2 | 1,06 | |
| nuclear factor (erythroid-derived 2)-like 3 | NFE2L3 | -1,10 | |
| cullin 3 | CUL3 | -1,00 | |
| glycogen synthase kinase 3 alpha | GSK3A | -1,02 | |

**Table 1. NRF2 target genes and their regulation upon mutant p53 silencing in 5 TNBC cell lines (result FD on average) – cont.**

## TABLE 2

| qPCR primers: | | |
|---|---|---|
| **Gene Name:** | **Primer sequence:** | **Direction:** |
| PSMA1 | ATACTTTCGGCAGCACCTCC | FW |
| PSMA1 | AGACCAACTGTGGCTGAACC | REV |
| PSMA2 | GTGCTTTGGCTCTTCGGGTA | FW |
| PSMA2 | GCTTTAATTCCCACGGACGG | REV |
| PSMA3 | GGCTGCAGTTTCATGTTAGGG | FW |
| PSMA3 | GATGGCACAGCCCCAATAAC | REV |
| PSMA4 | GTTAAGGGCTCCGTGGACAT | FW |
| PSMA4 | CCTGCATGTCCAATAGCTTCC | REV |
| PSMA5 | GTACGACAGGGGCGTGAATA | FW |
| PSMA5 | GCACACACCCTCTGATGTCT | REV |
| PSMA6 | GGGCCCAGGGATTGTGTTTA | FW |
| PSMA6 | GATGTAAGGCCACCCTGGTT | REV |
| PSMA7 | CAAGTGGAGTACGCGCAGGA | FW |
| PSMA7 | GCAGTTTGGCCACTGACTTCT | REV |
| PSMA8 | TGAATATGCCCAGGAAGCGG | FW |
| PSMA8 | ACTGCAAAAGCCATGCAGAC | REV |
| PSMB1 | CCCTTTGCAGCTGCGATTTT | FW |
| PSMB1 | GGGCTATCCCGCGTATGAAT | REV |
| PSMB2 | CTCATCGGTATCCAAGGCCC | FW |
| PSMB2 | GTCTCCAGCCTCTCCAACAC | REV |
| PSMB3 | TGAGTTGAAGGAAGGTCGGC | FW |
| PSMB3 | AAAGGTCTTCGGGTCCAACC | REV |
| PSMB4 | CGGAGGCTATGCTGATGGAG | FW |
| PSMB4 | AGCGTTCTACTAAGTCGCGG | REV |
| PSMB5 | GCTACCGGTGAACCAGCG | FW |
| PSMB5 | CAACTATGACTCCATGGCGGA | REV |
| PSMB6 | CACTCCAGACTGGGAAAGCC | FW |
| PSMB6 | GACAGCAGAAAATGCGGTCG | REV |
| PSMB7 | CACAGACATGACAACCCAGC | FW |
| PSMB7 | AGGGCTGCACCAATGTAACC | REV |
| PSMB8 | GCTCCTGGCTGACTTCTAGT | FW |
| PSMB8 | TGAACGTTCCTTTCTCCGTCC | REV |
| PSMB9 | GGCGTTGTGATGGGTTCTGA | FW |
| PSMB9 | AGAGAGTGCACAGTAGATGCG | REV |
| PSMB10 | AGCTACACGCGTTATCTACGG | FW |
| PSMB10 | CTGCGGTCCAGTCAGGTCTA | REV |
| PSMB11 | CGTGGCTATCGCTACGACAT | FW |
| PSMB11 | TGACACATGCTCCCATCCAC | REV |
| | | |
| TP53 | CTCCTCTCCCCAGCCAAAGA | FW |
| TP53 | GGAACATCTCGAAGCGCTCA | REV |
| | | |
| NRF1 (TCF11, NFE2L1) | TACGGGTGGACGTGGATACT | FW |
| NRF1 (TCF11, NFE2L1) | ACCAGCCAGGCATTTACCTC | REV |
| NRF2 ( NFE2L2) | TCCATTCCTGAGTTACAGTGTCT | FW |
| NRF2 ( NFE2L2) | TGGCTTCTGGACTTGGAACC | REV |
| | | |
| HO-1 | aactttcagaagggccaggt | FW |
| HO-1 | ctgggctctccttgttgc | REV |

| qPCR primers: | | |
|---|---|---|
| **Gene Name:** | **Primer sequence:** | **Direction:** |
| PSMC1 | TGGAGCTTCCTCTCACCCAT | Fw |
| PSMC1 | TGGCTGAGGTTTGGTTTGCT | Rev |
| PSMC2 | ACAGCCTTTACAGGTTGCCA | FW |
| PSMC2 | CTATCCACGCCCACTCTCATC | REV |
| PSMC3 | ATTGGGGGTTTGGACAAGCA | FW |
| PSMC3 | ATCAGCACCCCTTTTGGAGG | REV |
| PSMC4 | TCTGGAGGCTGTGGATCAGA | FW |
| PSMC4 | AGTGCATTGCTGTGCTTGTG | REV |
| PSMC5 | AGAGAAGATGGCGCTTGACG | FW |
| PSMC5 | CTCCGGAGGTTTTGGCTCTT | REV |
| PSMC6 | AACACAAGGAGATCGACGGC | FW |
| PSMC6 | CGATCTGCCCAACACTCTGTA | REV |
| PSMD1 | ATGGGAGGATGGAAGAGGCT | FW |
| PSMD1 | AACATGTAGCAGGCGTCGAA | REV |
| PSMD2 | CATGACTTCAGTGCCCAAGC | FW |
| PSMD2 | CGGAGATGATGTCAGCAGCA | REV |
| PSMD3 | GCGAATCAAAGCCATCCAGC | FW |
| PSMD3 | CAGCTCCACCACGATGAGAA | REV |
| PSMD4 | ACGTGGGCCTTATCACACTG | FW |
| PSMD4 | GATCTTGCCCTTGGGTTGGA | REV |
| PSMD5 | GCTCTTCTCCCTGCTTAACGA | FW |
| PSMD5 | CAGGTCAACCCTGAGGTTCC | REV |
| PSMD6 | TCCAGCAGTTCGGCAGTATC | FW |
| PSMD6 | ATGAGGGGCAAAAAGCCAGT | REV |
| PSMD7 | TTGATGTGAAGCCGAAGGACC | FW |
| PSMD7 | GCTCCAATTTCACTGGTCACG | REV |
| PSMD8 | TGGAACCGTAAAAGCCCCAA | FW |
| PSMD8 | TCACGGGCCAGAATTAGCTG | REV |
| PSMD9 | CGCAAACTGGGTCAGAGTGA | FW |
| PSMD9 | TGTTCACAGAGCCGAACTCC | REV |
| PSMD10 | AGCAGCCAAGGGTAACTTGAA | FW |
| PSMD10 | ACTCTCTCCTCATCACAGGCT | REV |
| PSMD11 | GCTTGCACTTCGGTATGCAG | FW |
| PSMD11 | GAGCTCTGCCCGGTAATCTG | REV |
| PSMD12 | TCGTCAAGATGGAGGTGGAC | FW |
| PSMD12 | ACGAGTCTGCTTTTCCAGAGA | REV |
| PSMD13 | ACGTACCGGGCTTCCTACAG | FW |
| PSMD13 | CAAAGCACGGATCCTGCACA | REV |
| PSMD14 | AGGAGGTATGCCTGGACTGG | FW |
| PSMD14 | TCCAGCACGGCCATGTTTT | REV |
| | | |
| Actin | CGCCGCCAGCTCACCATG | FW |
| Actin | CACGATGGAGGGGAAGACGG | REV |
| H3 | GAAGAAACCTCATCGTTACAGGCCTGG | FW |
| H3 | CTGCAAAGCACCAATAGCTGCACTCTGC | REV |
| GAPDH | CATGCCATCACTGCCACCC | FW |
| GAPDH | ACCTGGTCCTCAGTGTAGC | REV |

**Table 2. List of qPCR and ChIP primers sequences; primary antiobdies used for WB, ChIP and IP; siRNA sequences; – cont.**

## TABLE 2

| ChIP Primers: | | |
|---|---|---|
| **Gene Name:** | **Primer sequence:** | **Direction:** |
| PSMA1 ChIP Binding | AAGTCTGCGGGAGTTTGACG | FW |
| PSMA1 ChIP Binding | TTTTCCCGCCAGTCTCAGTT | REV |
| PSMA1 ChIP Non-binding | ATGTGGTCCTGGGTAAGGCA | FW |
| PSMA1 ChIP Non-binding | GCTTAGGGAAGCACAGGCTAA | REV |
| PSMA2 ChIP Binding | CCTCGACTACGCTGAAGACC | FW |
| PSMA2 ChIP Binding | TAAAGGAAAGGTGAGGGGCG | REV |
| PSMA2 ChIP Non-binding | TCGGTGCCACCTTTTCCTTT | FW |
| PSMA2 ChIP Non-binding | ACAGGTGAGCAGCATCAGTC | REV |
| PSMA3 ChIP Binding | AACCGAAGGAGGAGCCTTTG | FW |
| PSMA3 ChIP Binding | TTTCTCTGTGGCTCGTTCCG | REV |
| PSMA3 ChIP Non-binding | TGTAGGAAGGGGTCCAGTCA | FW |
| PSMA3 ChIP Non-binding | CCCATCCCTACCGTCATTTCC | REV |
| PSMB1 ChIP Binding | CGGCTTGTCCCTTTGGTAGT | FW |
| PSMB1 ChIP Binding | CGTTGCGCCATAGTTCTGAC | REV |
| PSMB1 ChIP Non-binding | CCAGATGGCTTAACAGTCCCA | FW |
| PSMB1 ChIP Non-binding | AGAGGGCTCTGGTGTTTACG | REV |
| PSMB5 ChIP Binding | GTAAGGGAAGTGAGGTCGGC | FW |
| PSMB5 ChIP Binding | GAAGCAGCAGCGATGTAACC | REV |
| PSMB5 ChIP Non-binding | CCCCAAATGGCTCTGACAGT | FW |
| PSMB5 ChIP Non-binding | TAGGTGAGGATGTGGGGGAG | REV |
| PSMB9 ChIP Binding | CTTCTCGCCTCTCCCTGC | FW |
| PSMB9 ChIP Binding | AGACAAGTGACGAGGCAGC | REV |
| PSMB9 ChIP Non-binding | ATCAGCAAACTCGCATGTAAAAG | FW |
| PSMB9 ChIP Non-binding | TGAAATTCACAAGTGCCCCAAAA | REV |
| PSMC1 ChIP Binding | CGTAGCGTCCCTAACGACTT | FW |
| PSMC1 ChIP Binding | GACCAGCGGAAAGAAACCCT | REV |
| PSMC1 ChIP Non-binding | GTCCGATAGGGGGAGTCAGT | FW |
| PSMC1 ChIP Non-binding | GGCTCCCACTGTCCTGTTTA | REV |
| PSMC6 ChIP Binding | GTGGAGTAGAAAGACGGGGC | FW |
| PSMC6 ChIP Binding | TAGGGTCCGCCATGATGAGA | REV |
| PSMC6 ChIP Non-binding | GACCCAGGTCATGTTCTCCC | FW |
| PSMC6 ChIP Non-binding | CCATGGATGTCTCTCCAAGTGT | REV |
| PSMD5 ChIP Binding | CGTCATCTAGGTCGCTGCTC | FW |
| PSMD5 ChIP Binding | GCCGACGAGGCTGTTTAACT | REV |
| PSMD5 ChIP Non-binding | CTGGAATCAAAGGACCTGGACT | FW |
| PSMD5 ChIP Non-binding | ACAGTCCTGCAAAGAACATACAT | REV |
| PSMD10 ChIP Binding | TCGCTGTCCCAGCAACTAC | FW |
| PSMD10 ChIP Binding | CGCGACGGGAAAAGAAAAGG | REV |
| PSMD10 ChIP Non-binding | TGGGCAAGGTTAGGAAGCAC | FW |
| PSMD10 ChIP Non-binding | GCCCGAGGGAAGAAGAACTG | REV |

| siRNAs: | |
|---|---|
| **Gene Name:** | **siRNA sequence:** |
| Control siRNA | All star negative control (1027281,Qiagen) |
| TP53 I | GACUCCAGUGGUAAUCUUAC |
| TP53 II | GGUGAACCUUAGUACCUAA |
| TP53 III | AGCAGUCACAGCACAUGAC |
| NRF1 (TCF11, NFE2L1) | CAGAAGCAGUGCCUAGUGA |
| NRF2 (NFE2L2) | GCACAGCAGAAUUCAAUGA |
| NRF2 (NFE2L2) II | GCAUUGGAGUGUCAGUAUG |
| PSMA2 | UGAAGAUCUGGAACUUGAA |
| STAT3 | GAAUCACGCCUUCUACAGA |
| NFYA | CAAUACCACCGUAUUCUUA |
| NFKB | GCCCUAUCCCUUUACGUCA |

| Antibodies: | |
|---|---|
| **Target protein name:** | **ID number, producer:** |
| p53 | sc-126, Santa Cruz |
| NRF1 (TCF11, NFE2L1) | sc-13031, Santa Cruz |
| NRF2 (NFE2L2) | ab62352, Abcam |
| PSMA2 | sc-54671, Santa Cruz |
| PSMB1 | sc-67345, Santa Cruz |
| PSMB9 (LMP2) | sc-28809, Santa Cruz |
| PSMC1 | ab3317, Abcam |
| CDKN1A (p21) | sc-397, Santa Cruz |
| PMAIP1 (NOXA) | OP180, Calbiochem |
| BCC3 (PUMA) | 4976S, Cell Signaling |
| KHSRP (KSRP) | ab150393, Abcam |
| Actin | A2066, Sigma |
| Acetyl-Histone H3 (Lys9) | 07-352, Merck |
| Histone H3 | ab1791, Abcam |
| p300 | 554215, BD Pharmmingen |
| Cleaved Caspase-3 | 9664S, Cell Siganling |
| PARP p85 | G734A, Promega |
| Mouse normal IgG | sc-2025, Santa Cruz |
| Rabbit normal IgG | sc-2027, Santa Cruz |

**Table 2. List of qPCR and ChIP primers sequences; primary antiobdies used for WB, ChIP and IP; siRNA sequences; – cont.**

# ACKNOWLEDGEMENTS

First of all, I would like to thank to my mentor Giannino Del Sal for giving me an opportunity to develop this story and for his valuable advices, enthusiasm, and encouragement over the course of my PhD. Your passion for science and persistence in looking for answers is an inspiring model of how to be a great scientist.

Work presented in this thesis was performed under the supervision of Prof. Giannino Del Sal and Dr. Dawid Walerych. I would like to give a special thanks to Dawid who was not only my tutor but a great friend that I knew I could rely on. You initiated the story and transferred on me Your unmatched enthusiasm and passion for science. Thank You for all of our meaningful discussions, having patience in teaching me how to work in a proper and efficient way as well as showing me the importance of asking the right questions.

For important contributions to our work special thanks should be given to: Dr. Antonio Rosato and Dr. Roberrta Sommaggio for mice experiments; Silvano, Emiliano, Yari for bioinformatics; Kasia G-W., Kasia R., and Eleonora for helping with some experiments, other collaborators for making this work possible and all Gianni Del Sal's lab members for constructive discussions.

I would like to thank Anna, Giovanni, Carmelo, Eleonora and Manuel not only for being wonderful coworkers with whom I could discuss my scientific doubts but also great friends that made my staying in Trieste feeling almost like home.

I thank also all the members of the Gianni Del Sal's laboratory team and my fantastic friends Bruna, Rudy, Luca, Edo that further caused, that Italy is a special place for me.

# APPENDIX

During the period of my PhD I have been collaborating in the following publications:

Garibaldi, F., Falcone, E., Trisciuoglio, D., Colombo, T., Lisek, K., Walerych, D., Del Sal, G., Paci, P., Bossi, G., Piaggio G., and Gurtner, A., (2016) "Mutant p53 inhibits miRNA biogenesis by interfering with the microprocessor complex." *Oncogene*

Marini, B., Kertesz-Farkas, A., Ali, H., Lucic, B., Lisek, K., Manganaro, L., Pongor, S., Luzzati, R., Recchia, A., Mavilio, F., Giacca, M., Lusic, M., (2015) "Nuclear architecture dictates HIV-1 integration site selection." *Nature*

Walerych, D., Lisek, K. & Del Sal, G., (2015) "Mutant p53: One, No One, and One Hundred Thousand." *Frontiers in Oncology*